

**INTERFACE PRESSURE AND VIBRATION COMFORT EVALUATIONS
OF AN AIR-CUSHION SUSPENSION SEAT**

Arash Naseri

A Thesis

In

The Department

Of

Mechanical and Industrial Engineering

Presented in Partial Fulfillment of the Requirements

For the Degree of Master of Applied Science (Mechanical Engineering) at

Concordia University

Montreal, Quebec, Canada

September 2011

© Arash Naseri, 2011

CONCORDIA UNIVERSITY

School of Graduate Studies

This is to certify that the thesis prepared

By: Arash Naseri

Entitled: INTERFACE PRESSURE AND VIBRATION COMFORT
EVALUATIONS OF AN AIR-CUSHION SUSPENSION SEAT

And submitted in partial fulfillment of the requirements for the degree of

Master of Applied Science (Mechanical Engineering)

Complies with the regulations of the university and meets the accepted standards with respect to originality and quality.

Signed by the final examining committee:

Dr. C.Y. Su _____ Chair

Dr. Y. Zeng _____ Examiner

Dr. Y. Zang _____ Examiner

Dr. G.J. Gouw, _____ Supervisor

Dr. S. Rakheja _____ Supervisor

Approved by _____
Dr. A.K.W. Ahmed MASC Program Director
Department of Mechanical and Industrial Engineering

_____ 2011

_____ Dean Robin Drew

ABSTRACT

INTERFACE PRESSURE AND VIBRATION COMFORT EVALUATIONS OF AN AIR-CUSHION SUSPENSION SEAT

Arash Naseri

The static and dynamic comfort performance of a suspension seat equipped with an air cushion with multiple air bladders are investigated through subjective and objective measurements of vibration transmission and body-seat interface pressure. The objective measures are obtained in terms of vibration transmission and body-seat contact pressure. The static and dynamic properties of the air cushion are initially characterized in the laboratory for different pre-loads and different inflation pressure combinations. For this purpose, a buttock shaped indenter is designed and fabricated to simulate seated body weight distribution over the cushion. This feature of the proposed indenter is assumed through measurements of buttock-cushion interface pressure distributions with a number of human subjects and the pre-loaded indenter. The results showed that the proposed indenter, unlike the standardized indenter (SAE J1051, 1988), yields more representative human-seat interface pressure distribution. The measured data further revealed concentration of contact pressure in the vicinity of the ischial tuberosities (IT). Consequently, the cushion surface was divided into nine different regions to characterize the load distributions in terms of contact force, mean pressure and contact area of the seated body over the buttocks, thighs, knees and the tail bone. The load distributions were measured with a total of 10 human subjects for nine different inflation pressure combinations, while seated with and without a back support. A questionnaire was also designed to assess the subjective comfort sensation of the subjects for different inflation pressure combinations. The subjective and objective responses revealed good correlation between the ischium pressure and the comfort sensation. A greater inflation pressure near the ischium region would thus cause greater discomfort.

The vibration transmission properties of the air cushion with and without the suspension were subsequently evaluated for different pressure combinations and white-noise random vibration. The vibration transmission properties of the seat were evaluated with the human subjects and equivalent passive loads. The results revealed bottoming the cushion under low and medium inflation pressures and thus higher vibration transmissibility. The objective measurements revealed that the suspension could attenuate the vibration but the natural frequency of the prototype suspension was too high for effective vibration attenuation. The mechanical suspension of the prototype seat, when combined with the polyurethane layer of the cushion and the inflated air bladders, showed a damped natural frequency close to the spinal resonance frequency.

Acknowledgment of Dedication

I would like to thank my supervisors, Dr. Subhash Rakheja and Dr. Gerard Gouw for initiating this project as well as for their technical, motivational and financial support throughout the completion of this thesis work. Their constant input has extended this learning experience far beyond the scope of this thesis.

I would also thank Mr. Anand Pranesh for his technical support and criticism during my work at CONCAVE.

I wish to thank Mr. Dainius Juras and all students and colleagues at CONCAVE who have volunteered their help during the experimental and analytical stages of this work.

I greatly thank and appreciate two important characters in my life, my dear friends Mr. Mahdi Shahparnia and Ms. Gohar Tajik whose pure friendship and love has motivated my social and academic life in North America, Also my parents for their constant support and love throughout my life, from the beginning of this long journey.

Table of Contents

List of Tables	ix
List of Figures	xi
List of Abbreviations	xv
List of Variables.....	xvi
1. INTRODUCTION AND SCOPE OF THE RESEARCH	1
1.1 Introduction.....	1
1.2 Review of the Literature	3
1.2.1 Biomechanics of Comfort and Seat Geometry	3
Natural Spine Posture	3
1.2.2 Evaluation of Comfort	7
1.2.3 Static Comfort.....	10
1.2.4 Dynamic Comfort	12
1.3 Seat Cushion Materials and Design	19
1.4 Scope and Objectives of the Thesis	25
1.5 Organization of the Dissertation.....	26
2. EXPERIMENTAL CHARACTERIZATION OF AN AIR SEAT CUSHION.....	28
2.1 Introduction.....	28
2.2 Prototype Seat Description	29
2.3 Cushion Characterization Methodology	30
2.3.1 Experimental Setup and Acquisition of Force-Deflection Characteristics	33

2.4	Indenter Design.....	35
2.4.1	Analysis of the Pressure Distribution	36
2.4.2	Verification of the Indenter Design	40
2.5	Static Force-Deflection Characteristics of the Seat Cushion.....	44
2.6	Dynamic Force-Deflection Characteristics of the Seat Cushion	46
2.6.1	Dynamic Damping Characteristics	49
2.7	Summary.....	51
3.	CORRELATION BETWEEN SUBJECTIVE COMFORT AND INTERFACE PRESSURE DISTRIBUTION	52
3.1	Introduction.....	52
3.2	Measurement of Body-Seat Pressure Distribution on Seat Cushion	56
3.2.1	Subjective Evaluations	59
3.2.2	Test Matrix and Methodology	59
	Table 3-4: Test matrix.....	63
3.3	Method of Analysis.....	63
3.4	Results and Discussions.....	64
3.4.1	Contact force, area and pressure - Intra-subject variability	64
3.4.2	Contact force, area and pressure distribution on the seat cushion	67
3.4.3	Correlation between subjective evaluations and objective force distributions	83
3.5	Summary.....	86
4.	DYNAMIC ANALYSIS OF SUSPENSION SEAT	88

4.1	Introduction.....	88
4.2	Static and Dynamic Properties of the Seat Suspension System	89
4.3	Experimental Characterization of Vibration Isolation of the Suspension	94
4.3.1	Test Apparatus	94
4.3.2	Test Matrix.....	98
4.3.3	Test Method	99
4.4	Resonant Frequencies of the Seat and the Structure.....	101
4.5	Vibration Transmissibility of the Inflatable Cushion.....	106
4.5.1	Cushion Vibration Transmissibility Loaded with Passive Loads	106
4.5.2	Cushion Vibration Transmissibility Loaded with Human Subject and Influence of Back Support.....	109
4.6	Vibration Transmissibility of the Suspension Seat.....	111
4.6.1	Vibration Transmissibility of Seat Suspension Loaded with a Passive Load	112
4.6.2	Vibration Transmissibility of Seat Suspension Loaded with Human Subjects and Influence of Back Support	115
4.7	Summary.....	118
5.	CONCLUSIONS AND RECOMMENDATIONS FOR FUTURE WORK	119
5.1	Highlights of This Research Thesis	119
5.2	Conclusions.....	120
5.3	Recommendations for Future Work	124

List of Tables

Table 1-1: Reported discomfort in local body segments through subjective evaluations [1, 5, 6].	9
Table 1-2: Reported resonant frequencies of the spine.	14
Table 2-1: Comparison of measured dynamic and static cushion stiffness values.	47
Table 3-1: A summary of studies reporting human-seat interface pressure and force	53
Table 3-2: Anthropometric attributes of the subjects [43].	60
Table 3-3: Air bladder pressure combinations of the seat cushion used in the experiments.	62
Table 3-4: Test matrix.	63
Table 3-5: The measured standard deviations of the mean contact force, area and pressure data acquired for each subject with eight different cushion inflation pressure configurations.	66
Table 3-6: Mean normalized force on the seat cushion of the subject sitting with and without a back support across eight cushion inflation pressures.	67
Table 3-7: Comparisons of total body-seat contact force measured for the eight cushion inflation pressure combinations (A to H) and two backrest supports.	71
Table 3-8: Comparison of the mean overall seat cushion force corresponding to eight cushion inflation pressure combinations and two backrest supports.	72
Table 3-9: Comparisons of mean force, area and pressure distributed over different seat regions (M01 to M09), when sitting with a full back support (B).	74
Table 3-10: Comparisons of mean force, area and pressure distributed over different seat regions (M01 to M09), when sitting with no back support (NB).	76
Table 3-11: Mean normalized distributed force and standard deviation of the mean (full back support).	78

Table 3-12: Mean normalized distributed force and standard deviation of the mean (no back support).	79
Table 3-13: Mean force percentage distribution of the user-selected cushion inflation pressure (G), with and without the back support.	86
Table 4-1: Static stiffness of the seat suspension.	91
Table 4-2: Measured damping coefficients in compression (C_c) and rebound (C_r).	93
Table 4-3: Selected combinations of individual bladders pressure coupled with locked and un-locked suspension.	99
Table 4-4: Seat components resonance frequencies - 70.2 kg passive load.	105

List of Figures

Figure 1-1: Location of center of gravity for different seating postures [6].	4
Figure 1-2 The geometric model of the spine while sitting [5].	5
Figure 1-3 (a) The lumbar support to realize an ideal pelvis rotation of 35 degrees, with 10 degrees seat pan inclination, 5 degrees depression into seat, and 120 degrees backrest incline [5]; (b) head flexion under an ideal backrest inclination and knee flexion [9].	7
Figure 1-4 Human-seat pressure distribution [18].	11
Figure 1-5: Influence of vehicle vibration spectrum on vibration attenuation performance of two suspension seats with different vibration transmissibility [17].	16
Figure 1-6: Stress-Strain Curve of a typical open cell PUF [34].	20
Figure 1-7: Integration of different air cells in an air-inflated seat cushion configuration [38].	22
Figure 1-8: Vertical amplitude transmissibility of (a) a standard foam cushion and (b) air cushion [25].	24
Figure 1-9: Pressure distribution at the human-seat interface: (a) foam; and (b) air cushion [25].	24
Figure 2-1: Schematic illustration of bladders within the cushion and the backrest.	30
Figure 2-2: Prototype suspension seat.	31
Figure 2-3: Experimental setup for measurements of force-deflection characteristics of seat cushions in accordance with SAE J1051 [39].	32
Figure 2-4: Schematic of the data acquisition and analysis system.	34
Figure 2-5: A schematic of the modified Staarink indenter [57] (values are in mm).	37
Figure 2-6: Finite element analysis of the cushion-indenter system: a) Cushion-indenter system b) Pressure distribution on the cushion c) Cushion deformation, the upper surface of the indenter is kept horizontal d) Cushion deformation; the lower surface of the indenter is in	

full contact with the cushion surface e) 3D picture of real subject interface pressure distribution f) 2D picture of human subject interface pressure distribution.	38
Figure 2-7: Buttock-Shaped indenter	39
Figure 2-8: Schematic illustration of the novel Electronics pressure mat (units are in mm)..	40
Figure 2-9: Schematic presentation of pressure division regions on the cushion (digits indicate number of sensors occupied).	41
Figure 2-10: Comparison of pressure distribution: a) Subject b) Indenter.	42
Figure 2-11: Comparisons of the contact force, peak pressure (PP), mean pressure (MP) and contact area (A) measured at the seat interface for human subject and the buttock-shaped indenter.....	43
Figure 2-12: Comparisons of static force-deflection characteristics of the seat pan with three different bladder pressures measured using the buttock-shaped and SAE indenters.....	45
Figure 2-13: Dynamic force-deflection characteristics of the cushion measured under deflections at 1, 2 and 4 Hz (inflation pressure = 1 psi, preload of 290 N).	48
Figure 2-14: Variations in the dynamic seat stiffness at a preload of 280 N as a function of the excitation frequency and inflation pressure.	48
Figure 2-15: Equivalent viscous damping coefficient as a function of frequency and inflation pressure.	50
Figure 3-1: Schematic of the different contact regions considered in the study.....	58
Figure 3-2: a) Body map of human-seat contact area for subjective zonal discomfort evaluations. b) Layout of air bladders within the seat cushion and their interactions. Regions: 1- tail bone, 2 - right cushion wing, 3 - right buttock, 4 - left buttock, 5-right thigh, 6- left thigh, 7- right under knee, 8-left under knee and 9-left cushion wing.....	58
Figure 3-3: Correlation between the body mass index (BMI) and the mean contact force, area and pressure of subjects sitting with full back support (B).	69

Figure 3-4 Correlation between the body mass index (BMI) and the mean contact force, area and pressure of subjects sitting without back support (NB).	70
Figure 3-5: Normalized force distribution over the nine sub-regions of the seat pan corresponding to different inflation pressure combination (A to H).	80
Figure 3-6: Contact area distribution over the nine sub-regions of the seat pan corresponding to different inflation pressure combination (A to H).	81
Figure 3-7: Mean pressure distribution over the nine sub-regions of the seat pan corresponding to different inflation pressure combination (A to H).	82
Figure 3-8: Mean normalized force distributions of individual sub-regions of the seat cushion judged as most comfortable by the subjects.	84
Figure 4-1: Typical suspension seat configuration [42].	90
Figure 4-2: Static force-deflection characteristics of the seat suspension.	92
Figure 4-3: Orientation of the dampers within the suspension mechanism.	93
Figure 4-4: Schematic of the whole-body vehicle vibration simulator (WBVVS) and the test suspension seat.	96
Figure 4-5: Schematic of the measurement and data acquisition system	97
Figure 4-6: Three-axis seat accelerometer pad mounted on (a) seat cushion and (b) seat pan.	100
Figure 4-7: Acceleration transmissibility of the seat with locked suspension and no cushion.	102
Figure 4-8: Suspension acceleration transmissibility with different passive loads.	103
Figure 4-10: PUF cushion acceleration transmissibility with a passive load of 70.2 kg and locked suspension.	104
Figure 4-9: Cushion air bags' location on the plastic support.	104
Figure 4-11: Bushing defects (left) and resulting damper eyes misalignment (right).	105

Figure 4-12: Comparison of acceleration transmissibility characteristics of the seat with locked suspension and cushion air bladders inflated at different pressures (passive loads). 107

Figure 4-13: Comparison of acceleration transmissibility characteristics of air cushion with different passive loads and inflation pressures (locked suspension). 108

Figure 4-14: Comparisons of acceleration transmissibility characteristics of the cushion with three different subjects and three inflation pressure combinations (locked suspension). 110

Figure 4-15: Comparisons of acceleration transmissibility characteristics of the suspension with different passive loads and inflation pressures (un-locked suspension). 113

Figure 4-16: Comparisons of acceleration transmissibility of the locked and un-locked suspension (passive load = 70.2 kg; 0 psi air cushion pressure). 114

Figure 4-17: Comparisons of acceleration transmissibility of the seat suspension with passive load and human subjects sitting without back support and 0 psi air cushion pressure. 116

Figure 4-18: Comparison of acceleration transmissibility of the seat suspension with subject sitting with and without the back support (un-locked suspension). 117

List of Abbreviations

A/D	Analog to Digital conversion
B	Back (refers to sitting with Backrest support)
BMI	Body Mass Index
BPD	Body Pressure Distribution
CCC	Custom Contoured Cushion
DDE	Dynamic Data Exchange
DMA	Direct Memory Access
DOF	Degree of Freedom
FE	Finite Element
FEA	Finite Element Analysis
ISO	International Standards Organization
IT	Ischial Tuberosities
f	frequency
LK	Locked
LVDT	Linear Variable Differential Transducer
LVT	Linear Velocity Transducer
MNiP _{max}	Mean Normalized Maximum Ischium Pressure
MP	Mean Pressure
NB	No Back Support (refers to sitting with no backrest support)
PP	Peak Pressure
Psi	Pound per Square Inch
PUF	Polyurethane Foam
r.m.s	Root Mean Square value

SAE	Society of Automotive Engineers
SEAT	Seat Effective Amplitude Transmissibility
SD	Standard Deviation
UNLK	Un-Locked
VDV	Vibration Dose Value
W	Weighting factor
WBVVS	Whole-Body Vehicular Vibration Simulator

List of Variables

A	Area
<i>a</i>	Acceleration
C	Equivalent Viscous Damping Coefficient
E	Energy dissipated
F	Force
ω	Circular Frequency
X	Peak Displacement Amplitude

1. INTRODUCTION AND SCOPE OF THE RESEARCH

1.1 Introduction

The comfort performance of a driver seat is a complex function of its support and vibration transmission properties. The comfort sensation of a seated body is strongly related to the seat cushion ability to distribute the body weight. A higher pressure concentration near the ischial tuberosities yields greater sensation of discomfort, while a higher contact pressure near the soft thigh tissues may adversely affect the blood flow to the legs [1]. The occurrence of localized high pressure zones at the human-seat interface is reported to cause soft tissue deformation leading to blood restriction in lower extremities resulting in discomfort.

A higher localized pressure concentration may encourage inadequate posture, which could contribute to physiological pain and discomfort [1]. A statically comfortable seat is associated with minimal muscular effort demand from the occupant to maintain the seated position, which is attributed to sufficient body support and contact with the seat, seat back and the floor. When considering the seat comfort in vehicles, the combination of static and dynamic effects should be taken into account. The static seat characteristics such as the seat geometry, hardness and support properties are thought to affect static comfort. It has been reported that prolonged exposure to inadequate supported posture is the cause of back pain, spinal disorders and abdominal pain, which contribute to sensation of discomfort [1, 5].

The design of an automotive seat thus necessitates careful consideration of the interactions between the occupant and the seat. Apart from the static comfort

performance, the dynamic comfort related to vibration transmitted to occupant forms an integral part of the seat design. This is particularly important in applications involving high magnitudes of whole-body vehicular vibration and prolonged exposure as in the case of heavy-road and off-road vehicles. Occupational exposure to such vibration has been associated with an array of musculoskeletal disorders, fatigue, discomfort and poor productivity [3, 10]. Objective measures have been defined to assess the vibration transmission properties of seats, while the static comfort performance is mostly assessed through subjective measures.

The subjective assessments involve repetitive field trials and often yield large variabilities [14]. Alternatively, it has been suggested the subjective comfort sensation may be related to human seat interface pressure distribution in an objective manner [14, 17, 19]. The comfort sensation, however, is related to a large number of seat design factors in a highly complex manner. These include: seat height, cushion properties, backrest angle, seat pan dimension, tilt angle and cushion contours, armrest, lumbar support and head rest. The design of seats for comfort thus necessitates true understanding of all the factors in addition to biodynamics of human posture in the seated position. Only minimal efforts have been made to establish correlations between the subjective evaluation of comfort and various seat design factors.

In this thesis, the occupant's perception of comfort is investigated in terms of human-seat interface pressure, both in static and dynamic environment, in addition to vibration attenuation performance of the seat. A suspension seat with air cushion and backrest comprising multiple inflatable air bladders is considered in order to facilitate different contact pressures in the localized contact zones. The contact pressure distributions of the seated occupants are characterized for various combinations of

cushion and backrest air bladders pressures and different sitting postures. The pressure distributions are correlated with the subjective comfort sensation of the human occupants. The vibration isolation properties of the air cushion with and without the suspension are further characterized to assess the dynamic comfort performance of the seat.

1.2 Review of the Literature

Seating comfort is a complex function of many seat design, vehicular and environmental factors, apart from the individual's anthropometry. The comfort assessments of seats thus necessitate consideration of all these factors. The reported studies on the relevant seat design factors are thus reviewed and summarized below so as to build the essential background and to formulate the scope of this research thesis.

1.2.1 Biomechanics of Comfort and Seat Geometry

Natural Spine Posture

The comfort performance of a seat design has been strongly related to its support characteristics in view of the spinal column support and shape. Although the ergonomics of sitting in an office environment has been extensively studied [1], the biomechanics of automobile driving posture has been addressed in a relatively fewer studies. The design of an automotive seat directly affects the driver's spinal support and the biomechanics. Inadequate support from the seat caused either by the poor seat design or unsuitable seating posture, contribute to sensation of discomfort [1]. Furthermore, low back pain is frequently reported by the operators of heavy vehicle, has been attributed to dynamic loading of the spine under vehicular shock and vibration and prolong sitting in a constrained space [2]. It has been reported that more than half of the heavy vehicle drivers' population suffers from premature degenerative changes in their spinal column

[4]. Furthermore, a posture that restricts the spine from maintaining its natural shape highly contributes to discomfort. The muscles surrounding the spine are continuously engaged in maintaining the natural curves of the column and experience fatigue during prolonged and awkward sitting postures. The most stable and natural shape of spine corresponds to that in a upright standing posture, where the head, back and buttock are aligned when posterior portion of each part touches a virtual wall [5]. When transition occurs from standing to a sitting posture, the pelvis rotates by nearly 40 degrees posteriorly, which causes center of gravity to fall above or posterior to the ischial tuberosities depending upon the backseat inclination. Figure 1-1 shows the location of the center of gravity and pelvic rotation when a person is leaning forward, sitting straight or leaning backward, with no back support[6]. This alters the distribution of the body mass on the seat and causes greater contact stresses on the soft tissues [6].

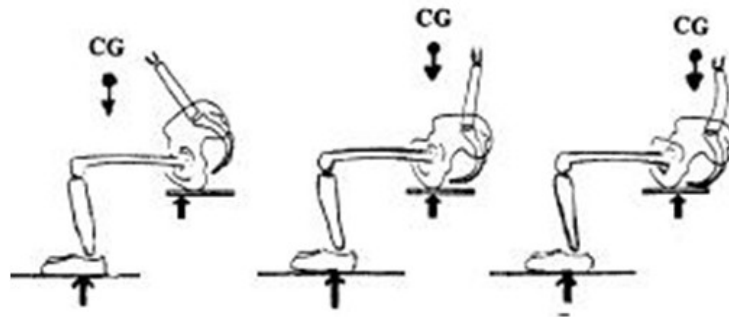


Figure 1-1: Location of center of gravity for different seating postures [6].

While the natural shape of the spine in seated posture affects the load distribution on the seat and thus the sensation of comfort, the thigh–trunk angle is another factor in determination of sitting posture. A higher back inclination would result in higher thigh – trunk angle and thus greater pelvic rotation, which not only engages back muscles for

posture control, but also transfers more body weight to the tailbone region. This causes greater concentrated pressure zones at the seat–human interface, and thus a sensation of discomfort [5]. It has been reported that 135 degree thigh – trunk angle is a neutral position for the thigh muscles [5], although such an inclination is not feasible for vehicular seating. Other seat characteristics such as seat pan inclination, seat height and lumbar support also contribute to thigh–trunk angle and hence the thigh muscle tension [6]. Harisan et al. [6] proposed a spinal model for seating applications and suggested that an optimal seat design is required to maintain a natural spine shape to achieve comfortable posture (Figure 1-2).



Figure 1-2 The geometric model of the spine while sitting [5].

The seat geometry and contouring of the cushion and the backrest play crucial roles in realizing a stable and comfortable posture. The static and dynamic properties of the resilient materials used in the seat also determine the support abilities and the vibration

transmission to the occupant. A soft foam material may help reduce the transmission of ride vibration of the vehicle, but could contribute to discomfort due to bottoming of the foam and pelvic rotation [5]. On the other hand, too hard a foam material tends to limit undesired pelvic rotation and help maintain neutral spine column, but causes high localized interface pressure and yields only limited vibration isolation [5]. The soft tissues and muscles surrounding the ischial tuberosities tend to deform when sitting, which causes greater contact of the bones with the harder cushion surface leading higher force at the interface. The presence of high localized pressure at the body-seat interface could limit the blood circulation and cause a sensation of discomfort [11].

The seat design is often initiated with selection of polyurethane foam (PUF) for the cushion and the backrest. The seat geometry and foam contouring is subsequently attempted to realize desired sitting postures. Harison et al. [6] have defined a normal pelvis rotation in standing posture in the order of 50 degrees between posterior - inferior to top margin of the acetabulum. Schoberth [12] measured the pelvis deviation as 10 degrees when changing posture from standing to mid-sitting position. The magnitude of pelvic rotation is strongly influenced by the seat geometries such as seat height, backrest angle and seat pan inclination as well as the foam hardness [5]. A few studies have also suggested the use of an adjustable lumbar support to achieve ideal pelvic rotation as shown in Figure 1-3 (a) [1, 5], although the design of an optimal lumbar support is a challenging task considering variation in the drivers' anthropometry.

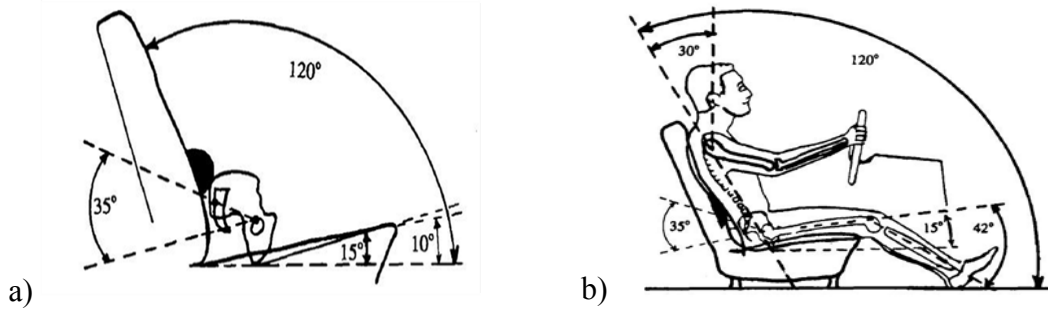


Figure 1-3 (a) The lumbar support to realize an ideal pelvis rotation of 35 degrees, with 10 degrees seat pan inclination, 5 degrees depression into seat, and 120 degrees backrest incline [5]; (b) head flexion under an ideal backrest inclination and knee flexion [9].

The optimum backrest angle and knee flexion have been reported as 120 degrees and less than 45 degrees, respectively. Such a seat design, however, restricts the head flexion around 30 degrees to ensure adequate visual field, as seen in Figure 1-3 (b) [9]. This would cause loading of neck muscles and thus the sensation of discomfort in the cervical region [13]. A lower backrest angle is thus desirable to limit the neck muscles loading. Through measurements of electromyography (EMG) activity of various back muscles, it has been shown that reducing the backrest angle from 120 to 100 degree does not greatly alter the back muscles activities, and yields head flexion in the order of 10 degrees [1, 11].

1.2.2 Evaluation of Comfort

The comfort performances of vehicle seats are evaluated using two approaches involving subjective and objective evaluations. Subjective evaluations address specific product features and sensation of comfort in a relative sense. Subjective methods are more widely used to assess seating comfort, which is known to be highly subjective and dependent upon individuals' physiological and physical well-being, and interactions with the seat. The subjective evaluations, however, pose considerable challenge in interpretations of the data due to extreme variabilities and poor repeatability [14].

Furthermore, subjective methods are not cost effective since they may involve large number of subjects and developments in several prototypes, while the data may not yield sufficient design guidance [14]. Although subjective methods have been employed to obtain relative comfort ranking of the seats, the large inter-subject variability, particularly, under varying vibration stimuli has also been recognized [15]. Subjective evaluations of seats, however, have been effectively used to indentify locations of localized discomfort sensations of different seat designs (Table 1-1). Table 1-1 summarizes the sources of subjectively evaluated discomfort.

Upon recognizing the limitations of subjective comfort evaluation methods, the need to develop reliable methods to measure the seat comfort quantitatively has been widely recognized [14, 19, 28, 38]. Although a number of objective measures have evolved, a generally acceptable approach does not yet exist.

Table 1-1: Reported discomfort in local body segments through subjective evaluations [1, 5, 6].

Region of Discomfort	Probable Cause
Buttock	Inappropriate distribution of body-seat interface pressure, related to either cushion characteristics or seating posture.
Under thighs/Knees	Insufficient cushion support leading to concentrated interface pressure.
Thighs' muscles	Greater thigh-trunk angle, which depends on seating posture and hip to pedal distance.
Lower back	Vibration and inadequate back/lumbar support.
Upper back/Shoulders	Improper backrest adjustment, seating posture or large head flexion.

Moreover, the proposed methods address specific or limited comfort measures and cannot assess the overall seating comfort. For instance, ISO – 7096 [16] has set forth a test method and acceptance criteria of suspension seats in view of their vibration isolation effectiveness, expressed in terms of seat effective amplitude transmissibility (SEAT). The standardized methodology has been widely used to obtain objective measures of vibration-related performance of suspension seats for heavy road and off-road vehicles [18]. A few studies have also attempted to derive objective measures of seating comfort related to the support properties of the seats [19], which are discussed in the following subsections. The objective methods, as in case of the subjective methods, involve a number of human subjects, while the data could be applied to develop analytical models for seeking design guidance in an efficient manner. The studies reporting objective methods may be grouped under static and dynamic comfort.

1.2.3 Static Comfort

‘Static Comfort’ refers to perception of seating comfort by the human occupants in a static environment, and is determined by the support properties and muscular demand imposed on the occupant, apart from the adjustability and the appearance. The static comfort evaluations are considered as reasonably good measures for assessing the support provided by the seat components such as backrest, seat pan, arm rests, seating height, and seat to pedals distances. Apart from these, the static comfort is also strongly influenced by the cushion firmness, as summarized earlier in section 1.2.1 [1, 5]. Hard cushions yield occurrence of concentrated pressure zones under the ischial tuberosities, and could adversely affect blood circulation with greater contact force on the soft tissues of the thighs. Soft cushions, on the other hand, may yield bottoming of the PUF and impose greater stresses on the femur bone [1, 14].

The force-deflection properties of the seats have been most widely investigated in the context of static seat comfort related to cushion stiffness properties [21]. Wolf [20] proposed a sag factor to describe the supportability of the PUF seats, defined as ratio of compression force of a foam sample corresponds to 65% deformation to that corresponds to 25% deformation of the total thickness. The sag factor is measured using a 200mm diameter circular disk indenter, as recommended in SAE 1051 [39]. The features of indenter together with the static force-deflection properties of the seats are further discussed in section 2.3 and 2.4. A sag factor of 2.8 was recommended as an indicator of good static comfort [20, 22].

Static seat comfort is normally associated with two factors: foam hardness and bottoming [21, 50]. Bottoming happens when the foam sample is subjected to a larger load, which is observed by a sharp increase in the gradient of the load–deflection curve.

Bottoming produces a sudden increase in stiffness due to the deformation of the seat structure under the seat cushion, which has been related to poor comfort performance [18]. The subject gradually felt more comfortable in the absence of bottoming effect with harder foams, however, while excessive foam hardness causes higher localized pressure around the ischial tuberosities (IT).

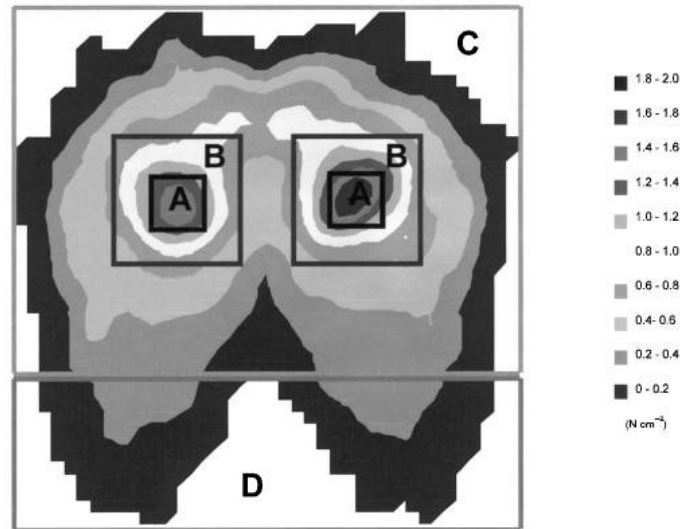


Figure 1-4 Human-seat pressure distribution [18].

A few studies have shown good correlation between the human-seat interface pressure concentration and the static comfort sensation [14, 28]. Ebe [18] established a linear relationship between the pressure around the ischial bones and the static seat comfort. Figure 1-4 demonstrates a typical pressure distribution measures at the human-seat interface, where the foam material was a low damping polyurethane with 50 mm in thickness. The zone A shows the highest contact pressure in the vicinity of the IT-s, followed by zone B covering the soft tissues around the IT bones. A few studies have suggested that greater pressure in zone A is directly related to greater sensation of discomfort by the subjects [14, 18, 28]. The IT bones carry a greater portion of the upper

body weight when sitting on hard seats, which causes greater deformation of the soft tissues surrounding IT and generates sensation of discomfort. The soft foams also exhibit similar trends when seat bottoming occurs [22]. In an attempt to quantify the seat static comfort, Frusti and Hoffman [14] divided the seat pan and the backrest of an automobile seat into nine different regions and measured the interface pressure in each individual region. On the basis of the observed correlations between the subjective evaluations of the static seat comfort and the contact pressure, the study proposed the following design guidance for a comfortable seat:

- The force under buttocks region should be 58% - 64% of total seat pan force.
- Force under thighs and knees should be 21% - 28% of the total seat pan force.
- Back rest force in the lower back area should be in the range of 58% - 65% of the total backrest force.
- Back rest force in the middle back area should be in the range of 25% - 32% of the total backrest force.
- Back rest force in the shoulder and upper area should not exceed 6% of the total backrest force.

The above trends have also been reported for a number of automotive seats in other study [28].

1.2.4 Dynamic Comfort

‘Dynamic comfort’ refers to occupants’ comfort sensation, while being exposed to vehicle vibration, arising from vehicle interactions with road irregularities. The dynamic tire-track interactions are generally transmitted to the seated occupant through the vehicle suspension, chassis and the seat. The dynamic comfort performance of a seat is directly related to static and dynamic characteristics of the seat and the vibration environment of the vehicle. The reported studies have specifically focused on the vibration transmission properties of seats for applications in heavy vehicles [44, 58]. This has been attributed to

various detrimental effects of vibration on the occupant health, comfort and rate of performance [10, 11, 44]. Prolonged exposure to whole-body vehicular vibration has been associated with spine and supporting structures injuries, particularly the low back pain (LBP) [10, 11, 46, 47]. The vast majority of the heavy road and off-road vehicles, wheeled and tracked, exhibit dominant vehicle ride vibration at frequencies up to 10 Hz. This frequency range mostly envelopes the reported resonant frequencies of the spine and the supporting structure (Table 1-2). The exposure to vehicle vibration thus induces resonant stresses in the spine and the supporting structure leading to injuries over prolonged exposure. It is thus vital to design seats that can attenuate vibration in the vicinity of the spinal resonances [11]. A number of low natural frequency suspension seats have thus been developed to protect the driver from potentially injurious vibrations. The dynamic comfort performances of such seats have been investigated analytically as well as experimentally [7, 33, 36]. While the vast majority of the studies have evaluated the dynamic performance of seats through laboratory and field measurements, relatively few studies have attempted development and analyses of linear and nonlinear analytical models of the seats to derive design guidance [33, 36]. These models generally include linear and nonlinear stiffness due to suspension and the cushion, nonlinear suspension damping, and mass-equivalent occupant model, although a few have implemented biodynamic occupant models [36]. The results from the analytical and experimental studies have been widely used to seek design guidance and to assess the dynamic comfort performance of the seats.

Table 1-2: Reported resonant frequencies of the spine.

Authors	Reported Spine Resonant Frequencies
Wilder et al [45]	4.75 Hz, 9.5 Hz, 12.7 Hz
Panjabi et al [47]	4.4 Hz
Christ and Dupuis [24]	4.0 Hz

The dynamic comfort and vibration isolation effectiveness of the seats are generally assessed using frequency-weighting defined in ISO-2631-1 [2]. The standard also provides methods for assessing the vibration exposure of seated occupants, comfort performance, and the potential health risks associated with vibration exposure. The standard requires measurement and analysis of vibration in the 0.5 to 80 Hz range. The vibration isolation effectiveness of the suspension seats are widely reported in terms of SEAT, derived as [42]:

$$SEAT = \frac{\sum_i (W(f_i) a_s(f_i))^2}{\sum_i (W(f_i) a_b(f_i))^2}$$

where $W(f_i)$ is the W_K - frequency weighting corresponds to center frequency f_i of the i^{th} third octave band, and $a_s(f_i)$ and $a_b(f_i)$ are the rms acceleration measured at the seat-occupant interface and the seat base, respectively. A SEAT value below 1.0 indicates attenuation of vibration by the seat. A value above 1.0 implies amplification of vehicle vibration by the seat and thus its poor dynamic comfort performance [42]. Automotive seats generally exhibit SEAT values in the 60% to 80% range [42], while off-road vehicle seats often exhibit SEAT values above 1 [42]. The SEAT values are strongly dependent upon the vertical vibration spectra of the vehicle, which is attributed to nonlinear

behavior of the suspension seat. Figure 1-5 illustrates the influence of vibration spectrum on the SEAT values of two seats, denoted as 'A' and 'B' together with their acceleration transmissibility [17]. As shown in the figure, one stimulus is mostly dominant in the 4-8 Hz range, while the other is dominant between 0 and 4 Hz. Seat A with its resonance frequency around 3 Hz yields superior attenuation of the first spectrum whereas seat B with resonance at 5 Hz amplifies the first spectrum of vibration. However, seat B is superior to seat A, when the dominant frequency occurs in the 0 and 4 Hz range. In the context of dynamic seating comfort, a few studies have investigated dynamic body pressure distribution and its correlation with subjective comfort rating [14, 28]. The frequent movement of the driver on the seat has been associated with sensation of discomfort [29]. A few studies have employed 3D motion cameras to capture the postural shifting tendencies of the occupants [19].

Owing to difficulties associated with mounting of 3D cameras in the vehicle, it was proposed to monitor the movement of the driver's left leg as an indicator of the postural shift. Alternatively, the postural shifting tendencies can be conveniently captured through measurement of pressure distribution at the seat. Since the body-seat interface pressure sensing system is very sensitive to small changes in contact pressure, an adequate definition for "pressure change" in a dynamic environment is essential. It has been suggested that pressure variations exceeding 5% of total pressure for the seat pan and 15% for the back support be considered as a dynamic pressure variation [30]. Such variations are considered indicative of subject's movement arising from discomfort and to prevent numbness or to adapt more comfortable posture. Such variations, however, are often caused by voluntary movements of the occupant that can not be associated with a discomfort sensation. Prolonged sitting in confined space, as in the case of driving, has

also been known as a cause of increased discomfort [31]. This may in-part be attributed to sustained levels of higher pressures at the body-seat interface, particularly around the ITs.

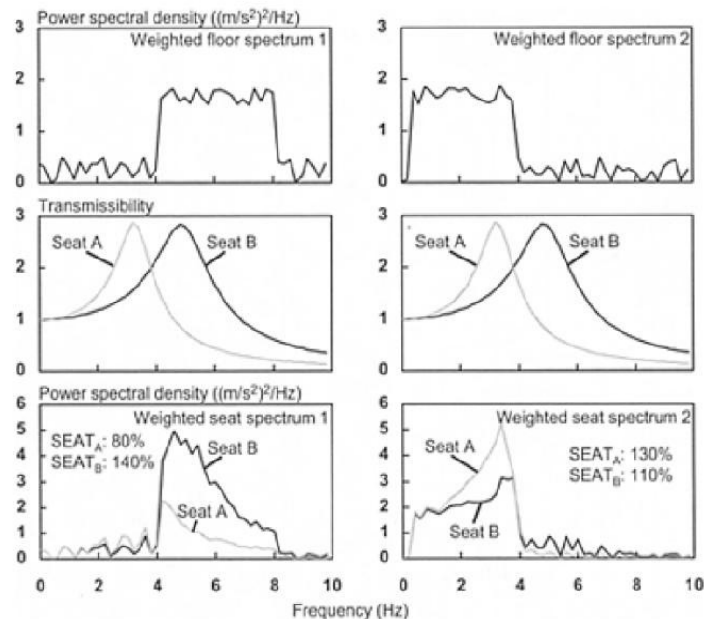


Figure 1-5: Influence of vehicle vibration spectrum on vibration attenuation performance of two suspension seats with different vibration transmissibility [17].

The occupants tend to alter their posture either to reduce or shift the pressure concentrations. A few studies have identified increase in the trunk, hip and torso angles with increasing driving duration [32]. An increase in torso angle tends to decrease in the pressure on the buttock and the tail bone. A strong correlation between the pressure variable and the body movement has been established from a video analysis [29, 30], suggesting strong relationship between the body discomfort sensation and pressure variations.

The variations in contact pressure are also caused by the vehicle vibration and shock. The effects of sinusoidal vibration, magnitude and frequency on the variation and distribution of body-seat contact pressure, ischium pressure, contact area and force

between the seated occupant and a visco-elastic seat has also been investigated [8]. The study revealed that a softer cushion provides greater contact area, and thus more evenly distributed contact pressure and reduced concentration of contact pressure around the ITs. The mean normalized maximum ischium pressure (the ratio of peak ischium pressure to the static ischium pressure), was observed to be largest in the vicinity of the resonance frequency of the occupant-seat system (2.5-3 Hz). The peak normalized pressure, in case of a rigid seat was observed in the vicinity of the vertical mode resonance of the body (4.5-5.0 Hz). These results suggest relatively larger body-seat interface pressure and thus greater discomfort near the resonances of the body and body-seat system.

Ebe et al. [33] investigated the dynamic comfort performance of seats of different static properties under different vibration magnitudes. The study concluded that softer foams are generally perceived as more comfortable, while they exhibit greater sensitivity to change in vibration magnitude. The static characteristics of the seat such as stiffness, contouring and geometry mostly determine the static sitting comfort, while the dynamic properties affect the dynamic comfort in the presence of vibration. The vibration or dynamic comfort of seats are objectively evaluated by considering vibration transmission properties of seats and vibration characteristics of the seated body in accordance of ISO-2631-1 [2]. The standard recommends the use of frequency-weighted root-mean-square (*rms*) acceleration for assessing comfort performance and the vibration dose value (VDV) under relatively higher intensity vibrations with greater crest factors. It has been shown that VDV is better correlated with vibration discomfort [21]. Through experimental assessments of seats with different static and dynamic characteristics, it is concluded that the static and dynamic comfort performances of seats are related to both the static and dynamic properties. In a significant vibration environment, however, the dynamic

properties primarily affect the comfort performance. Heavy road and off-road vehicles employ a suspension at the driver's seat, often referred to as a dynamic seat. A dynamic seat comprises a polyurethane foam (PUF) cushion seat pan and the backrest supported on either a mechanical or pneumatic suspension. In order to provide a controlled posture for subjects with varying anthropometric body sizes, such seats are designed to provide various adjustments such as backrest angle, height, fore-aft distance and in some cases the armrest. The suspension mechanism and characteristics are determined based on the target vehicle and its vibration environment. Such seats are usually tuned to provide isolation of vibration above 2 Hz [42]. Such suspensions, however, provide limited travel to ensure adequate driver reach to the controls. Owing to their low natural frequency (1 to 1.5 Hz) and limited travel, these often incur suspension bottoming or topping under vehicle operations on rough off-road terrains or on urban roads, and thereby transmit high intensity vibration or shocks to the occupants [23, 42]. Exposure to such high intensity vibration or repetitive shock motions has been associated with extreme discomfort and health effects.

Wu and Griffin [35] measured the SEAT (seat effective amplitude transmissibility) value of a suspension mechanism in its full range of operation (from bottom stop to top stop). Under low vibration, the suspension remains nearly locked due to friction and thus the seat serves more like a conventional static seat. With increasing vibrations the suspension acts as a vibration isolator and its transmission properties are strongly related to the suspension frequency and the damping properties. Under intense vibration, the suspension tends to top or bottom leading to shock motions of the occupant. Rakheja et al. [7] further showed that the suspension design involves a difficult compromise between the vibration and shock isolation performances.

1.3 Seat Cushion Materials and Design

The static and dynamic comfort performance of a seat is strongly related to the seat cushion design and material. The seat cushions are primarily designed to provide adequate body support, which determines the comfort sensation or the “show-room comfort” performance of the seat. Furthermore, the density, resilience and visco-elastic properties of the widely-used polyurethane foams (PUF) directly affect the dynamic comfort apart from the static comfort performance. Both the static and dynamic properties of a PUF cushion/material, however, are strongly influenced by the preload (occupant weight), deflection and rate of loading (frequency and magnitude of vibration), in a highly nonlinear manner [37]. While considerable efforts have been made to experimentally characterize different properties of various PUF materials and seat cushions, only minimal efforts have been reported on modeling of seat cushions [36].

The properties of a typical PUF material are best described by its force-deflection or stress-strain curves, as illustrated in Figure 1-6 [34]. Under application of a small load, the foam behaves as an elastic material, while the buckling of the foam cells progresses under increasing loads leading to relatively lower stiffness. Further increase in the load leads to total cell buckling with rapid increase in the stiffness of the foam. The hysteresis of the PUF materials and air flows in the open cell structure also constitute the damping properties of a seat. The hysteresis and thus the damping of a PUF cushion are also strongly dependent upon the preload, magnitude and the rate of deflection [34, 40].

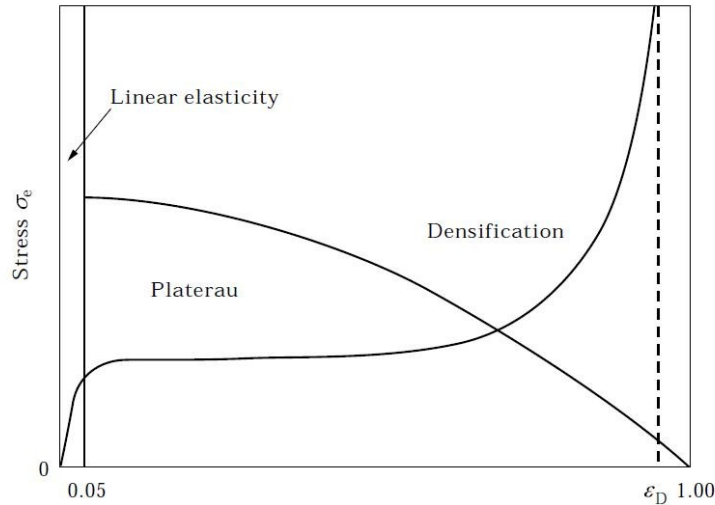


Figure 1-6: Stress-Strain Curve of a typical open cell PUF [34].

A few studies have analyzed the PUF performance in terms of distribution of human-seat interface pressure under static sitting and under vehicular vibrations as stated earlier. These have established that softer PUF provides the occupant with greater comfort sensation since the contact pressure is more evenly distributed over the contact area of the human body with the seat pan as well as the backrest. Soft foams, however, tend to bottom easily and could thus cause considerable discomfort and high vibration transmissibility to the body. Alternatively, relatively harder PUF seats protect the heavier subjects against bottoming and yield enhanced sensation of stability; but cause concentrated pressure zones for the lighter subjects. Blair et al. [41] investigated the effect of chemical structure of PUF on dynamic and static characteristics of the seat cushions and concluded that cushions with moderate hardness and high thickness yield lowest vibration transmissibility at low frequencies and near the resonance frequency. It has been further shown that thick PUF cushions yield lower stiffness and higher deflections [37]. However, the hysteresis loss for a thicker PUF sample was observed to be less than that of the thin foam, which led to higher vibration transmissibility. At

frequencies close to resonance frequency of the human body, close to 5 Hz the thinner foam provided less transmitted vibration, while the thicker foam exhibited greater vibration attenuation at frequencies above 5 Hz.

The current design trends in automotive seating demand relative thin cushions in order to accommodate electric control drives beneath the seat and to realize light weight structure design. The seat cushions are thus designed with a combination of PUF material and an additional elastic material so as to minimize the PUF bottoming. The various reported studies on experimental characterization of seat cushions have invariably concluded that [37]:

- Static and dynamic characteristics of the PUF cushions are highly dependent on the occupant's body weight and magnitude of the vibration.
- Dynamic characteristics of the PUF cushions are in correlation with the foam thickness. In the range of the vehicle's dominant frequencies, different foam thicknesses are required to achieve the best response.
- Static characteristics and pressure distribution of the PUF are also dependent on the foam hardness. Differences in individuals' body weight require different foam hardness.
- Foam seat cushions can not conform to different buttocks shapes and individual body dimensions.
- PUF cushions compress over time and provide less cushioning.

Concepts in inflated air cushions have been proposed to achieve compact and flexible designs so as to accommodate occupants with widely varying body weight [25, 61, 62]. Such seat cushions offer considerable potential advantages for applications in automobiles and heavy road and off-road vehicles. These include the potential to achieve variable stiffness, improved ability to conform to individuals' buttocks shape, possibility of integrating multiple air cells with different inflation pressure and shape over the entire

cushion contact area and possibility of achieving vibration attenuation by interconnecting different air cells.

The air cells, however, yield minimal damping and could thus yield amplification of the vehicle vibration. These seats offer attractive potential to achieve flexible support properties and more even distribution of contact pressure. Figure 1-7 illustrates a seat cushion with many different air cells over the contact area [38].

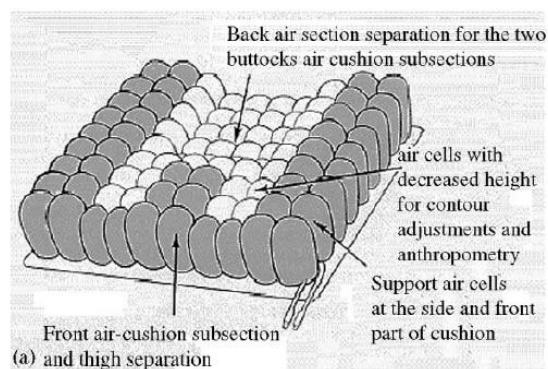


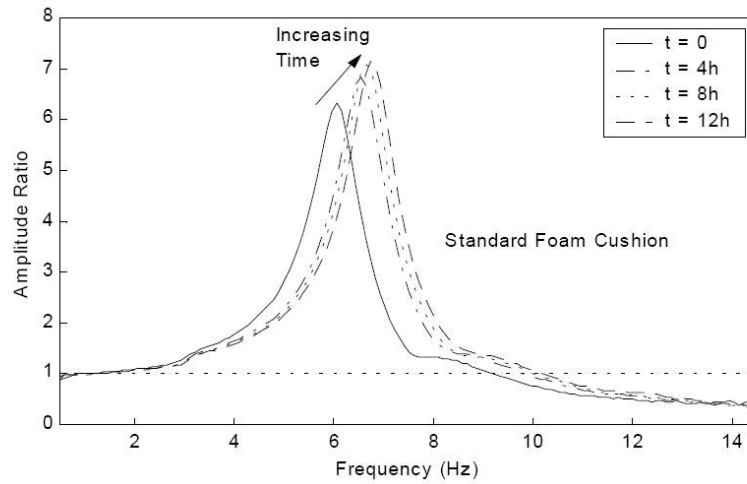
Figure 1-7: Integration of different air cells in an air-inflated seat cushion configuration [38].

Hostens et al. [38] investigated a prototype air cushion seat for agricultural machinery, which employed five different air bags in a custom contoured cushion (CCC) seat. These included: two air bags under the ITs, one under the thighs, and two in the backrest. The air bags within the seat pan consisted of different air cells configured to form desired contours for the individuals. All five air bags were connected individually to a central air reservoir, while the occupant could adjust the inflation pressure individually or through interconnections. Experiment showed that the air cushion subsections could greatly contribute to uniform interface pressure distribution, yield greater subjective evaluation of comfort. Ahmadian et al. [25] conducted a comparative analysis of air-inflated and foam seat cushions for truck seats through measurements of vibration transmission and

pressure distribution. Both cushions displayed almost identical natural frequencies, and nearly identical damping property as determined from the rate of decay of the response to a step input. Consequently both seats revealed comparable acceleration transmissibility characteristics, such as seen in Figure 1-8 [25]. The study also investigated the stiffening effect of the cushion under continuous loading over a 12-hour duration. While both the seats revealed stiffening tendency with time, the stiffening of the air seat was relatively less. The two seats however, revealed considerably different human-seat interface pressure maps (Figure 1-9).

The results showed that the air cushion seat yields larger contact area, more uniform contact pressure, while conforming to the individual buttocks' shape. Boggs et al. [26] investigated the performance of air-inflated cushions for applications in truck seats. In the study, the drivers were permitted to adjust the seat and the pressure over a duration of approximately one week so as to identify comfortable posture and adjustments. The total area of the seat pan was subsequently divided into four zones enveloping the left and right side of the seat pan along the thighs, the ITs, the tailbone region and front of the cushion beneath the left and right knees. The inflation pressure in each area was adjusted by each individual driver, and the static pressure distributions were measured for both foam and air cushion seats before and after the driving experience to eliminate the dynamic effect of driving. Results showed that for both cushions the pressure distributions before driving had similar patterns; however after the driving experience the foam cushion displayed higher concentrated pressure zones under the IT bones.

a)



b)

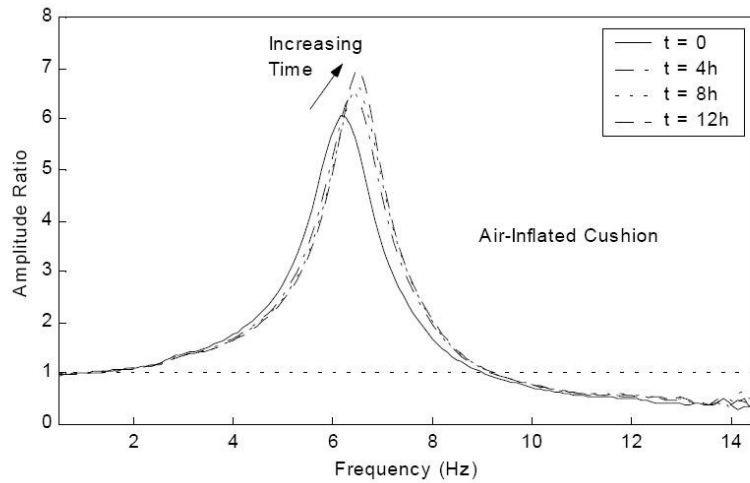


Figure 1-8: Vertical amplitude transmissibility of (a) a standard foam cushion and (b) air cushion [25].

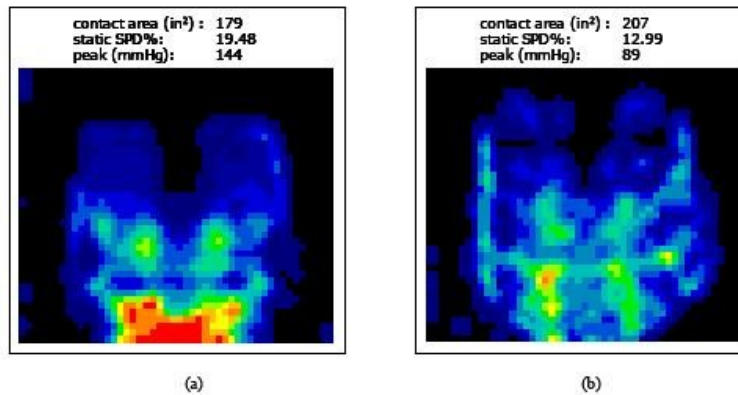


Figure 1-9: Pressure distribution at the human-seat interface: (a) foam; and (b) air cushion [25].

1.4 Scope and Objectives of the Thesis

From the review of relevant reported studies, it is evident that the sensation of comfort in an automotive seat is a complex function of seat dimensions, sitting posture, seat pan and backrest mechanical properties, contact pressure and its distribution, driving environment, and the vehicle characteristics apart from the subject anthropometry. The comfort performance of automotive seats have been mostly evaluated via subjective means. These have also attempted to identify the sources of discomfort and pain in a vehicle seat. Such an approach could yield important design guidance for the seats but would require repeated measurements with a large number of subjects, and prototype seats. More recent studies have attempted to develop objective methods to assess the seating comfort. Body pressure distribution (BPD) at the human-seat interface has been considered as an important and effective objective measures to assess comfort. However the correlation between the interface pressure magnitudes, their ranges and the location of their occurrence with comfort ratings has not yet been established. A seat designed with a number of independent or interconnected airbags could yield more desirable inter force pressure to promote sitting comfort. Furthermore, such a design would offer extreme flexibility for the occupant to adjust to desirable contact pressure. In addition, the reported studies on BPD have been limited to static seating, while the comfort assessments without considering the dynamic nature of driving have not been attempted. Dynamic seats have demonstrated effective attenuation of vibration, when the suspension mechanism is properly tuned in accordance with the vibration environment. Besides, the static and the dynamic properties of a suspension seat play an important role in determining the vibration and sitting comfort. Cushion material, being the main interface between the seat frame and the human body, can greatly affect the overall comfort

sensation. The static properties of a seat cushion have been invariably characterized using a 200 mm diameter indenter in accordance with SAE J1013. The results obtained from such an indenter can not be considered reliable since the contact pressure distribution differs substantially from the human-seat interface pressure. The design and assessments of alternate indenters that can reproduce the body-seat interface pressure distribution are thus highly desirable.

The overall objectives of this thesis are formulated to analyze methods for characterization of static properties of seats and comfort performance in an objective manner. The study is conducted with an air cushion comprising a number of independently inflatable airbags to achieve varying interface pressure distributions. The specific objectives of the study include:

- a) Design and fabricate a human buttocks-shaped indenter for characterization of mechanical properties of the PUF and the air cushion seats on the basis of measured human-seat interface pressure data.
- b) Measure the stiffness and damping characteristics of the PUF and the air cushion seats using the buttock-shaped indenter and compare with the data obtained with standardized SAE indenter.
- c) Perform subject comfort assessments of the air cushion seat using different inflation pressure combinations, and acquire human-seat interface pressure data. Attempt correlations between the subjective assessments and objective pressure data.
- d) Evaluate vibration isolation performance of the prototype air cushion seat with and without a mechanical suspension.

1.5 Organization of the Thesis

This thesis is organized in five chapters describing the systematic realization of the above-stated objectives. The highlights of the relevant reported studies are presented in Chapter 1 together with the scopes and objectives of the present study. The design of a prototype suspension seat with multiple inflatable air bladders within the cushion and the

backrest is described in Chapter 2 together with the design of buttock-shaped indenter for characterizing the static and dynamic properties of the cushion. The resulting mechanical properties of the cushion are compared with those identified from the standardized SAE indenter. In chapter 3, an experimental design is presented for evaluating the seating comfort through subjective assessments and via measurements of human-seat interface pressure. The correlation between the subjective results and the pressure distribution is also investigated. Chapter 4 presents the dynamic analysis of the suspension seat mechanism with the inflatable air cushion. The vibration transmission properties of the air cushion seat with and without the suspension are investigated. The mechanical properties of the seat suspension are measured and various natural frequencies of the seat and its structure are identified. Major conclusions, guidelines and recommendations for possible future studies regarding comfort evaluations of seat via pressure measurement and the effectiveness of the air cushion application are presented in chapter 5.

2. EXPERIMENTAL CHARACTERIZATION OF AN AIR SEAT CUSHION

2.1 Introduction

Mechanical properties of seat cushions highly contribute to the comfort performance of seats. The cushion stiffness determines the effectiveness of the cushion to distribute the interface pressure, and provides support in both dynamic and static environments [5]. Seat cushions, as a medium between seat structure and the human body, also play crucial role in attenuation of vibration, which is frequently measured by hysteresis loss [5]. The force-deflection characteristics of polyurethane foam cushions (PUF) used in automotive seat industry have been reported to be highly non-linear [34]. The stiffness and hysteresis loss, and thus the support and vibration attenuation characteristics may depend on the individuals' body weight, seating posture and seat-buttocks contact area. In light of this, the analysis of cushion mechanical properties is yet another objective measure to compare automotive seats.

In this chapter, experimental methods for characterizing stiffness and damping properties of a seat cushion with various inflatable air bladders are explored. A buttock-shaped indenter is realized for measurement of cushion properties that could yield contact pressure distribution comparable to that encountered with a human subject. The validity of the indenter is illustrated through measurements of force and pressure distribution over the cushion loaded with the indenter and a human subject. The static and dynamic force-deflection properties of the seat are subsequently measured to estimate dynamic stiffness and equivalent damping constants in the 1 – 5 Hz range for three different inflation pressures, 0, 3.44 kPa and 6.88 kPa (0, 0.5 and 1.0 psi), of the seat cushion air bladders.

2.2 Prototype Seat Description

The seat used in this study was a prototype bus/truck suspension seat with a wide seat pan and backrest to accommodate a wider range of occupants. Both the seat pan and the backrest were designed with side wings to offer greater lateral support. The seat pan consisted of a cover, 5-cm thick PUF and four air bladders located under the foam. The thickness of the foam was greater at the side cushion wings compared to the mid-section. The bladders were individually connected to an air compressor and controlled by the driver via pneumatic valves provided at the side of the seat for easy access. Each square-shaped bladder was 18 cm wide and was capable of withstanding an inflation pressure up to 34.47 kPa (5 psi). Two of the bladders were located under the buttocks and other two bladders were positioned under the thighs. The total fore and aft travel of the seat pan was 7 cm, while the vertical travel was 11 cm. In order to eliminate an asymmetric pressure distribution at the human-seat interface, the two bladders under each region were pneumatically connected to each other. The backrest also consisted of a cover with 2-cm thick foam and five air bladders. One bladder was located in the lumbar area, and the other four covered the mid-back, upper back, left and right cushion wings, respectively. The configuration of the air bladders is illustrated in Figure 2-1. The suspension mechanism of the seat employed 2 dampers and an air spring. The total suspension travel of the seat was 11 cm, while the seat height could be adjusted by the air spring via a pneumatic valve. Figure 2-2 displays the prototype seat used in this study.

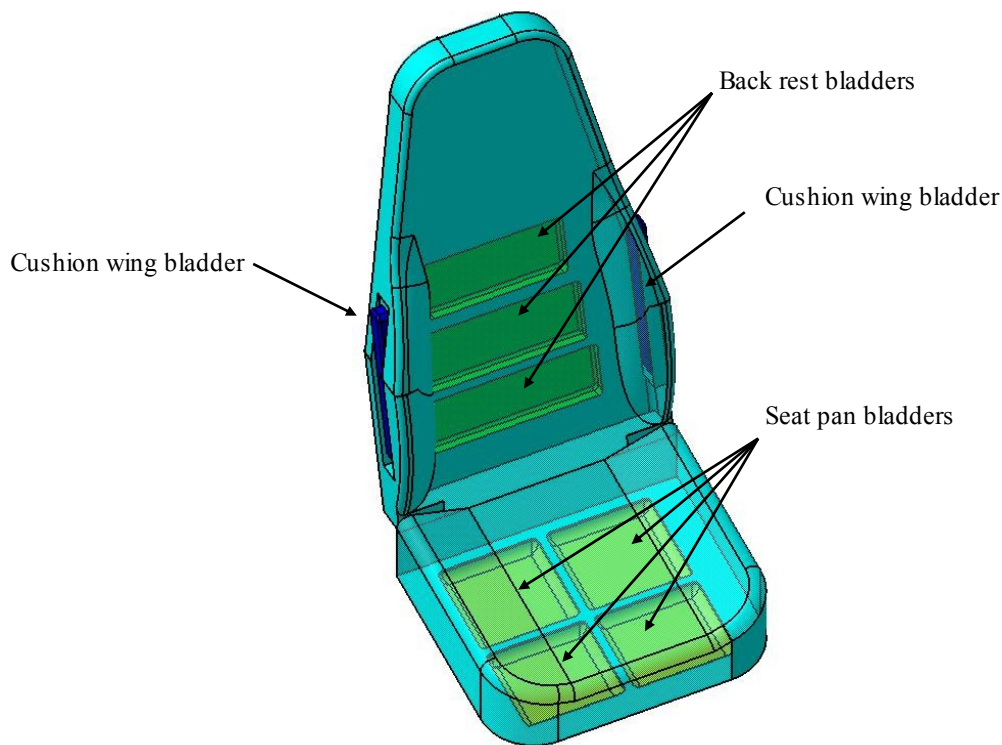


Figure 2-1: Schematic illustration of bladders within the cushion and the backrest.

2.3 Cushion Characterization Methodology

The characterization of the test cushion was initially performed in accordance with the standardized procedure recommended in SAE J1051 [39]. This standard provides a method to obtain force-deflection data of finished (or unfinished, when specified) cushion components of seats for off-road work machines. The standard, however, does not provide any acceptance criterion. The test apparatus comprises the following:

- a) A 200 mm diameter, rigid, flat, or curved indenter, as shown in Figure 2-3. The indenter force shall be applied through a rigid or a swivel joint capable of accommodating the angle of the top surface of the test seat cushion.



Figure 2-2: Prototype suspension seat.

- b) A platform capable of positioning the top surface of the test seat parallel to and centered with the jointed indenter and not to restrict the normal breathing or deformation of the test seat.
- c) An apparatus capable of applying the desired force and measuring the deflection of the indenter into the test seat cushion.

The standard test procedure requires that the test specimen be conditioned, un-deflected and un-distorted at $22^{\circ}\text{C} \pm 2^{\circ}\text{C}$ and relative humidity of $50\% \pm 2\%$ for at least 12 hours prior to testing. The test shall be performed at least 96 hours after the manufacture of the raw materials used in the test seat (foam and elastic components other than the metal components, etc.). The test procedure involves following systematic tasks [39]:

1. Mount the specimen with the top surface parallel to and centered with the indenter. The 200 mm diameter indenter shall be used for both the seat-pan and backrest cushion. In case of components with unusual shape and contours, a minimum 80% of the indenter area must be in contact.

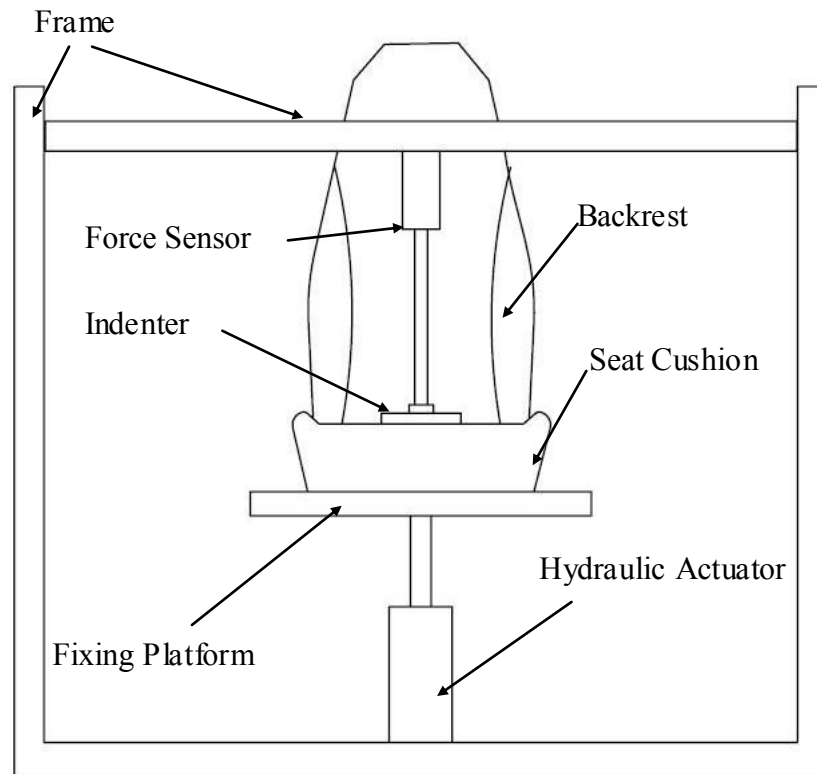


Figure 2-3: Experimental setup for measurements of force-deflection characteristics of seat cushions in accordance with SAE J1051 [39].

2. Pre-flex the test seat 3 times by compressing and releasing the force at a rate of 100mm/min. The specimen shall be compressed as follows.
 - Seat-pan cushion: 1334 N
 - Backrest cushion: 664 N
 - All other components shall be compressed to 20 % of the original thickness
 - Allow 10 ± 5 minutes relaxation for the specimen to stabilize after pre-flexing before continuing with the test.
3. Apply a 45 N pre-load to the 200 mm diameter indenter on to the base where the deflection will be measured and set the deflection to zero.
4. For the 200 mm indenter, apply an incremental load slowly, no greater than 220 N to minimize shock. Allow the test seat to stabilize for 1 minute then measure the deflection. Continue this incremental procedure without removing the preceding force until the maximum load of 1334 N for the seat cushion and 664 N for the backrest cushion is reached. When incremental deflection is used, the specimen shall be compressed to not less than 20% of its original thickness.

5. After reaching the maximum force, reduce the force slowly (minimize shock) in 222 N maximum intervals, allowing 1 minute for the test specimen to stabilize before measuring deflection at each increment.
6. Return time: Deflect the cushion to $25\% \pm 2.5\%$ of un-deflected cushion and hold for 1 min. Release the load for 0.5 s or less and record the time taken to return to the un-deflected condition.

Since the operating environment and the conditions for the off-road vehicles greatly differ from those of a city bus and other heavy road vehicles, the maximum loads applied to the seat cushion in the force-deflection test were modified. The application of the 1334 N load, as described in SAE J1051 standard, would cause excessive deflection in the cushion and the seat structure. Also the implementation of air bladders inside the seat pan required further attention in adjusting the maximum applied load on the seat pan. The air bladders could only withstand a maximum inflation pressure of 34.47 kPa (5 psi). Considering that a typical vehicle seat cushion accommodates 70 – 75% of the total body weight of the driver [8], the maximum allowable load was limited to 1200 N with increments of 45 N.

2.3.1 Experimental Setup and Acquisition of Force-Deflection Characteristics

Figure 2-3 illustrates a schematic of the setup used to measure the both static and dynamic mechanical properties of the cushion. The setup consists of a 4500 N Sensotek load cell, a linear velocity transducer (LVT) and a built-in Schaevitz LVDT. The measured force and deflection data were acquired using the dSPACE hardware and software. The data were acquired at a rate of 360 Hz and analyzed to derive the force-deflection and force-velocity properties of the seat cushion. Figure 2-4 displays a schematic chart of the data acquisition and analysis of the static and dynamic cushion characteristics.

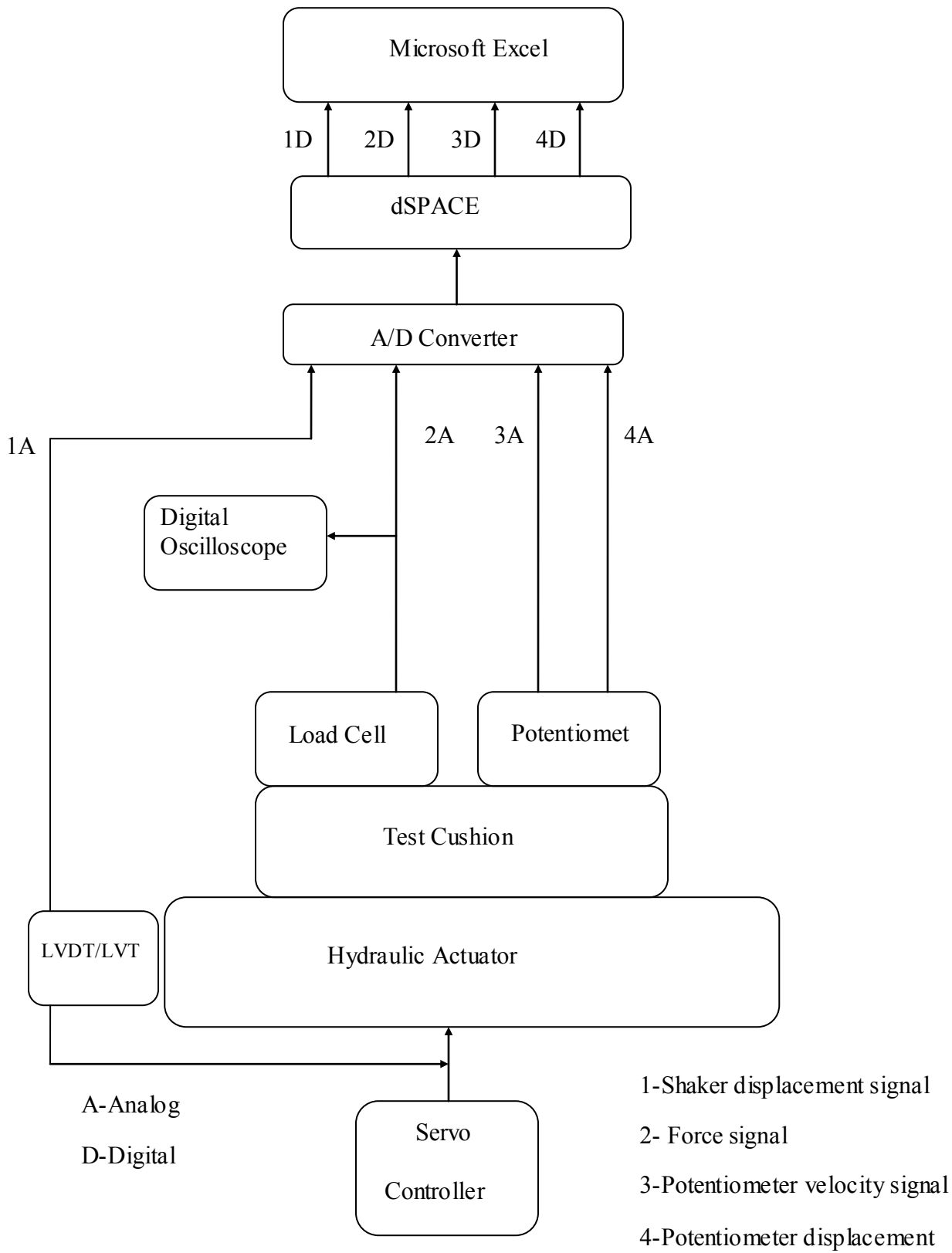


Figure 2-4: Schematic of the data acquisition and analysis system.

2.4 Indenter Design

The comfort evaluation of automotive seats, when measured in a short-term, is relatively easy when performed subjectively. The subjective evaluation is fundamentally a survey of potential users as they compare the relative “feel” of different seat features [54]. The subjective evaluations, however, require large population of subjects of different height, body weight, age and race. This method thus mandates the manufacturers to fabricate and install many prototype seats with various modifications. The process becomes even more complex because the subjective evaluations tend to be influenced by many other factors such as health, age and environment, which are not directly related to the seat features [55]. The subjective evaluations, therefore, generally yield excessive variabilities [55] and pose considerable challenges in view of interpretations.

Limitations of the subjective comfort assessment method have generated the necessity to seek objective measures to predict seat comfort. In order to achieve objective measures for evaluation, the study must contain subjective evaluations to be correlated with essential objective factors, if any. Some of these recommended methods are measurement of interface pressure and vibration transmissibility. In the context of pressure measurement at the human-seat interface, the cushion mechanical properties play an important role.

It has been reported that use of human subjects does not provide repeatable results, even with the same subject, equipment and the environment [56]. Undetectable shifts in posture are reported as the main cause of variations in pressure distribution measurements. A few standardized procedures have been developed to measure the cushion stiffness in a consistent manner [39], which invariably employ rigid indenters for

loading of the cushion. However these indenters are not compatible with real human buttocks shape and contact surface. For instance, the 20 cm diameter indenter recommended in SAE J1051 can simulate loading only in the vicinity of the tuberosities, although the magnitude of contact pressure would be far greater than that expected in the human-seat interface. The indenter design, defined in the Japanese standard [52] on the other hand, tends to distribute the interface pressure that is somewhat comparable to that of real human subject on the seat cushion. It is thus desirable to design indenters that can simulate the pressure distribution in a reasonable and repeatable manner.

In this study, a human buttocks-shaped indenter is designed for characterization of visco-elastic properties of the seat cushions. The design is based on measured human-seat interface pressure. A preliminary indenter shape was initially conceived on the basis of design recommended in ISO 16840-2 [57], which is a modified version of the shape proposed by Staarink [60]. Figure 2-5 displays the overall shape and dimensions of the indenter. The indenter was made of high density poly-ethylene (PE).

2.4.1 Analysis of the Pressure Distribution

The indenter-cushion pressure distribution was estimated through development and analysis of a finite-element model of the indenter and the PUF. The analysis, however, considered the seat cushion as an elastic material as opposed to the open-cell PUF element. The resulting pressure map could thus be considered as a qualification parameter of the pressure profile of the indenter. The elastic properties of the cushion material in the study were taken from the measured force-deflection data for a typical seat. The finite-element analysis (FEA) was performed considering different loads and the results were used to identify resulting pressure distributions.

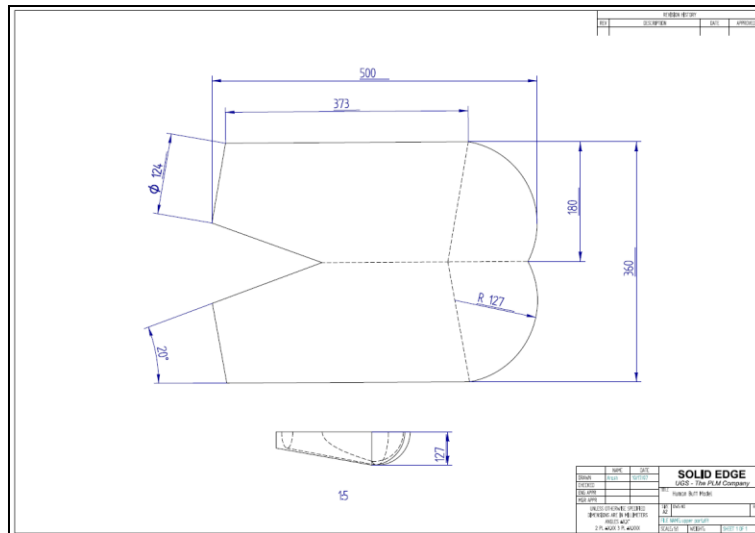


Figure 2-5: A schematic of the modified Staarink indenter [57] (values are in mm).

As an example, Figure 2-6 illustrates the FE model of the indenter-cushion system, cushion deflection and the pressure distribution under a cushion deformation of 40 mm. The deformation of the cushion loaded by the indenter is shown in Figure 2-6 (a), while the resulting pressure distribution at the cushion and the initial cushion deformation with indenter held horizontal are illustrated in Figure 2-6 (b) and Figure 2-6 (c), respectively. Figure 2-6 (d) illustrates the deformation profile with indenter being in full contact with the cushion surface. The thighs region under the indenter is in full contact with the cushion. The resulting pressure distribution is shown in Figure 2-6 (b). Orange zone in Figure 2-6 (b) represents the highest contact pressure, which would be expected to occur under the ischial tuberosities (IT) in case of a human subject. During the analysis, the contact area between the indenter and the cushion was derived under gradually loading, starting from the buttocks and ending with the full contact. As demonstrated, two orange circles represent the highest deformation in the cushion in the IT regions. Figure 2-6 (e) and (f) also illustrate the typical pressure distribution measured in this study with a human subject seated on an automotive seat cushion. The figures illustrate the measured

pressure profiles in 3D and 2D, respectively. Considering that the FE model was developed taking into account only elastic properties of the cushion, the results are considered adequate to assess the performance potential of the indenter only in a qualitative sense. The comparison of the measured and estimated pressure profiles suggest reasonably good similarity in the pressure distribution in the buttock region.

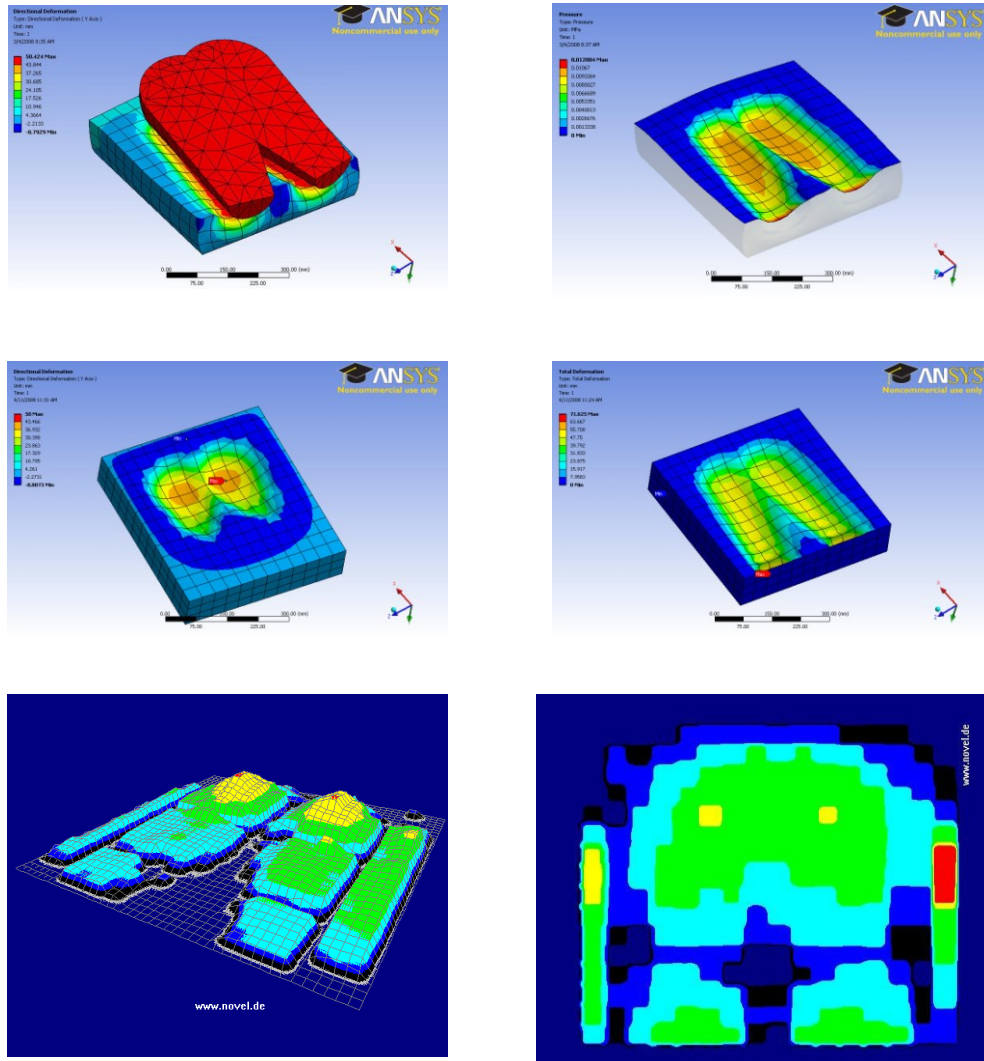


Figure 2-6: Finite element analysis of the cushion-indenter system: a) Cushion-indenter system b) Pressure distribution on the cushion c) Cushion deformation, the upper surface of the indenter is kept horizontal d) Cushion deformation; the lower surface of the indenter is in full contact with the cushion surface e) 3D picture of real subject interface pressure distribution f) 2D picture of human subject interface pressure distribution.

Following the preliminary finite element analysis of the pressure distribution, a buttock-shaped indenter was subsequently fabricated through CNC machining. Considering the largest portion of the upper body weight of a seated subject is transferred to the seat via the IT region, the point of application of the load was selected on the symmetry line above and between the IT bones. Figure 2-7 pictorially shows the indenter and the fixation used to attach the indenter to a load cell for measurement of the imported force.

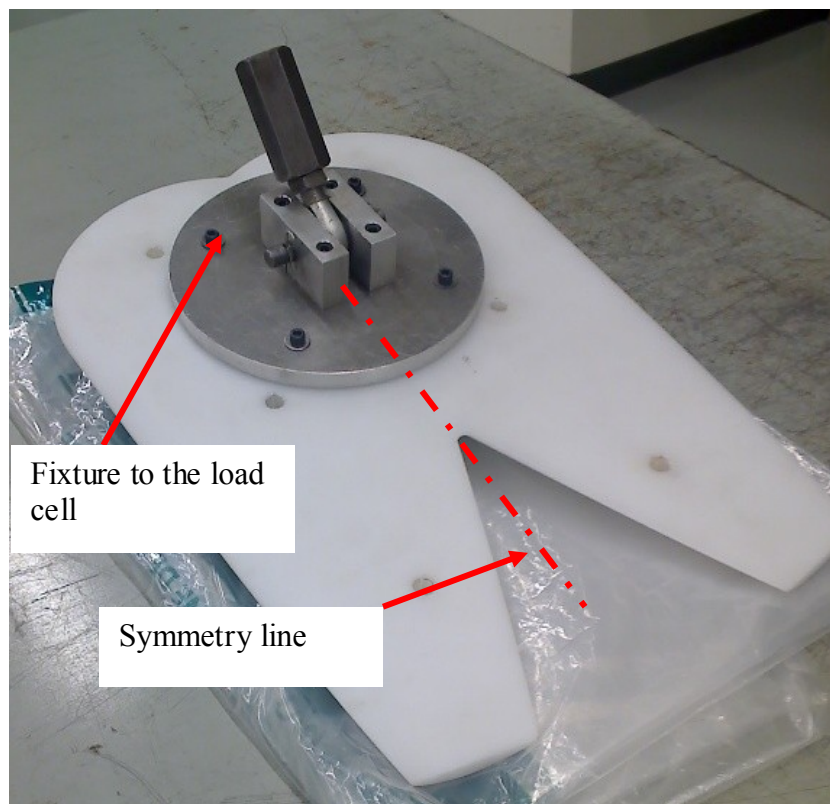


Figure 2-7: Buttock-Shaped indenter

2.4.2 Verification of the Indenter Design

The indenter design, realized in this study, was verified in view of its pressure distribution under static loads. For this purpose, an experiment was designed to measure the indenter pressure distribution while loading the prototype seat. The indenter pressure distribution was acquired using *EMED* measurement system manufactured by *Novel Electronics*. The pressure measurement technology consists of a flexible capacitive type sensor matrix, a portable data conditioning and data acquisition, *PLIANCE* system. The pressure mat consists of 16x16 sensor matrix molded in a 2 mm elastomeric mat. The total sensitive area of the mat is 1536.64 cm², covered by 256 sensors, each 2.45 × 2.45 cm. A threshold pressure value of 0.25 N/cm² was selected for the seat pan measurements. Figure 2-8 shows a schematic illustration of the pressure mat. The seat with the pressure mat and the indenter was placed on a platform. Each measurement was taken twice at a rate of 20 Hz for 10 seconds to verify good repeatability of the data.

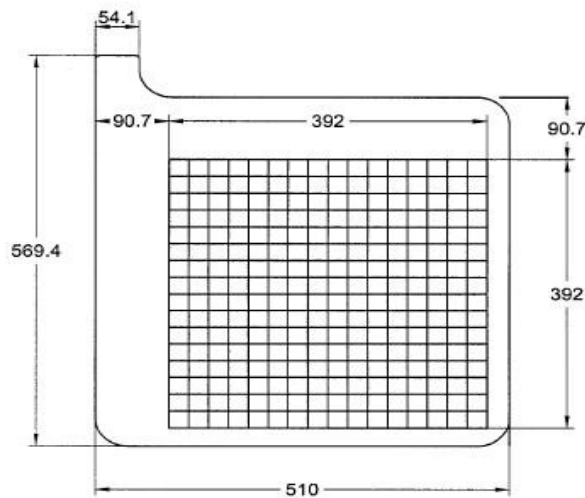


Figure 2-8: Schematic illustration of the novel Electronics pressure mat (units are in mm)

During each experiment, the peak pressure (PP), mean pressure (MP), contact area (A) and total contact force (F) were measured apart from the pressure distribution. For this purpose, the cushion area was divided into 9 different regions. These included the region in the vicinity of right and left tuberosities, thighs, knees, and the left and right wings of the cushion, as shown in Figure 2-9. The pressure, force and contact area data were acquired and analyzed for each region. Figure 2-9 also shows the number of sensors enveloped by each region.

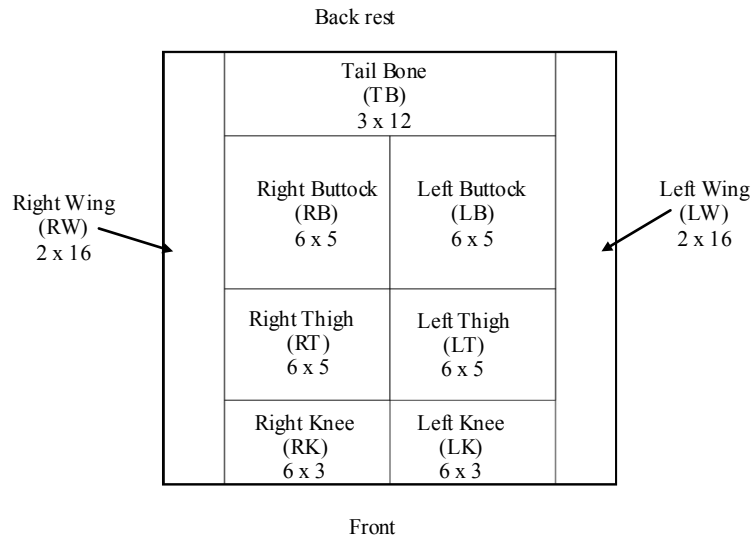


Figure 2-9: Schematic presentation of pressure division regions on the cushion (digits indicate number of sensors occupied).

To simulate the subject's upper body weight transferred to the seat cushion, a few lead shot bags were used to load the indenter. The subject participating in this experiment weighted 65 kg. However, some portion of the total body weight is transferred to the floor through the feet. Hence the subject's load measured on the cushion was only 49.2 kg. The cushion inflation pressure was adjusted to 10.34 kPa (1.5 psi) and 5.17 kPa (0.75 psi) for the buttocks and the thighs region, respectively. Figure 2-10 illustrates the pressure distribution measured with the loaded indenter and the subject seated on the cushion.

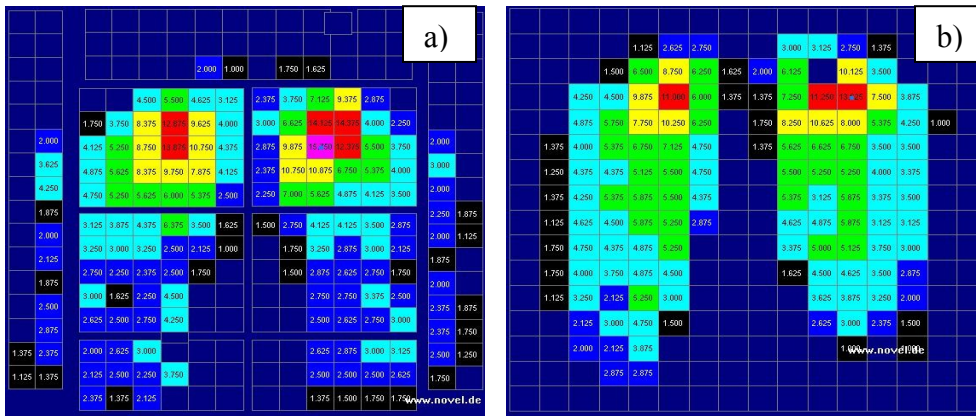


Figure 2-10: Comparison of pressure distribution: a) Subject b) Indenter.

The results were compared in terms of force over the regions, peak pressure, mean pressure and contact area, as shown in Figure 2-11. It was intended to select the subject so that the body weight carried on the cushion as well as the buttocks shape and the contact area are close to that of the indenter, although the differences could not be avoided. The comparison revealed:

- In both cases the percentage of the body weight which was transferred onto the seat pan indicated nearly 75% of the total body weight.
- Indenter was not able to simulate the pressure distribution over the cushion wings areas or under the thighs. This is attributed to relatively narrow width of the indenter, conical geometry of the thighs and the fact that in real human body, some of the soft tissues displace from under the buttocks to the sides when seated.
- In all measurements except the PP, the indenter shows more symmetry than the subject in the left and right side values. Since the PP is the instantaneous measure of the maximum pressure recorded by the pressure mat, it is not an effective measure for comparison.
- In the force distribution graph, both the indenter and the subject exhibit comparable values in the IT region. However in the thighs region, the indenter shows lower values compared to the subject. This is explained by the fact that human body distributes some of the load to the side wings and under the thighs. This is also observed in the PP, MP and contact area graphs.
- The indenter seems to be capable of simulating the pressure and force distribution symmetrically in the ITs and thighs regions. The presence of soft tissue and deformation in case of the subjects results in more distribution of load to side wings and under the thighs.

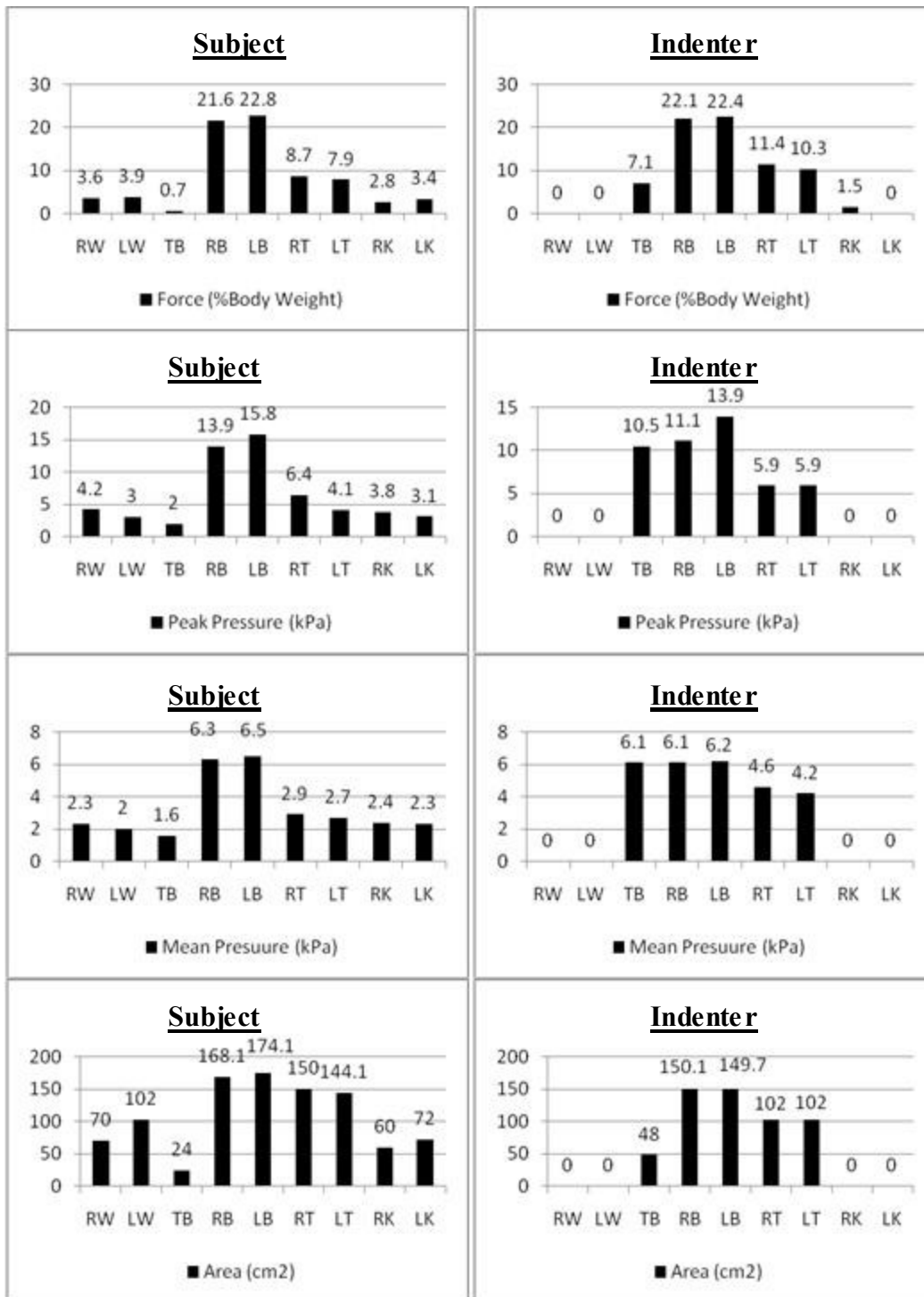


Figure 2-11: Comparisons of the contact force, peak pressure (PP), mean pressure (MP) and contact area (A) measured at the seat interface for human subject and the buttock-shaped indenter.

2.5 Static Force-Deflection Characteristics of the Seat Cushion

The static force-deflection characteristics of the seat pan were measured following SAE J1051 procedure. For this purpose, the seat cushion was installed in the test platform, shown in Figure 2-3, where the buttock-shaped indenter replaced the 20 cm diameter standardized indenter, shown in Figure 2-7. Since the PUF used in the seat pan is relatively soft, a preload greater than 720 N resulted in total bottoming of the cushion with zero inflation pressure. The force-deflection properties of the seat cushion were characterized using three different inflation pressures of the air bladders: 0 kPa (0 psi), 3.44 kPa (0.5 psi) and 6.88 kPa (1.0 psi). The cushion was preloaded prior to the test, while the preload varied with the inflation pressure. Therefore, for each configurations of the inflation pressure, the preload was selected such that the bottoming of the cushion did not occur.

Furthermore, the bladders' pressure varied with the preload. In order to maintain the desired pressure under a selected preload, the cushion was first deformed to each preload value then inflated to the required pressure. The indenter load was subsequently increased gradually and the resulting force-deflection data were recorded. Figure 2-12 shows the static force-deflection characteristics of the seat pan corresponding to selected inflation pressure. The measurements were subsequently repeated using the SAE J1051 indenter. The results are also presented in Figure 2-12. The results clearly show that the SAE indenter underestimates the cushion static stiffness in all cases. It can be attributed to the relative small contact area of the SAE indenter compared to that of the buttock-shaped indenter, which in turn leads to greater deflection of the cushion in the vicinity of the indenter.

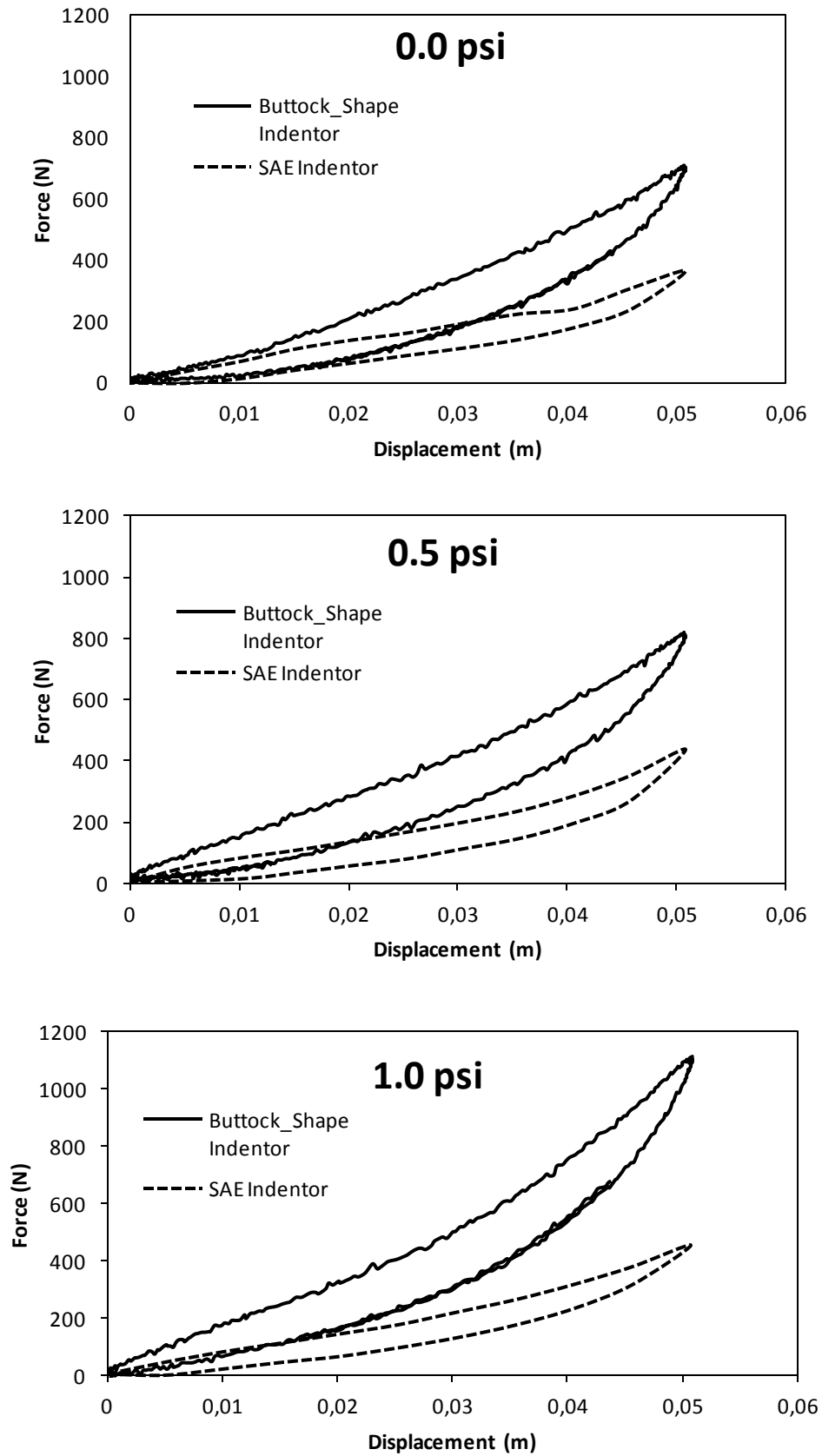


Figure 2-12: Comparisons of static force-deflection characteristics of the seat pan with three different bladder pressures measured using the buttock-shaped and SAE indentors.

Measured data reveals that the cushion stiffness increases with increase in the air bladder pressure, as it would be expected. The results also exhibit considerable hysteresis attributable to the PUF covering of the cushion. The maximum hysteresis measured by the SAE indenter in all three cases is approximately 160 N. The static force-deflection characteristics of the seat clearly show non linear visco-elastic property of the seat cushion with the preload. The equivalent linear stiffness of cushion could be estimated corresponding to a specific preload and inflation pressure.

2.6 Dynamic Force-Deflection Characteristics of the Seat Cushion

The dynamic comfort and vibration attenuation properties of a seat cushion are related to its dynamic force-deflection characteristics, which in case of PUF cushion differ from the static force-deflection properties [40]. With regards to dynamic comfort of a seat, the cushion stiffness is highly dependent on preload, amplitude and frequency of excitation. The dynamic stiffness constant is derived from the mean force deflection data in the vicinity of the selected preload value, while the indenter load is applied at a selected frequency.

In a vehicular environment, the inflation pressure is adjusted once the subject is seated. The dynamic tests were designed in a similar manner. A chosen preload was initially applied and the desired pressure was subsequently adjusted prior to the dynamic loading. In case of no inflation pressure (0 psi), the cushion was compressed to the mid thickness prior to the dynamic test. Since the dominant frequency of heavy road and off-road vehicles is in the range of 1.5 to 2.5 Hz for sprung mass and the natural frequency of the human body varies in the 4 to 5 Hz range [27], the dynamic characterization of the cushion were undertaken in the 1-5 Hz frequency range. For each inflation pressure, the

dynamic load was applied by imposing sinusoidal deflection of the indenter at different frequencies in the 1-5 Hz range. The measurements were also performed under different magnitudes of deflections, varying from 4.5 mm to 6.25 mm peak. As an example, Figure 2-13 illustrates the force-deflection characteristics of the cushion inflated at 6.88 kPa (1 psi) and subject to 6.25 mm deflection at 1 and 2 Hz, and 4.5 mm deflection at 4 Hz.

The results demonstrate that the hysteresis magnitude increases with increase in excitation frequency and the amplitude. The dynamic stiffness of the cushion was subsequently estimated in the vicinity of selected preloads. Table 2-1 summarizes the cushion dynamic stiffness measured at different frequencies in the 1-5 Hz range where the whole-body vibration tend to be predominated in most road and off-road vehicles. The results are presented for a preload of 280 N. The table also lists the static stiffness of the cushion corresponding to the selected inflation pressure. The results clearly show that the dynamic stiffness at low excitation frequencies tends to be lower than the static stiffness. The dynamic stiffness, however, exceeds the static stiffness at higher frequencies. Such a trend is also evident from the few studies reporting dynamic stiffness [8] and is attributed to reduced relaxation time of PUF at higher frequencies.

Table 2-1: Comparison of measured dynamic and static cushion stiffness values.

Cushion Inflation Pressure kPa (psi)	Static Stiffness (N/m)	Dynamic Stiffness (N/m)				
		Frequency (Hz)				
		1	2	3	4	5
0 (0)	19357	16994	17600	17903	17355	19749
3.44 (0.5)	20794	19153	20369	20707	20562	22811
6.88 (1)	30120	20584	22372	23072	23566	26764

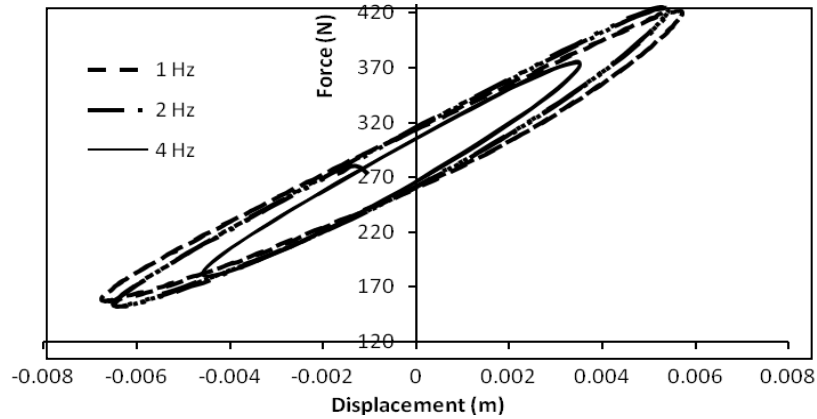


Figure 2-13: Dynamic force-deflection characteristics of the cushion measured under deflections at 1, 2 and 4 Hz (inflation pressure = 1 psi, preload of 290 N).

The dynamic stiffness tends to increase significantly at 5 Hz, as it is seen in Figure 2-14, irrespective of the inflation pressure. The results also suggest that variations in the dynamic stiffness of the seat cushion are relatively small under vibrations up to 4 Hz. The rapid increase in stiffness at 5 Hz excitation is most likely caused by collapse of PUF cells and air bladders, and reduced relaxation time.

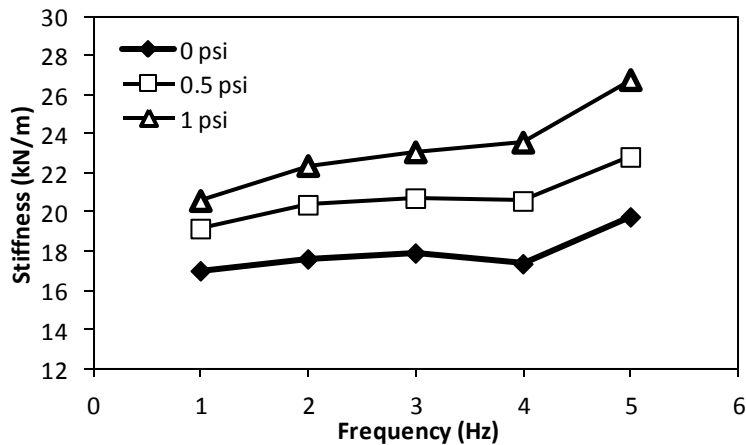


Figure 2-14: Variations in the dynamic seat stiffness at a preload of 280 N as a function of the excitation frequency and inflation pressure.

2.6.1 Dynamic Damping Characteristics

The measured dynamic force deflection data are also applied to estimate equivalent viscous damping of the PUF cushion. The viscous damping constant is estimated from the energy dissipated by the cushion over a cycle of oscillation. The energy dissipated per cycle is estimated from the force deflection data, such that [40]:

$$\Delta E = \oint F_{DC} dx \quad (2.1)$$

Where F_{DC} is the dissipative force and ΔE is the energy dissipated per cycle. The common approach to calculate the cushion equivalent damping is to equate the dissipated energy to that of a viscous damper [40]:

$$\Delta E = \pi \omega C_c(\omega, X) X^2 \quad (2.2)$$

Where C_c is the equivalent viscous damping coefficient, ω is the circular frequency and X is the peak displacement amplitude. By equating equations (2.1) and (2.2), the equivalent viscous damping is calculated in the vicinity of the excitation frequency and amplitude, also denoted as the local equivalent damping constant [40]:

$$C_c(\omega, X) = \frac{\Delta E}{\pi \omega X^2} \quad (2.3)$$

The damping behavior of cushions is mainly related to air flow through the cellular configuration of PUF foam for soft foams, and due to hysteresis for the hard foams.

Figure 2-15 illustrates variations in the local equivalent damping coefficient estimated for the prototype seat cushion. In the 1 to 5 Hz frequency range, while the magnitude of deflection was limited to 0.006 m, it is clearly seen in the figure that the damping coefficients decrease significantly with the excitation frequency. Lower frequencies are accompanied by higher damping coefficient which can be attributed to more airflow through the cellular foam configuration. Such trends have also been reported in a few studies on the PUF seat cushion [25, 61].

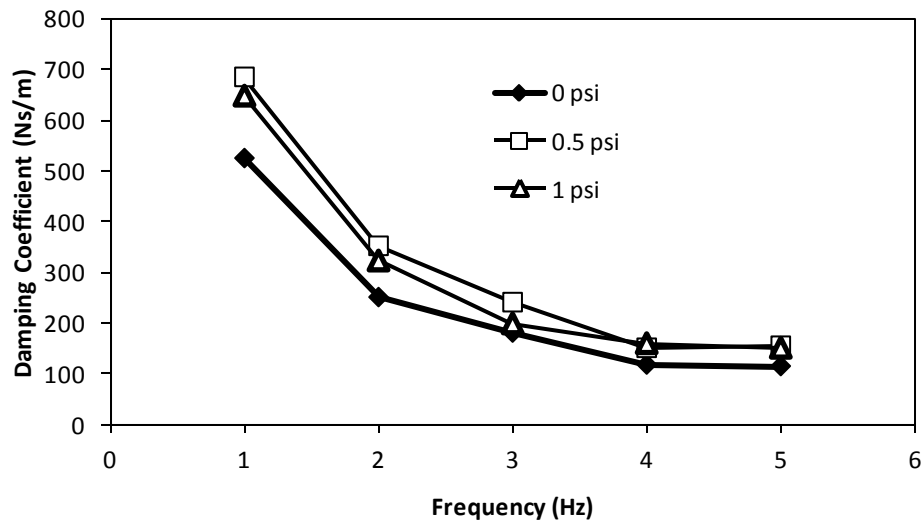


Figure 2-15: Equivalent viscous damping coefficient as a function of frequency and inflation pressure.

Results also show that the inflated seat cushion yields only slightly higher equivalent damping constant. Furthermore, the damping constants obtained under inflation pressures of 3.44 kPa (0.5 psi) and 6.88 kPa (1.0 psi) are quite comparable. The results thus suggest that the cushion damping effect is primarily attributable to the PUF cushion covering.

2.7 Summary

Comfort performance of an automotive seat in a dynamic environment is highly correlated with seat characteristics such as seat geometry, contour and stiffness [42]. In this chapter the cushion stiffness of the prototype seat has been measured in the static and dynamic environments. Since the prototype seat cushion has built-in air bladders which can be individually inflated, the influence of inflation pressure has also been taken into account. The static stiffness of the cushion was measured using different inflation pressure of 0.0, 3.44 and 6.88 kPa (0.0, 0.5 and 1.0 psi). Furthermore, the effect of different pre-loads has been studied to account for different body weights. In addition to that, the dynamic force-deflection characteristic of the cushion and the air bladders was measured in the 1-5 Hz frequency range to account for dominant resonant frequencies of the vehicle and the human body. The current practice to measure seat cushion stiffness is given by the SAE J1051 standard. However, the indenter used in this standard employs a round steel disc which does not represent the human body-seat interface surface. Hence a buttock-shaped indenter was fabricated following ISO 16840-2 practice to measure the seat cushion stiffness in static and dynamic environments. In order to verify the similarity of contact pressure distribution of the indenter to that of the human subject, the interface pressure was verified using pressure mapping technology. The results showed that the buttock-shaped indenter yields interface pressure around the ITs that is comparable with the human subjects, while the ISO-recommended indenter yields significantly lower stiffness. Furthermore, the static and dynamic stiffness of the seat cushion was objectively measured using the buttock-shaped indenter. In chapter 3, the comfort characteristics of the prototype seat are measured objectively and a correlation with the subjective comfort is attempted.

3. CORRELATION BETWEEN SUBJECTIVE COMFORT AND INTERFACE PRESSURE DISTRIBUTION

3.1 Introduction

From the commercial point of view, the first impression of an automobile by the customers is highly influenced by the static seat comfort, following the exterior and interior design. The static seat comfort, also referred to as “showroom comfort”, is thus an important marketing feature of an automobile [28]. The ultimate goal in quantifying comfort of an automobile seat is the ability to “design in” comfort. A more desired target is to predict the comfort as early as possible in the design process of a seat. This provides the engineers the opportunity of adjusting the seat features such as contours, cushion hardness, seat cushion dimensions, etc., in an effort to improve the comfort level of the seat and accommodate larger range of occupants [14].

The comfort perspective of a seat, however, is dependent upon a number of seat design features such as seat geometry, backrest and cushion inclinations, seat height, and elasticity and support properties of the seat cushion and the backrest. Furthermore, a generally acceptable objective measure of the comfort does not yet exist. A few studies have suggested that the support and thereby the comfort property of a seat could be related to body-seat interface pressure, although the desirable pressure profiles do not yet exist. The studies reporting human-seat pressure distribution and their relations with comfort have been discussed in Chapter 1 [24-29, 48, 49]. The highlights of these studies are also summarized in Table 3-1.

Table 3-1: A summary of studies reporting human-seat interface pressure and force

Lead Authors	Measurements	Objectives	Seat Type	Equipments	Anthropometric Factors/Posture	Duration	Subjects
Raphael [28]	Seat pan and backrest pressure, contact force and effective area of each region	Definition of a comfortable range for interface pressure, force and contact area on each cushion region	2 automotive seats	Pressure mat 16X16 cells	Hands on steering wheel, Right foot on pedal, seat adjusted to most comfortable posture	30 s short term, 3 hrs long term	15 male, 15 female (short term), 4 male and 4 female (long term)
Frusti [14]	Segmental pressure, Pressure range, Formulation of comfort criteria	Definition of a comfortable range for interface pressure on each cushion region	5 automotive seats	Pressure mat 44X48 cells	Typical driving posture	-	70 male, 70 female
Andreoni [19]	Sitting strategies, Pressure distribution	Definition of various sitting strategies in automobile seats	NR†	TECKSCAN pressure mat	Most comfortable driving posture, one foot on the pedal, asymmetric seating posture	1 s	7 male, 1 female
Husten [38]	Peak pressure at human-seat interface	Effect of backrest inclination on buttocks pressure, Correlation between BMI and pressure distribution, Comparison of pressure distribution between foam and air cushions	Agricultural machinery seats	Pressure mat	Most comfortable driving posture, Feet hanging, No armrest, Backrest inclinations: 110-130-145 degrees	16 min	10 male
Ahmadian [25]	rms pressure, pressure distribution area	Comparison between air cushion and foam cushion, Damping characteristics, Cushion stiffening	Truck seat	Single axis test rig, Indenter, Pressure mat	NR†	12 hr	Indenter
Wu [8]	Interface mean and peak pressure and force under vertical vibration	Effect of magnitude and frequency on IT pressure, force and contact area, Ischial PP	Visco elastic seat cushion	Novel pressure mat, single axis whole body vehicle simulator	Horizontal seat pan, seat height 420 mm, erect posture with and without back support	NR†	6 male

† Not Reported

Raphael et al. [28] investigated the effect of cushion stiffness on comfort prediction via subjective evaluations and pressure mapping technique. In order to simulate different cushion stiffness at various contact regions, including the ITs and the thighs, different foam materials were installed on the vehicle seat. The study measured the pressure distribution percentage in each contact region and the frequency of postural shifts over prolonged sitting. Finally, the subjective evaluation data were used to define desirable pressure and contact force ranges in each region. In a similar manner, Frusti et al. [14] measured seat comfort by correlating pressure measured at the contact interface and subjective evaluations. The study involved five sedan category vehicle seats and subjectively evaluated the comfort level in the laboratory as well as in the vehicles. The seat cushion area was divided into 15 regions and the body pressure percentage in each individual segment was measured to identify comfort pressure ranges for each region according to the subjective evaluation.

In another study performed by Andreoni et al.[19], sitting strategy was studied using combined optoelectronic system for motion capture and pressure sensors. The study revealed two sitting strategies, which affect the seat pan loading and three strategies directly related to backrest pressure distribution. It was found that subjects tend to adapt an asymmetric seating posture where peak pressure (PP) occurs under the left IT and a relatively greater load is supported by the right thigh. The study also showed that larger subjects tend to transfer more of the upper body load to the lumbar region, while smaller subjects distribute the load more evenly on the backrest.

The subjective comfort could be enhanced by providing variable or adaptive contact pressure at the body-seat interface, which cannot be realized from the fixed PUF seats.

Alternatively, air cushion seats could provide design flexibility for the occupant to vary contact over prolonged sitting depending upon the posture assumed and the intensity of vibrations. Hostens et al. [38] and Ahmadian et al. [25, 26] performed interface pressure distribution measurements of air cushion seats under vehicular vibration. The study concluded an increase in mean pressure with increase in body mass index. It was suggested that in order to prevent capillary occlusion and pressure discomfort, the interface pressure must not be greater than 20 to 30 mmHg (0.27-0.40 N/cm²). The sustained pressure tolerance of seated body, however, varies over the entire contact region. A higher pressure in the vicinity of IT-s would be acceptable, while a higher pressure near the soft thigh muscles could cause capillary occlusions. It would thus be desirable to design seats with a number of air bladders that would allow selection of different pressure in different regions.

In studying the human comfort evaluation of vehicle seats, the pressure mapping technique has also been utilized in dynamic environments. Wu et al. [8] studied the effect of vibration magnitude and frequency on IT pressure, contact force and contact area as well as the maximum ischial PP obtained from the measurements. It was concluded that the maximum ischium pressure and effective contact area occur near the resonance frequency of coupled human-seat system (2.5-3 Hz) on soft seats and it increases with increase in magnitude of vibration.

In this chapter, it is intended to quantitatively measure the cushion comfort by correlating the objective measurements to subjective evaluations. For this purpose, the total area of the seat cushion was initially divided to sub-sections covering nine regions at the human-seat cushion interface. This would allow measuring contact pressure, force

and area for individual regions independently. Ten adult male subjects participated in the experiment. In order to simulate different cushion hardness, an inflatable cushion was used which would allow the experimenter to modify the cushion stiffness under buttocks and thighs independently. In order to eliminate asymmetric loading of the cushion the built-in air bladders within the cushion PUF were symmetrically interconnected so that the left and right-hand-side air bladders would inflate symmetrically. Subjective evaluation of each cushion stiffness was performed using a ranking questionnaire (Appendix A), which allowed each subject to individually rank each anatomical region using a body-seat interface map.

3.2 Measurement of Body-Seat Pressure Distribution on Seat Cushion

An experiment was designed to measure body-seat interface pressure distribution under static sitting condition and to examine correlation, if any, between the pressure distribution and the subjective comfort sensation. In particular, the subjective discomfort assessments are evaluated in relation to ranges of localized pressure concentrations, and those of desired cushion air bag pressure. The prototype seat facilitated selection of different cushion pressure and thus the stiffness over different contact regions, namely the buttocks, thighs, and the tail bone. The experiments were thus conducted for different inflation pressure of cushion air bladders, while the contact pressure distributions were acquired in NOVEL EMED system, as briefly described in section 2.4. The seat cushion surface was divided into 9 different regions, while the contact pressure distribution, force and contact area were measured over each zone. Since the software employed to acquire data from the pressure mat refers to each zone as a “Mask”, hereafter each zone is marked with letter “M”. Zone M01 encompasses the area around the tail bone known as sacro-iliac region, as shown in Figure 3-1. Pressure in this zone is most affected by

backrest inclination. This zone is covered by 36 sensors and has a total sensing area of 216.09 cm². Zones M02 and M09 cover the lateral wings of the cushion as seen in Figures 3-1 and 3-2. These zones depending on the contour and design may cause excess force on femur bone and create sensation of discomfort. The summation of these two zones covers a total of 64 sensors with total area of 384.2 cm².

It has been widely reported that the majority of the seated body is supported by the buttocks region, which may lead to higher concentrated contact pressure [22]. To investigate this contact pressure values, which could be better correlated with subject's comfort or discomfort, the buttocks contact area was divided into zones M03 and M04, covering a total area of 180.07 cm² in each region. The thighs' contact region comprising soft tissues could lead to discomfort sensation, should the contact pressure exceed capillary pressure value. In this experiment the corresponding areas are enveloped by zones M05 and M06, as shown in Figures 3-1 and 3-2 each with total area of 180.07 cm².

It should be noted that longitudinal dimension of the cushion may effectively alter the pressure distributions within the areas under the knees. These regions are also sensitive to excess force that may occur for relatively longer cushions compared to the buttock popliteal length. In order to investigate the pressure and force distribution within these contact areas, two additional zones, M07 and M08, were considered with sensing area of 108.04 cm² each. For the prototype cushion used in the study, these two zones were relatively small compared to the overall dimension of the upper legs.

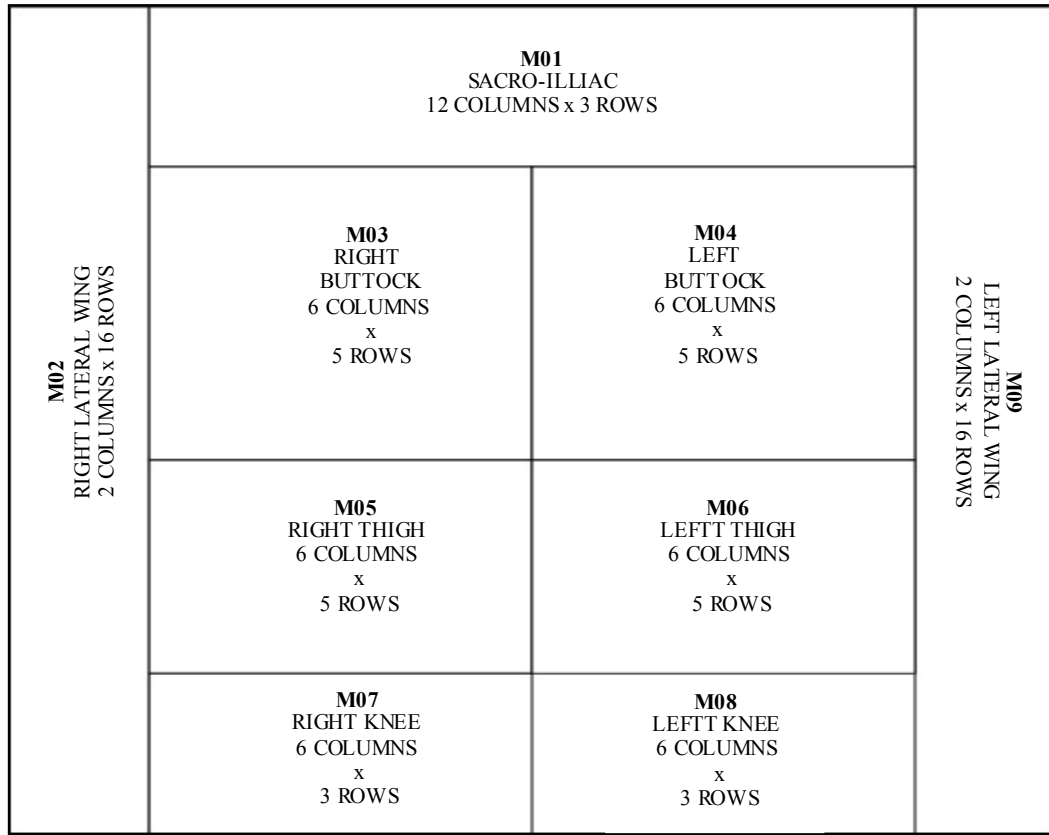


Figure 3-1: Schematic of the different contact regions considered in the study.

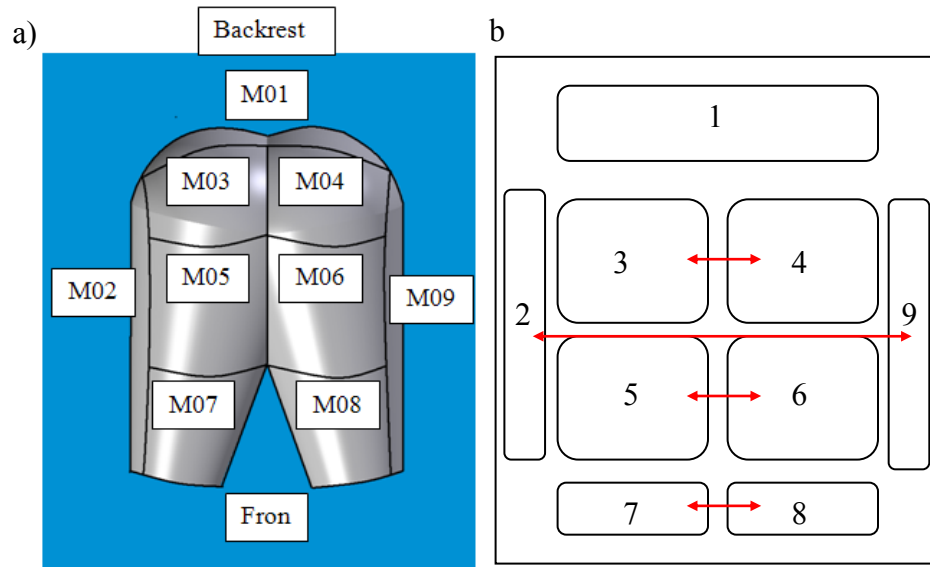


Figure 3-2: a) Body map of human-seat contact area for subjective zonal discomfort evaluations. b) Layout of air bladders within the seat cushion and their interactions. Regions: 1- tail bone, 2 - right cushion wing, 3 - right buttock, 4 - left buttock, 5-right thigh, 6- left thigh, 7- right under knee, 8- left under knee and 9- left cushion wing.

3.2.1 Subjective Evaluations

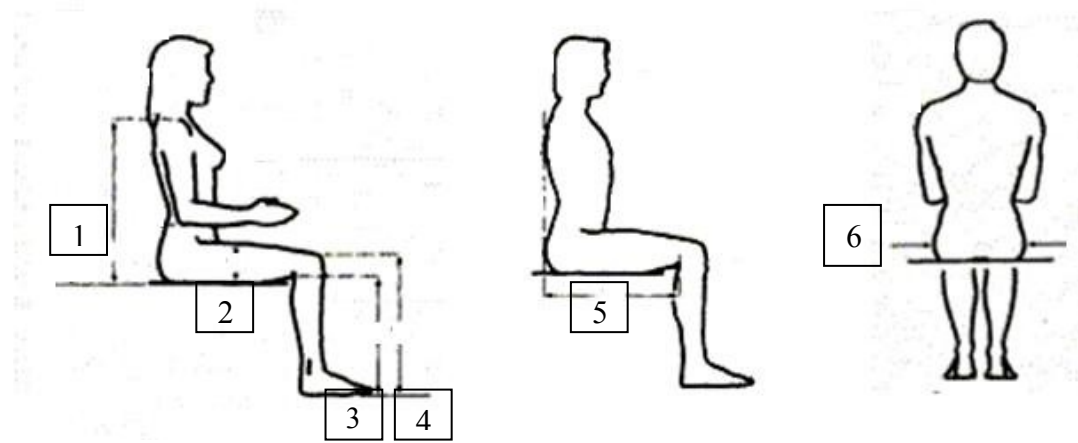
The experiments involved different inflation pressures of the air bladders in the thighs and buttocks regions, as described previously. The subjective sensation of sitting comfort or discomfort of the prototype seat with each inflation pressure setting was also attempted. For this purpose, a questionnaire was designed to seek participant's sensation of comfort or discomfort with respect to different contact zone. The correlation between subjective data, and objective pressure and force values were subsequently attempted. This includes a map of 9 zones superimposed on the body-seat contact area and a category partitioning scale inspired by Shen and Parsons [17]. Each subject was supplied with a scale and a body map to evaluate related pressure and force corresponding to each contact zone, as shown in Figure 3-2. The evaluation scale range varied from 1 to 5, 1 being the most uncomfortable and 5 being the most comfortable condition. Ten adult male subjects were recruited for the study. Each subject was briefed with the experiments goals and methodology, and was asked to sign a consent form that had been approved by Human Research Ethics Committee at Concordia University. Table 3-2 summarizes some of the anthropometric attributes of the subjects.

3.2.2 Test Matrix and Methodology

The design process of a seat requires knowledge of probable force distribution and thus the local probable discomfort areas at the body seat interface. The stiffness variations over the cushion surface may lead to considerable variations in the contact pressure over different zones. Discomfort may be caused by large pressure concentration within a local zone.

Table 3-2: Anthropometric attributes of the subjects [43].

Subject:	1	2	3	4	5	6	7	8	9	10
Gender:	Male	Male	Male	Male	Male	Male	Male	Male	Male	Male
Age:	36.00	23	29.00	26	22	27	30	29	26	37
Static Weight (kg):	64.8	104.0	54.2	80.0	62.4	65.0	85.4	86.6	75.0	87.8
Standing Height (m):	1.73	1.88	1.65	1.75	1.76	1.78	1.78	1.74	1.83	1.76
BMI (kg/m ²):	21.7	29.4	19.9	26.1	20.1	20.5	27.0	28.6	22.4	28.3
1. Sitting shoulder height (cm):	55.0	62.0	56.0	63.0	62.0	62.0	60.0	59.0	61.0	63.0
2. Thigh thickness (cm):	11.0	18.0	12.0	13.5	13.5	14.0	14.0	13.0	145.0	13.0
3. Popliteal height (cm):	49.0	50.0	45.0	44.0	47.0	47.0	47.0	47.0	48.0	54.0
4. Knee height (cm):	59.0	63.0	53.0	56.0	56.5	58.0	57.0	58.0	58.0	43.0
5. Buttock-popliteal-length (cm):	49.0	56.0	37.0	48.5	48.0	49.0	50.0	49.0	48.0	48.0
6. Hip breadth (cm):	39.0	48.0	34.0	41.0	36.0	37.0	41.5	38.0	39.0	42.0



A low contact pressure in certain regions may also not be desirable, since it is an indication of inadequate body support. In order to simulate different distribution of cushion stiffness, the experiment was designed to seven “pre-selected” and one “user-selected” stiffness/pressure settings. These were realized by selecting different inflation pressures in different bladders. These are labeled from ‘A’ to ‘G’ and the selected pressure settings in the buttocks and thighs regions airbags are summarized in Table 3-3.

The interconnection between air bladder 3 and 4 permit symmetric contact pressure and cushion stiffness around the right and left tuberosities. In a similar manner interconnection between bladders 5 and 6 permit identical contact pressure supporting right and left thighs. The symmetric pressure distribution about the longitudinal axis is expected to eliminate the potential discomfort sensation by the subject due to asymmetric loading. Among the nine zones, only seven were selected to study the contact pressure distribution and the subjective discomfort sensation. The regions 7 and 8 were ignored due to lack of consistent contact across the subjects. Owing to the limited cushion dimension in the longitudinal direction, 8 out of the 10 subjects did not exhibit sufficient contact in these regions. The experiments involved pressure variation in the range of 0.0 to 10.34 kPa (1.5 psi). The chosen variations in pressure are denoted from A to H and summarized in Table 3-3. Pressure combinations A to H simulate the overall cushion hardness perception of the subject. The study also considered an additional air bladder pressure combination that was selected by the subject and judged to be most comfortable. The inflation pressure corresponding to the subject-selected setting is denoted by “G” in Table 3-3.

Table 3-3: Air bladder pressure combinations of the seat cushion used in the experiments.

Combination	Buttocks Pressure (psi)	Thighs Pressure (psi)
A	0	0
B	0.75	0.75
C	1.5	1.5
D	1.5	0
E	0	1.5
F	0.75	1.5
H	1.5	0.75
G	USER-selected	USER-selected

The initial experiments were performed with subjects assuming controlled posture, namely, vertical lower leg and horizontal thighs orientation, as reported in a few studies [5]. For this purpose the height of the feet support was varied to achieve desired posture. The subjects, in general, found this sitting position uncomfortable. It was thus decided to allow the subjects to assume a posture considered comfortable. For this purpose, the seat cushion was installed on an air suspension so as to achieve variations in the seat height by varying the air suspension pressure. The subjects, however, were asked to sit upright in driving-like posture with their back unsupported and supported against the backrest. The seat backrest was inclined at an angle of 100 degrees with respect to the horizontal plane while the hands were placed on the thighs.

The measurements with subjects thus involved two modes of back supports (NB - no back support, B - full back support) and 8 seat cushion bladder inflation pressure combinations (settings A to G). Each experiment was repeated 3 times to further study repeatability of subjective and objective measurements. The study thus involved 48 measurements per subject, as summarized in test matrix in Table 3-4.

Table 3-4: Test matrix.

Factor	Variations
Back Support	NB, B
Inflation pressure settings	A, B, C, D, E, F, H, G (Subject - Selected)
Seat height	Subject - Selected
Seat to feet distance	Subject - Selected
Repeats	3

Each subject was asked to sit on the seat with the pressure sensing mat assuming the desired pressure. The inflation pressures in individual air bladders were subsequently adjusted in accordance with a chosen combination (A to H). The subject was then asked to stand up and move away from the seat to permit cushion relaxation for 3 to 5 minutes. The subject was subsequently asked to assume the same posture and the pressure setting of individual bladders were examined and fine-tuned to ensure the selected inflation pressure combination. The subject was advised to sit for a duration of 3 minutes, while the contact pressure was recorded over duration of 30 seconds. The subject was then advised to stand up from the seat and answer the questionnaire in the adjacent laboratory, while referring to the seat cushion map and the scale. Each measurement was subsequently repeated after a rest interval ranging from 5 to 10 minutes.

3.3 Method of Analysis

The analysis of the collected data from the interface pressure measurement was carried out to evaluate contact force (F_n), contact area (A_n) and mean pressure (MP_n) for each individual anatomical region denoted by M01 to M09. Since the peak pressure (PP) within each region represents only an instantaneous value of the measured pressure over

the entire test duration, this measure is considered to be inappropriate to identify comfort pressure ranges. Due to high dependency of the contact force within each region on the body weight supported by the cushion, the contact force data was normalized to the total subject body weight supported by the cushion. Owing to the greater variation in the body weight, the normalized force data are expected to facilitate interpretations and possible correlations between the objective and subjective evaluations. Furthermore, this may yield important design guidelines for automotive seats. The normalized contact force data corresponding to each cushion inflation combination (A to G) were thus analyzed to identify comfort ranges reported by individual subjects. Owing to large variations in the comfort ranking corresponds to each pressure combination, the global ranges of contact force was reported only when a minimum of 8 out of 10 subjects assigned same ranking (1 to 5) to each global comfort level.

3.4 Results and Discussions

3.4.1 Contact force, area and pressure - Intra-subject variability

Due to the fact that the peak pressure (PP) is only an instantaneous maximum value of the pressure on a pressure sensor recorded during the data acquisition process, it does not provide adequate information on general force distribution. The mean pressure was thus utilized for the analysis. The measured data revealed considerable variations in all the measures across the subjects. This is mostly attributable to variations in the subject anthropometry. Furthermore, the measured data acquired for the same subject but different combinations of air bladder pressures also revealed large variations in the total contact force, contact area and mean contact pressure.

Table 3-5 shows the mean and the standard deviations (SD) in the force, area and mean pressure data acquired for each subject over eight cushion inflation pressure configuration labeled from A to H. The large standard deviation (SD) in the measured data for each subject is quite evident, and suggests significant affect of the cushion inflation pressure combinations. The results also show considerable scatter in the mean force, area and pressure, which are directly related to subject anthropometry, particularly the body weight and the build. The results in Table 3-5 are further used to study the proportion of total body weight supported by the prototype seat in a typical driving posture with and without the back support. In order to provide comparison among the force distribution of the subject population, the total seat cushion force was normalized by subject's total body weight for each cushion inflation pressure combination. The resulting normalized mean force values, expressed in percent body weight are summarized in Table 3-6 for each subject, with and without back support. The results clearly show that the body weight supported by the seat cushion is greater when sitting without a back support. It is should be noted that the mean normalized force reported for each subject was calculated as a mean value over the eight cushion inflation pressure. Tables 3-5 and 3-6 also list the body mass index (BMI) of each subject that provides knowledge on the body mass distribution for each subject and is further used for segmental normalized force distribution in the following sub-sections.

Table 3-5: The measured standard deviations of the mean contact force, area and pressure data acquired for each subject with eight different cushion inflation pressure configurations.

Full Back Support (B)							
Subject	BMI (kg/m ²)	Force (N)		Area (cm ²)		Mean Pressure (kPa)	
		Mean	SD	Mean	SD	Mean	SD
1	21.7	375.25	39.31	1037.46	157.64	3.66	0.44
2	29.4	522.29	20.39	1265.11	72.18	4.14	0.29
3	19.9	303.16	21.18	985.84	90.69	3.09	0.21
4	26.1	449.12	17.25	1205.77	86.05	3.74	0.34
5	20.1	336.33	28.95	1035.72	128.82	3.28	0.33
6	20.5	400.39	17.87	1106.40	53.92	3.62	0.18
7	27.0	483.40	17.23	1227.29	52.09	3.94	0.12
8	28.6	551.50	25.03	1299.84	67.43	4.25	0.17
9	22.4	398.83	16.46	1110.84	106.44	3.61	0.25
10	28.3	463.78	58.36	1075.28	216.38	4.38	0.41

No Back Support (NB)							
Subject	BMI (kg/m ²)	Force (N)		Area (cm ²)		Mean Pressure (kPa)	
		Mean	SD	Mean	SD	Mean	SD
1	21.7	414.43	21.14	960.53	120.62	4.35	0.36
2	29.4	689.69	28.14	1405.84	33.35	4.91	0.21
3	19.9	360.90	39.10	1007.09	140.21	3.61	0.29
4	26.1	632.33	22.27	1310.36	47.50	4.83	0.13
5	20.1	479.33	30.14	1129.42	76.76	4.25	0.17
6	20.5	472.13	44.30	1185.39	87.37	3.98	0.21
7	27.0	604.26	29.07	1297.42	32.66	4.66	0.18
8	28.6	661.45	41.83	1304.37	76.68	5.07	0.22
9	22.4	502.96	40.52	1169.21	122.27	4.31	0.18
10	28.3	588.81	30.16	1234.85	62.44	4.78	0.30

Table 3-6: Mean normalized force on the seat cushion of the subject sitting with and without a back support across eight cushion inflation pressures.

Full Back Support (B)			No Back Support (NB)		
Subject	BMI (kg/m ²)	Force(%)	Subject	BMI (kg/m ²)	Force(%)
1	21.7	58%	1	21.7	64%
2	29.4	50%	2	29.4	66%
3	19.9	56%	3	19.9	67%
4	26.1	56%	4	26.1	79%
5	20.1	54%	5	20.1	77%
6	20.5	62%	6	20.5	73%
7	27.0	57%	7	27	71%
8	28.6	64%	8	28.6	76%
9	22.4	53%	9	22.4	67%
10	28.3	53%	10	28.3	67%

Figures 3-3 and 3-4 show correlations between the body mass index (BMI) and the contact force, area and the mean pressure on the seat cushion for subjects seated with and without the backrest support. It is shown that the interface force, area and mean pressure increase with increase in subject BMI, however, a greater correlation is observed between the BMI and the contact force and mean pressure, compared to the mean contact area for both sitting postures. This is attributed to greater variations in the subjects anthropometry, particularly the buttocks dimension. The results also show that sitting without a back support yields relatively larger mean contact pressure.

3.4.2 Contact force, area and pressure distribution on the seat cushion

The measured pressure data are further analyzed to derive the distribution of contact force and pressure over different contact regions of the seat, as described in Figures 3-1 and 3-2. The distribution of contact force and pressure over the contact regions M01 to M09 could yield considerable knowledge towards localized discomfort sensation and design guidance for seat cushions. The analysis of the data, however,

suggested that contact force and pressure characteristics are strongly influenced not only by the subject anthropometry but also the seat inflation pressure. As an example, Table 3-7 summarizes the variations in the body weight supported by the seat (total contact force) with different inflation pressure combinations (A to H) for each subject. The results clearly show considerable variations in the body weight supported by the seat with varying inflation pressures. These suggest that varying the cushion inflation pressure alters the subject posture and thus the contact pressure distribution. The table also lists the inflation pressures (buttocks/thighs) in psi units. For sitting without a back support, an increase in the pressure of the buttocks and thighs air bladders, in-general, yields increasing portion of body weight supported by the seat (combinations A, B and C). This trend, however, is not consistent when sitting with a back support. The variations in the inflation pressure in one of the seat regions may shift the body weight to another region resulting in greater variation in the contact force. This was clearly observed from the measured data. Increasing the thigh region pressure resulted in increased contact pressure on the thighs and higher contact force on the buttock region.

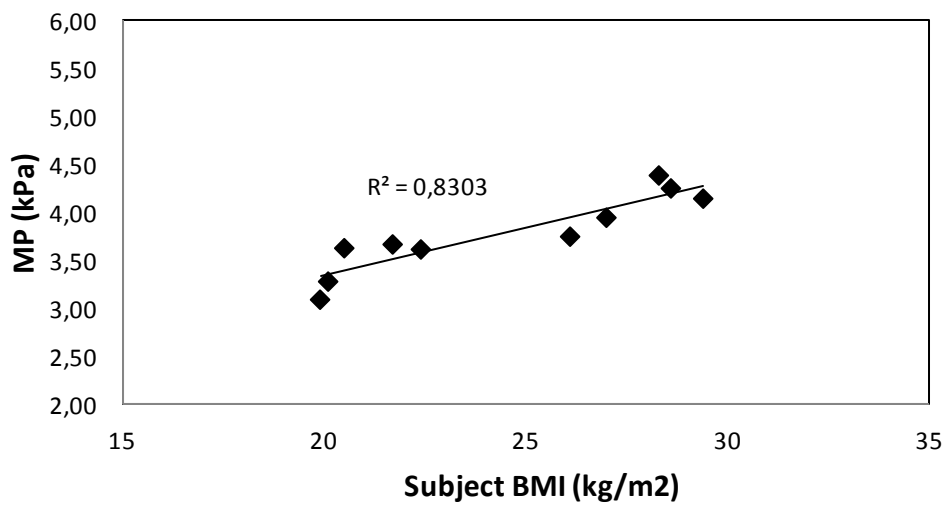
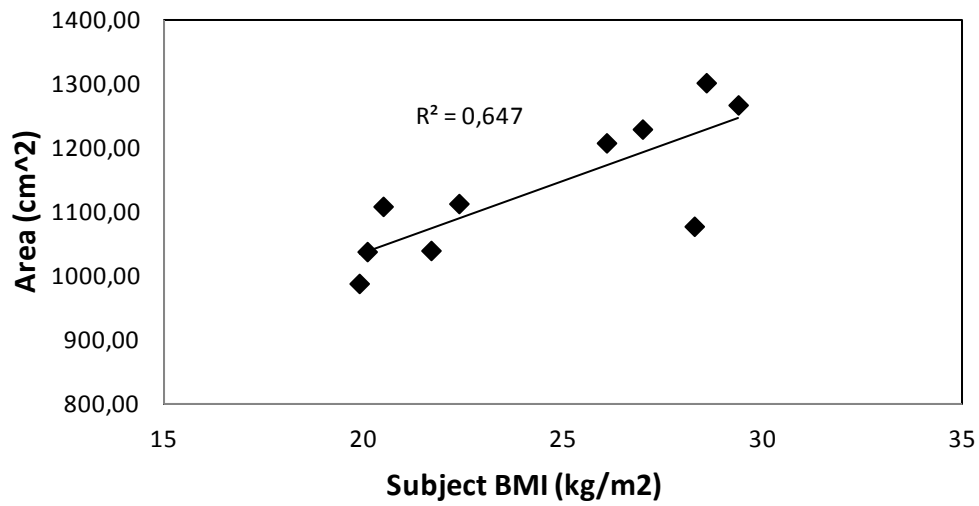
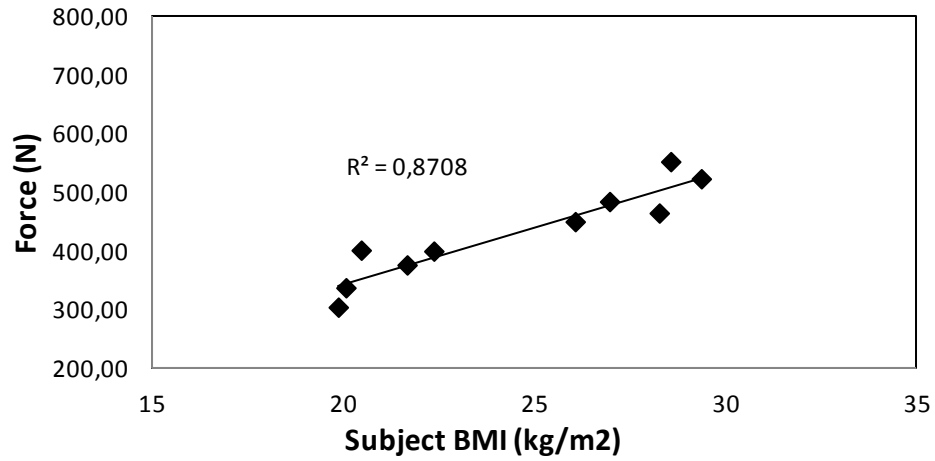


Figure 3-3: Correlation between the body mass index (BMI) and the mean contact force, area and pressure of subjects sitting with full back support (B).

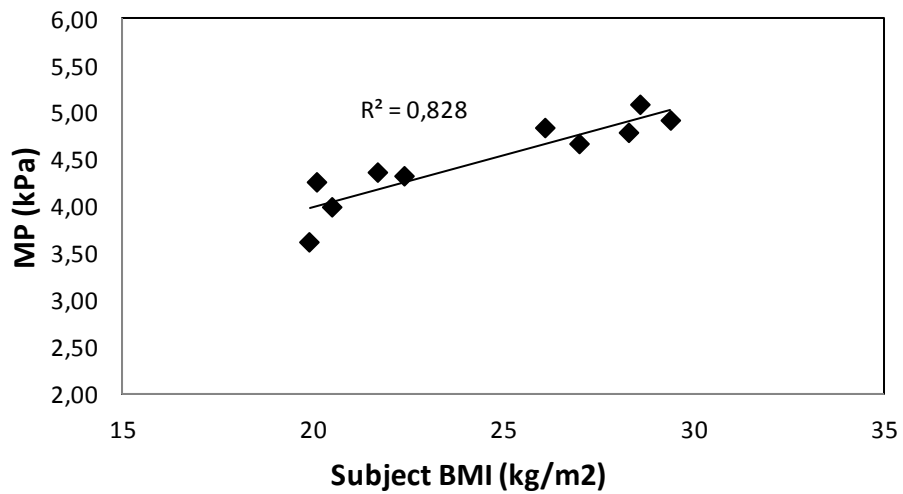
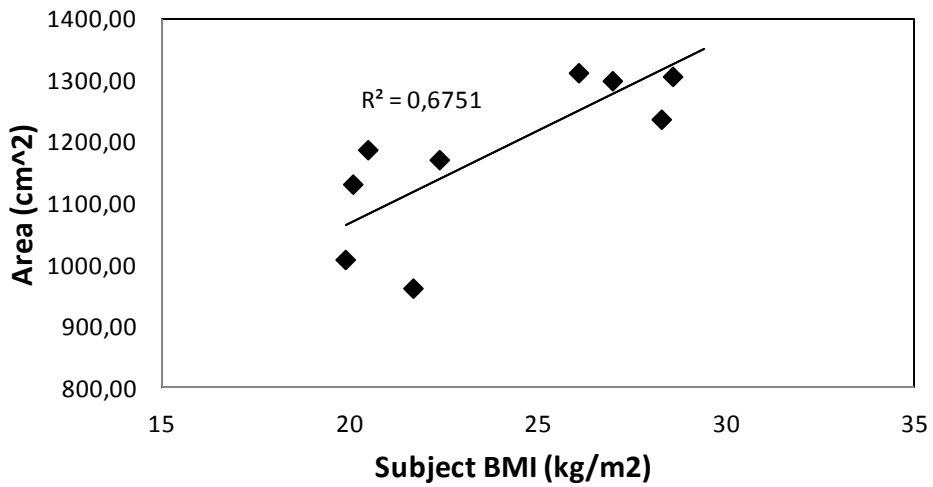
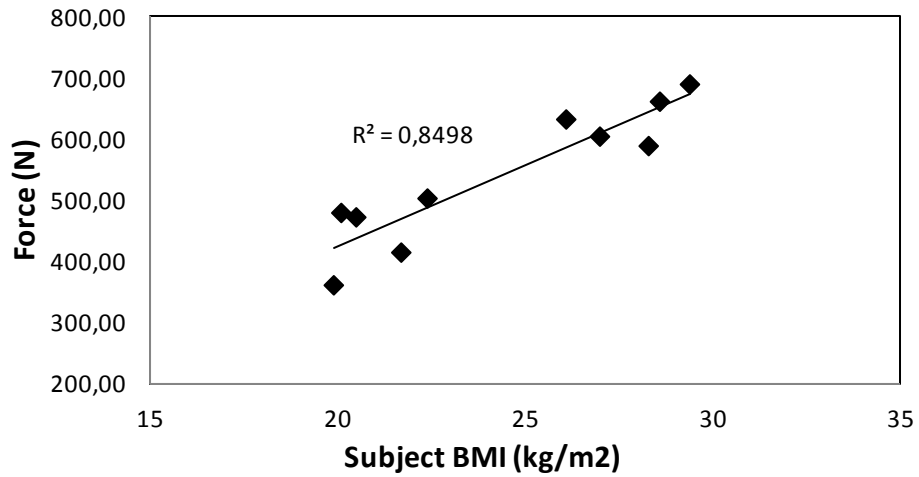


Figure 3-4 Correlation between the body mass index (BMI) and the mean contact force, area and pressure of subjects sitting without back support (NB).

Table 3-7: Comparisons of total body-seat contact force measured for the eight cushion inflation pressure combinations (A to H) and two backrest supports.

Subject	Seat Cushion Inflation Pressure Combination (Full back support)							
	A (0,0)	B (0.75, 0.75)	C (1.5, 1.5)	D (0, 1.5)	E (0, 1.5)	F (0.75, 1.5)	G	H (1.5, 0.75)
1	326.98	339.54	380.25	331.45	373.99	414.51	425.72	409.56
2	539.94	496.73	558.91	519.07	514.39	515.40	531.53	502.33
3	291.51	303.32	335.09	278.46	324.52	318.34	277.88	296.16
4	424.12	427.96	459.00	453.81	448.99	478.44	446.52	454.11
5	321.57	336.46	368.92	296.93	380.11	347.10	334.85	304.73
6	383.64	381.27	425.56	382.42	414.88	419.92	393.99	401.47
7	487.33	472.25	493.37	452.96	468.63	504.39	497.59	490.71
8	510.74	559.10	571.75	524.32	577.11	579.01	541.86	548.08
9	387.12	399.68	398.21	369.90	423.83	415.75	400.20	395.95
10	499.96	495.35	527.71	478.29	517.44	420.75	375.05	395.73

Subject	Seat Cushion Inflation Pressure Combination (No back support)							
	A (0,0)	B (0.75, 0.75)	C (1.5, 1.5)	D (0, 1.5)	E (0, 1.5)	F (0.75, 1.5)	G	H (1.5, 0.75)
1	414.32	435.44	410.60	393.76	393.76	427.65	448.08	391.81
2	641.66	706.92	691.25	662.80	725.32	716.97	676.94	695.65
3	380.22	341.72	362.99	290.50	430.92	365.97	362.37	352.52
4	629.07	638.22	620.61	604.27	679.19	641.94	626.47	618.89
5	478.87	488.69	493.64	449.78	532.72	495.45	454.29	441.17
6	458.41	489.90	459.22	435.67	552.91	516.76	429.09	435.11
7	602.95	615.31	596.83	567.46	660.16	623.62	578.78	588.95
8	631.33	700.44	635.63	631.06	732.57	698.12	631.67	630.81
9	518.41	517.39	514.16	461.00	568.36	529.68	458.76	455.92
10	542.49	569.13	556.26	594.51	618.04	626.38	593.50	610.16

The mean contact force values and the corresponding standard deviations are computed across the subjects and summarized in Table 3-8 for each inflation pressure combination. The results show large standard deviation (SD), which is attributed to differences in subject anthropometry. The results also exhibit the general trend in increasing contact force with increasing pressure in both the thighs as well as buttocks regions.

Increasing the buttock pressure alone with fixed thighs pressure revealed inconsistent trends. For instance, for 0 psi thigh pressure, an increase in buttock pressure from 0 to 1.5 psi (combinations A and D) resulted in lower contact force for both the sitting postures. This suggests shifting of the body weight towards the legs of a seated subject. On the other hand, for the fixed higher thighs pressure of 1.5 psi, increase in buttock pressure (combinations E, F and C) resulted in relatively small change in the contact force, when sitting without a back support. This suggests relatively small change in the sitting posture. An opposing trend, however, is observed with the back supported posture, where increase in buttocks contact pressure yields, lower contact force suggesting greater shifting of weight towards the legs. Owing to the lack of definite trends in the total body force on the seat cushion, the measured data were analyzed to obtain distributions of contact force on different regions of the seat. These may provide the knowledge on shifting tendencies. Table 3-9 and 3-10 present the mean contact force, mean contact area and mean of mean interface pressure, derived for each of the seat cushion regions (M01 to M09), while sitting with and without a back support, respectively. The tables also present standard deviations in mean force (SD-F), mean contact area (SD-A) and mean of mean interface pressure (SD-MP).

Table 3-8: Comparison of the mean overall seat cushion force corresponding to eight cushion inflation pressure combinations and two backrest supports.

Pressure Combination		A (0,0)	B (0.75, 0.75)	C (1.5, 1.5)	D (0, 1.5)	E (0, 1.5)	F (0.75, 1.5)	G (user selected)	H (1.5, 0.75)
B	Mean	417.29	421.17	451.88	408.76	444.39	441.36	422.52	419.88
	SD	88.66	83.45	83.38	89.45	76.89	78.92	84.67	83.70
NB	Mean	529.77	550.31	534.12	509.08	589.40	564.25	526.00	522.10
	SD	95.29	117.66	104.93	120.45	116.07	115.86	107.13	119.15

The results clearly show extreme variability in all of the measures, which is mostly attributed to anthropometric variations. The variability in the force data could be somewhat reduced by normalizing the contact force with the standee body weight. The mean normalized distributed forces (\bar{F}) for different inflation pressure combinations are summarized in Table 3-11 and 3-12 respectively, for the back supported and unsupported postures. The results show negligible force in the knees region, rating from 1.2% to 3.6% (region M07 and M08) of the total body weight when sitting with back support. The maximum contact force occurs in the buttocks region in the vicinity of the tuberosities (regions M03 and M04) in the range of 20% to 28.3 %. The thighs region (M05 and M06) support 7% to 15% and the side wings (M02 and M09) support 7% to 12 % of the total body weight, respectively. The tail bone region (M01) supports 8% to 10% of the total body weight when sitting with full back support. On the other hand, when sitting with no back support the percentage of the body weight supported by the tail bone region (M01) is 4% to 8%. This is attributed to the shifted body weight towards the IT regions and the thighs regions. When sitting with no back support the maximum contact force measured on the tuberosities (M03 and M04) was 28% to 36% which declares the body mass shift towards the buttocks and the upper legs. Also the percentage of the body weight supported by the thighs (M05 and M06) was increased to 11% - 18% and 9% - 14% for the side wings (M02 and M09), respectively. The knees region (M07 and M08), however, showed an increased value of 2.5% to 6%.

Table 3-9: Comparisons of mean force, area and pressure distributed over different seat regions (M01 to M09), when sitting with a full back support (B).

		Inflation Pressure Combination							
Sub-region		A (0,0)	B (0.75, 0.75)	C (1.5, 1.5)	D (0, 1.5)	E (0, 1.5)	F (0.75, 1.5)	G (user selected)	H (1.5, 0.75)
M01	mean F	72.09	74.02	63.74	82.64	62.55	67.01	77.45	76.98
	mean A	164.83	176.67	147.16	167.23	168.77	164.15	177.99	162.46
	mean MP	4.08	3.96	3.99	4.53	3.54	3.87	4.19	4.56
	SD -F	38.51	32.80	35.50	40.50	28.67	28.75	29.74	31.73
	SD -A	46.68	44.95	59.82	54.78	45.79	44.88	38.35	46.54
	SD -MP	1.34	1.10	1.06	1.45	0.84	0.94	0.99	0.84
M02	mean F	36.93	33.42	25.35	23.10	40.69	33.45	34.27	22.28
	mean A	135.74	128.20	103.52	91.55	141.97	123.96	124.95	91.72
	mean MP	2.66	2.51	2.34	2.32	2.82	2.69	2.74	2.29
	SD -F	15.46	14.21	14.71	14.22	12.17	13.89	11.43	13.50
	SD -A	41.69	30.72	48.24	42.19	26.17	40.22	32.92	43.86
	SD -MP	0.48	0.52	0.41	0.55	0.38	0.72	0.53	0.77
M03	mean F	85.86	83.92	99.30	103.53	73.48	85.52	86.42	103.94
	mean A	178.84	177.14	173.05	177.60	175.83	176.30	177.25	177.57
	mean MP	4.81	4.74	5.70	5.81	4.18	4.84	4.88	5.85
	SD -F	12.92	10.87	18.94	17.47	11.93	14.70	15.41	13.69
	SD -A	6.90	5.05	18.87	4.11	5.17	4.56	4.87	3.03
	SD -MP	0.75	0.58	0.68	0.88	0.64	0.75	0.88	0.70
M04	mean F	89.67	86.60	108.55	106.54	77.26	88.25	87.71	106.51
	mean A	173.03	172.48	176.81	174.11	169.43	170.97	169.79	173.01
	mean MP	5.17	5.02	6.14	6.11	4.56	5.15	5.15	6.15
	SD -F	13.82	10.62	14.98	15.48	9.69	11.05	14.26	11.32
	SD -A	8.57	7.65	6.37	5.61	8.88	7.84	8.71	6.19
	SD -MP	0.62	0.54	0.81	0.77	0.51	0.50	0.65	0.53
M05	mean F	43.34	45.29	52.02	30.55	58.64	54.20	43.01	33.58
	mean A	145.07	154.14	157.74	112.08	164.34	158.72	144.77	135.98
	mean MP	2.84	2.88	3.26	2.48	3.54	3.38	2.94	2.47
	SD -F	22.13	15.84	18.00	23.05	14.01	15.15	16.01	11.00
	SD -A	26.22	18.16	14.08	38.26	18.02	19.71	31.82	27.53
	SD -MP	1.04	0.78	0.96	1.12	0.58	0.73	0.75	0.61

Table 3-9: (continued)

		Inflation Pressure Combination							
Sub-region		A (0,0)	B (0.75, 0.75)	C (1.5, 1.5)	D (0, 1.5)	E (0, 1.5)	F (0.75, 1.5)	G (use selected)	H (1.5, 0.75)
M06	mean F	30.69	35.62	43.86	21.65	51.17	45.35	32.23	29.43
	mean A	126.32	133.64	136.42	101.58	144.16	137.09	120.89	117.56
	mean MP	2.31	2.62	3.18	2.05	3.51	3.28	2.64	2.53
	SD -F	15.90	12.09	12.80	10.18	13.73	12.56	13.70	11.97
	SD -A	25.58	18.36	17.25	33.56	15.94	20.21	40.16	34.14
	SD -MP	0.81	0.57	0.60	0.38	0.58	0.58	0.71	0.59
M07	mean F	7.47	8.46	10.23	1.79	15.50	12.46	8.15	4.15
	mean A	47.41	48.80	51.08	13.70	64.33	58.39	48.87	29.38
	mean MP	1.52	1.65	1.84	1.01	2.28	2.14	1.41	1.20
	SD -F	5.08	6.49	9.37	2.93	10.37	8.28	7.14	2.97
	SD -A	30.06	30.68	30.31	22.83	29.49	30.36	33.02	19.48
	SD -MP	0.27	0.24	0.45	0.57	0.40	0.45	0.54	0.47
M08	mean F	4.83	6.12	7.02	1.42	10.80	9.45	6.03	4.61
	mean A	34.00	36.59	38.27	12.23	49.22	46.23	37.81	31.37
	mean MP	1.24	1.61	1.81	0.84	2.13	1.85	1.41	1.32
	SD -F	3.31	3.72	3.25	1.27	5.24	4.24	3.66	2.34
	SD -A	18.95	18.21	13.39	10.47	13.03	20.10	22.45	15.59
	SD -MP	0.42	0.25	0.31	0.47	0.55	0.70	0.55	0.48
M09	mean F	46.41	47.71	41.99	37.54	54.28	45.66	47.25	38.41
	mean A	150.29	156.38	144.05	135.29	160.22	143.00	149.05	138.93
	mean MP	3.00	2.94	2.81	2.60	3.33	3.10	3.12	2.74
	SD -F	16.47	17.99	17.89	17.16	16.58	19.49	17.06	15.49
	SD -A	35.86	33.60	34.99	43.47	32.10	42.19	39.25	41.52
	SD -MP	0.65	0.75	0.64	0.75	0.57	0.72	0.73	0.60

Table 3-10: Comparisons of mean force, area and pressure distributed over different seat regions (M01 to M09), when sitting with no back support (NB).

		Inflation Pressure Combination							
Sub-region		A (0,0)	B (0.75, 0.75)	C (1.5, 1.5)	D (0, 1.5)	E (0, 1.5)	F (0.75, 1.5)	G (use selected)	H (1.5, 0.75)
M01	mean F	61.22	67.38	34.47	49.00	70.56	57.77	49.79	47.11
	mean A	160.71	154.01	99.49	122.57	157.10	137.87	131.94	116.20
	mean MP	3.64	4.09	2.94	3.68	4.19	3.80	3.40	3.60
	SD -F	25.30	37.00	23.44	30.98	40.10	37.54	32.76	34.60
	SD -A	41.58	43.79	48.20	48.65	48.36	55.06	61.75	56.50
	SD -MP	0.78	1.30	1.25	0.96	1.36	1.29	1.01	1.18
M02	mean F	52.42	45.64	32.85	31.64	51.41	45.18	39.53	28.25
	mean A	158.94	144.27	110.41	112.00	151.12	144.07	132.20	102.74
	mean MP	3.27	3.08	2.85	2.72	3.31	3.04	2.90	2.62
	SD -F	12.63	17.32	16.69	15.58	17.96	16.97	16.98	15.72
	SD -A	27.03	30.56	44.68	46.02	38.33	29.44	37.97	43.40
	SD -MP	0.42	0.66	0.44	0.31	0.63	0.64	0.54	0.44
M03	mean F	114.08	116.42	114.00	132.89	106.91	110.28	117.15	136.49
	mean A	178.60	175.13	170.02	170.49	176.99	174.87	170.89	178.27
	mean MP	6.36	6.57	6.55	7.57	6.00	6.24	6.73	7.64
	SD -F	24.53	28.87	33.43	39.96	25.80	26.11	31.09	20.71
	SD -A	4.68	13.65	24.24	27.71	9.70	14.46	20.70	4.05
	SD -MP	1.29	1.37	1.44	1.78	1.30	1.20	1.44	1.06
M04	mean F	117.24	117.11	127.57	140.53	111.47	115.61	124.40	137.77
	mean A	175.45	178.21	175.67	179.33	177.02	177.50	179.55	178.82
	mean MP	6.68	6.56	7.24	7.83	6.28	6.50	6.93	7.70
	SD -F	18.96	17.06	22.25	22.57	20.96	16.23	19.89	18.80
	SD -A	9.77	4.10	9.47	2.27	7.53	4.53	1.65	2.56
	SD -MP	0.96	0.88	1.05	1.23	1.07	0.82	1.09	0.98
M05	mean F	58.12	64.04	72.57	53.66	73.22	72.77	64.18	52.05
	mean A	160.05	167.09	168.68	144.38	164.50	171.01	165.61	161.91
	mean MP	3.53	3.75	4.25	3.45	4.34	4.21	3.80	3.16
	SD -F	25.66	23.98	25.53	37.15	22.64	20.96	29.49	16.70
	SD -A	19.60	21.84	12.96	37.71	24.86	13.90	12.70	14.58
	SD -MP	1.26	1.15	1.29	1.78	0.94	0.99	1.52	0.79

Table 3-10: (continued)

		Inflation Pressure Combination							
Sub-region		A (0,0)	B (0.75, 0.75)	C (1.5, 1.5)	D (0, 1.5)	E (0, 1.5)	F (0.75, 1.5)	G (use selected)	H (1.5, 0.75)
M06	mean F	42.40	49.71	64.24	38.22	64.46	60.33	47.70	47.89
	mean A	142.67	150.36	157.79	134.55	155.90	153.29	151.90	146.67
	mean MP	2.90	3.28	4.04	2.75	4.09	3.91	3.11	3.23
	SD -F	14.92	11.68	16.36	13.99	16.08	13.21	13.12	13.51
	SD -A	24.83	16.26	13.87	22.42	16.64	12.39	13.16	11.57
	SD -MP	0.68	0.62	0.79	0.72	0.86	0.65	0.68	0.70
M07	mean F	14.90	19.43	22.81	10.62	28.27	24.76	16.17	12.01
	mean A	67.83	71.13	73.10	53.27	73.67	75.99	69.68	59.16
	mean MP	1.93	2.45	2.82	1.66	3.41	3.05	2.17	1.99
	SD -F	12.17	15.03	17.20	11.39	21.19	15.89	10.49	5.23
	SD -A	39.22	35.30	36.03	40.88	39.15	32.20	34.14	21.19
	SD -MP	0.62	0.74	0.77	0.54	1.08	0.71	0.43	0.2
M08	mean F	10.03	13.67	16.41	6.81	19.35	17.70	12.02	11.98
	mean A	54.35	57.28	59.12	40.47	60.81	62.80	60.62	59.01
	mean MP	1.63	2.23	2.64	1.40	2.90	2.74	1.94	1.98
	SD -F	5.05	7.02	7.45	4.58	9.41	6.32	3.88	4.38
	SD -A	21.57	18.04	17.67	23.40	21.63	11.34	12.37	12.13
	SD -MP	0.69	0.68	0.77	0.59	1.08	0.62	0.38	0.46
M09	mean F	59.26	57.03	49.21	45.72	63.76	59.85	53.50	48.55
	mean A	152.06	148.38	133.04	130.97	150.67	151.02	147.72	139.77
	mean MP	3.78	3.67	3.55	3.26	4.07	3.82	3.47	3.27
	SD -F	22.52	25.33	21.95	23.93	27.95	25.17	22.06	23.68
	SD -A	40.96	38.92	37.64	45.76	44.94	35.36	34.47	35.72
	SD -MP	0.71	0.90	0.81	0.89	0.93	0.95	0.84	0.98

Table 3-11: Mean normalized distributed force and standard deviation of the mean (full back support).

Sub-region	Parameter	Inflation Pressure Combination							
		A (0,0)	B (0.75, 0.75)	C (1.5, 1.5)	D (0, 1.5)	E (0, 1.5)	F (0.75, 1.5)	G (user selected)	H (1.5, 0.75)
M01	mean \bar{F}	0.095	0.094	0.081	0.105	0.080	0.086	0.101	0.099
	SD	0.047	0.032	0.040	0.044	0.028	0.032	0.035	0.034
M02	mean \bar{F}	0.047	0.043	0.032	0.028	0.053	0.043	0.044	0.027
	SD	0.015	0.013	0.015	0.014	0.010	0.014	0.010	0.014
M03	mean \bar{F}	0.114	0.112	0.132	0.137	0.097	0.114	0.114	0.138
	SD	0.011	0.016	0.025	0.018	0.014	0.020	0.014	0.021
M04	mean \bar{F}	0.119	0.116	0.145	0.142	0.103	0.118	0.116	0.143
	SD	0.013	0.020	0.022	0.023	0.016	0.021	0.017	0.026
M05	mean \bar{F}	0.056	0.060	0.069	0.041	0.077	0.072	0.057	0.044
	SD	0.026	0.022	0.028	0.037	0.015	0.021	0.023	0.010
M06	mean \bar{F}	0.038	0.046	0.057	0.028	0.067	0.059	0.041	0.039
	SD	0.013	0.010	0.010	0.010	0.013	0.012	0.014	0.013
M07	mean \bar{F}	0.010	0.012	0.014	0.003	0.021	0.017	0.011	0.006
	SD	0.007	0.011	0.015	0.005	0.017	0.013	0.012	0.004
M08	mean \bar{F}	0.006	0.008	0.010	0.002	0.015	0.013	0.008	0.006
	SD	0.005	0.006	0.006	0.002	0.009	0.007	0.005	0.003
M09	mean \bar{F}	0.060	0.062	0.054	0.048	0.071	0.059	0.062	0.050
	SD	0.019	0.020	0.018	0.018	0.019	0.022	0.020	0.017

Table 3-12: Mean normalized distributed force and standard deviation of the mean (no back support).

		Inflation Pressure Combination							
Sub-region	Parameter	A (0,0)	B (0.75, 0.75)	C (1.5, 1.5)	D (0, 1.5)	E (0, 1.5)	F (0.75, 1.5)	G (user selected)	H (1.5, 0.75)
M01	mean \bar{F}	0.078	0.085	0.042	0.061	0.088	0.071	0.061	0.057
	SD	0.026	0.036	0.024	0.028	0.040	0.038	0.035	0.033
M02	mean \bar{F}	0.069	0.058	0.041	0.039	0.067	0.058	0.051	0.035
	SD	0.012	0.016	0.015	0.015	0.019	0.014	0.016	0.014
M03	mean \bar{F}	0.151	0.154	0.149	0.174	0.142	0.145	0.154	0.181
	SD	0.032	0.037	0.037	0.051	0.038	0.028	0.037	0.027
M04	mean \bar{F}	0.155	0.155	0.169	0.186	0.148	0.154	0.166	0.183
	SD	0.021	0.019	0.023	0.024	0.026	0.021	0.026	0.023
M05	mean \bar{F}	0.077	0.085	0.097	0.071	0.096	0.096	0.086	0.067
	SD	0.041	0.037	0.041	0.060	0.030	0.030	0.047	0.014
M06	mean \bar{F}	0.055	0.065	0.084	0.049	0.085	0.079	0.062	0.062
	SD	0.015	0.010	0.015	0.013	0.019	0.011	0.009	0.011
M07	mean \bar{F}	0.021	0.027	0.032	0.015	0.040	0.034	0.022	0.016
	SD	0.019	0.024	0.028	0.018	0.035	0.027	0.017	0.008
M08	mean \bar{F}	0.013	0.018	0.023	0.009	0.027	0.024	0.016	0.016
	SD	0.007	0.010	0.013	0.006	0.015	0.011	0.007	0.008
M09	mean \bar{F}	0.076	0.072	0.063	0.057	0.082	0.076	0.068	0.061
	SD	0.024	0.025	0.022	0.024	0.031	0.024	0.022	0.023

Figures 3-5 to 3-7 illustrate the mean contact normalized force, area and pressure, respectively, distributed over nine regions on the seat cushion for the eight inflation pressure combinations. The results are compared for both sitting postures, B and NB. It is clearly shown that in-general (with and without back support) 20% to 36% of the seated human body weight is supported by the IT regions (M03 and M04) and 8% to 18 % by the thighs region (M05 and M06). The rest of the body weight is carried onto the side wings (M02 and M09) with 7% to 14%, the regions under the knees (M07 and M08) with 1.2% to 6% and the tail bone (M01) with 4% to 10% of the total seated body weight. Depending on the cushion inflation pressure, the contact force ratios change and in some cases only a minimal contact between the subject body and the region may exist.

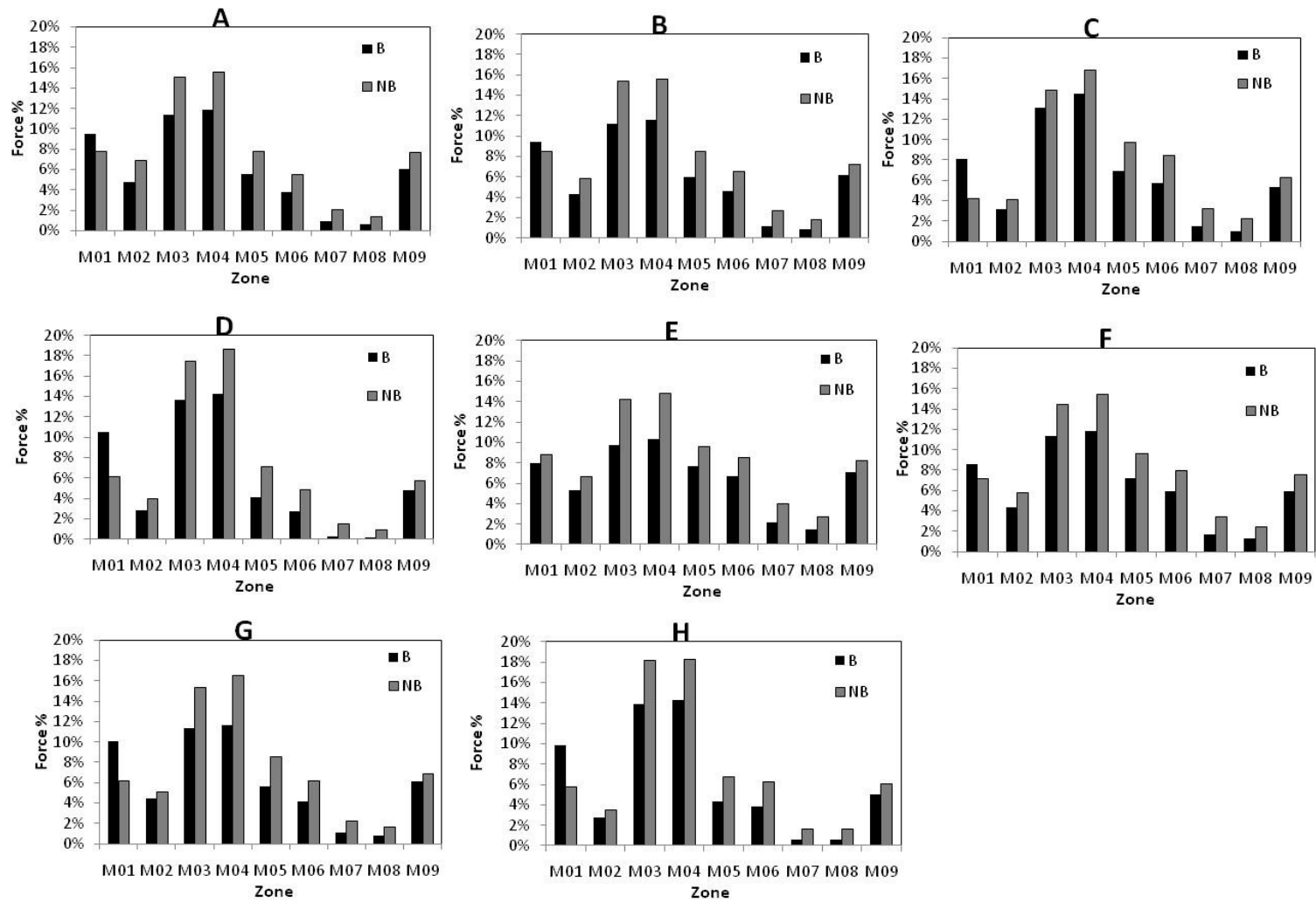


Figure 3-5: Normalized force distribution over the nine sub-regions of the seat pan corresponding to different in flat ion pressure combination (A to H).

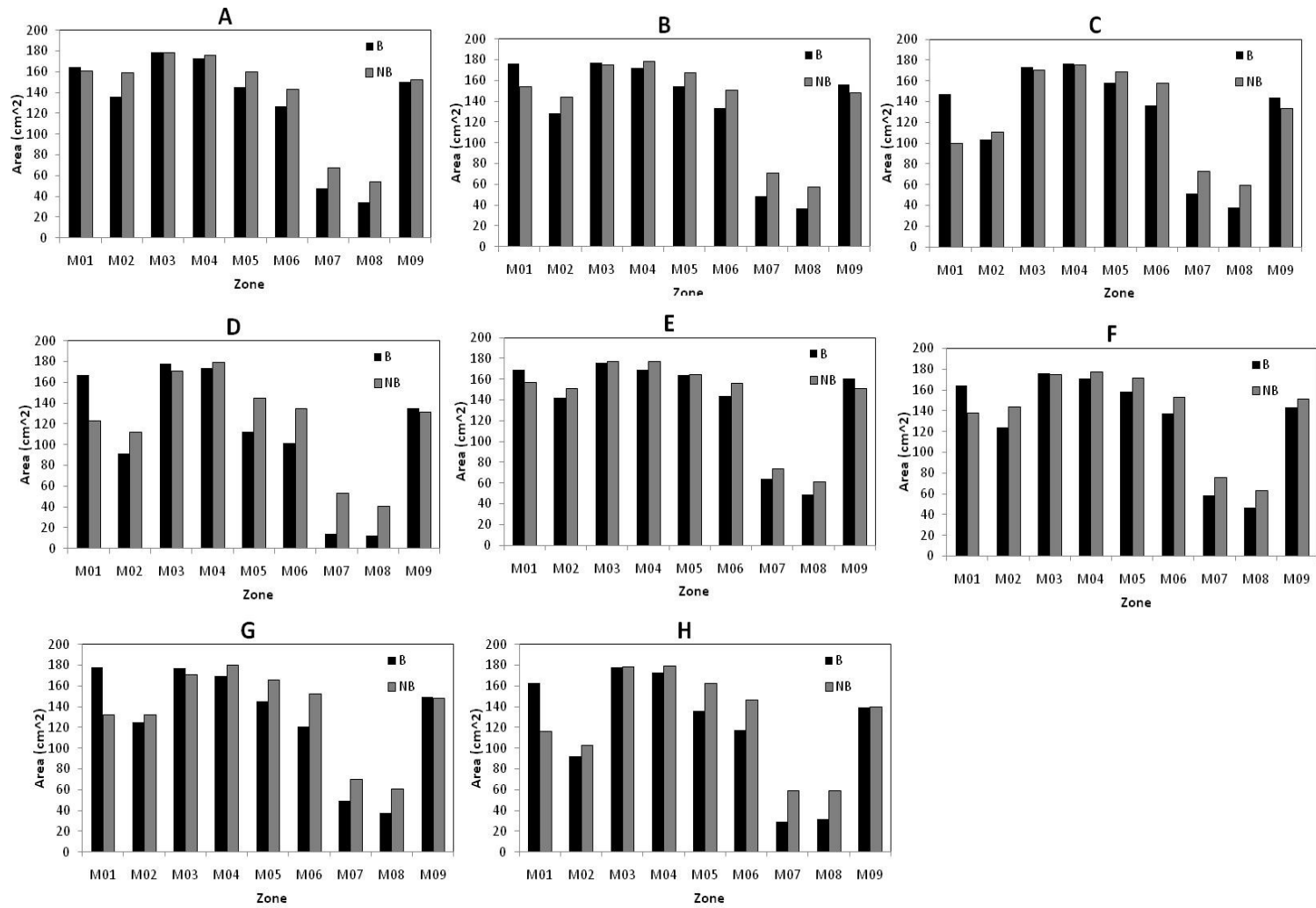


Figure 3-6: Contact area distribution over the nine sub-regions of the seat pan corresponding to different inflation pressure combination (A to H).

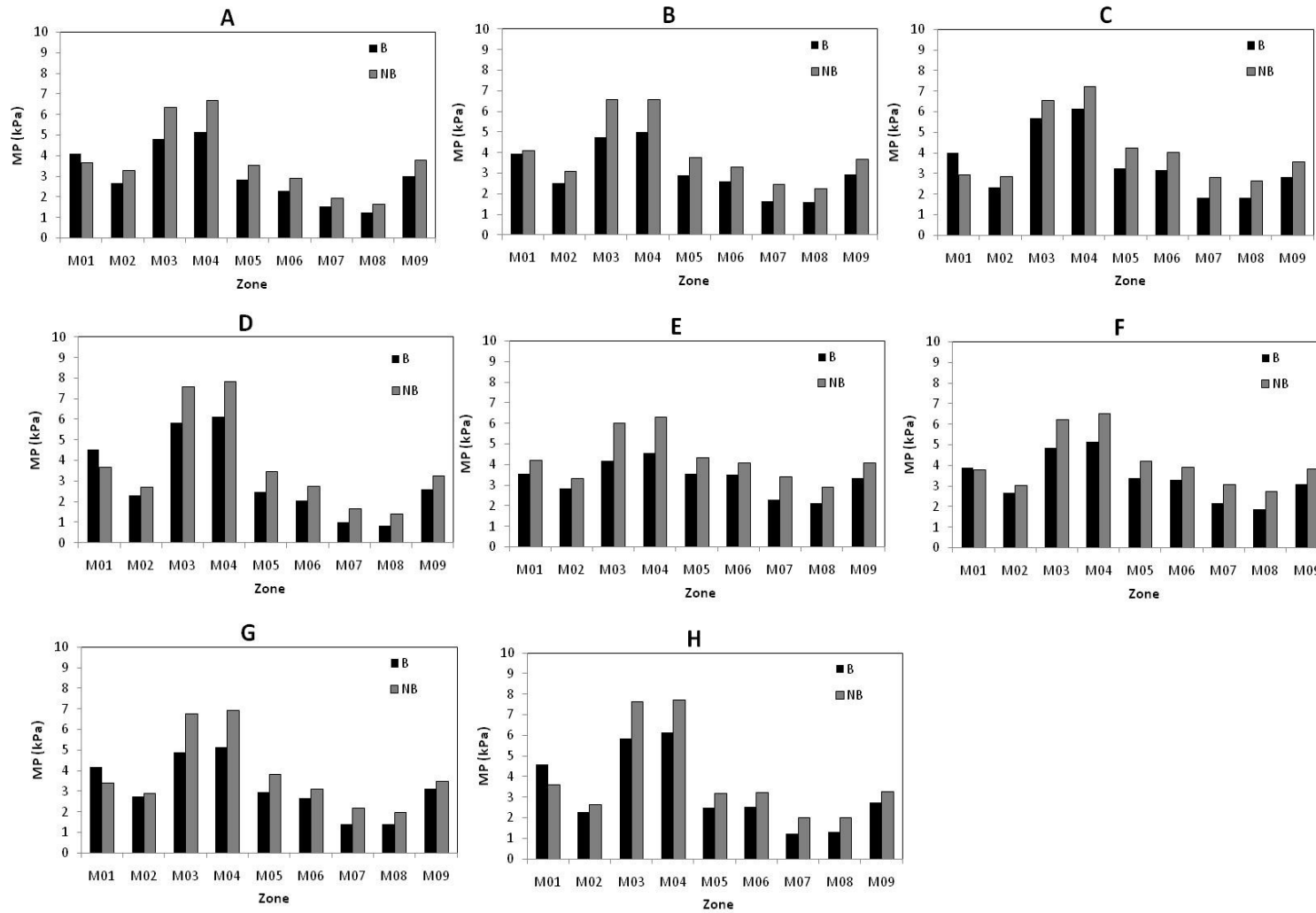


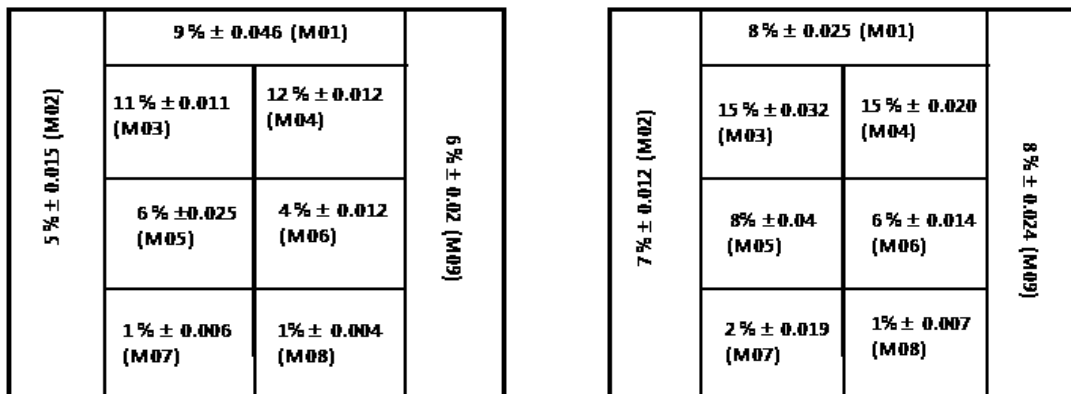
Figure 3-7: Mean pressure distribution over the nine sub-regions of the seat pan corresponding to different inflation pressure combination (A to H).

3.4.3 Correlation between subjective evaluations and objective force distributions

Although a few studies have proposed a contact force/pressure-based objective measure of the seating comfort, its correlation with subjective comfort sensation has not been established [19, 25, 32, 38]. In this study, the correlation between the subjective assessment and the objectively-measured force distribution is attempted. For this purpose, the force distributed over different regions of the seat are derived and normalized with respect to total body weight in order to account for variations in the subjects' weight. The normalized force distribution over the nine seat segments, presented in section 3.4.2, are considered in conjunction of subjective rankings of comfort sensation for all the inflation pressure combinations (A to H). While attempts were also made to correlate the contact area and mean pressure with the subjective rankings, the results in this study have been limited to correlations with normalized force only. This was attributed to wide variation in contact area and mean pressure among the subjects, and lack of an adequate normalization factor to reduce the extent of variability in these measures. The normalized force distributed over each individual sub-region across the subject population together with the mean subjective ranking of the same region was evaluated to identify a correlation if any. Among all the pressure settings, the one with highest comfort ranking (5) was reported as the most comfortable force distribution. The analyses were performed for both sitting posture involving supported and unsupported back.

The subjective rankings of the seat with different inflation pressures were initially analyzed. The results revealed that the subjects were not capable of distinguishing between rankings 4 (comfortable) and 5 (very comfortable). Same conclusion was made for the ranking 1 (very uncomfortable) and 2 (uncomfortable). Therefore the data corresponds to rankings 4 and 5, and 1 and 2 were combined to define a clear judgment of a 'comfortable' and 'uncomfortable' setting. This suggests that the chosen pressure combinations or the test

population were not sufficient to identify the degree of comfort and discomfort. The ranking 3 was considered as an uncertain judgment and thus excluded from the analysis. The subjective data could thus be grouped in ‘comfortable’ or ‘uncomfortable’. Such a grouping would be considered inadequate for assessing seating comfort. The correlations of these groups with the objective measures, however, could yield significant knowledge, particularly a methodology for further studies. Figure 3-8 summarizes the mean normalized force distribution for each sub-region of the seat, which were derived for the seat inflation pressure setting judged as the most comfortable by the subjects. This pressure setting corresponded to setting (A) with completely deflated air bladders under the thighs and the ITs. These results suggest that the subjects in general preferred a soft seat with un-inflated air bladders under the ITs and the thighs regions. The seating compliance in this case is provided by the PUF layer of the cushion. This is most likely attributed to the shape and position of the air bladders inside the air cushion, which assume an oval profile when partially or fully inflated. The oval shape of the inflated air bladders contributes to localized pressure concentration under the ITs and thighs region and yield a sensation of discomfort.



a) Full back support (B)

b) No back support (NB)

Figure 3-8: Mean normalized force distributions of individual sub-regions of the seat cushion judged as most comfortable by the subjects.

The results further suggest that a cushion with large number of small size air bags would be more desirable so as to limit the localized pressure concentrations. In both sitting postures, with and without the back support, the normalized force in the thigh regions is substantially smaller than those in the tail bone, side wings and the IT regions. This suggests that the subjects prefer to have just enough pressure under the thighs to provide postural support in addition to distribute the force evenly; however, most of the force is carried onto the IT regions regardless of the backrest support condition.

The results also showed that an increase in the force distribution in the tail bone region provided more comfort sensation when changing the sitting posture from no back support to a fully supported back. This is explained by the fact that sitting with a supported back yields greater contact of the tail bone with the seat. The small difference observed between the left and the right regions (thighs, knees, wings and the ITs) are partly attributed to the individuals non-symmetrical sitting habit and in-part to the resolution of the measurement system. Results also showed that the subjects were not generally able to distinguish comfort and/or discomfort feelings within the knees region. This is attributed to the fact that the knees were not always in contact with the seat cushion for some of the subjects, only partial or minimal contact could be observed for other subjects. The contact of the knees with the seat was mainly influenced by the cushion length and the subject anthropometry. Shorter subjects felt excess contact force under their knees due to relative short upper legs. On the other hand, taller subjects did not experience knees contact with the seat cushion.

During the subjective evaluations, the subjects were asked to adjust the cushion inflation pressure under the buttocks and the thighs regions to a level judged to be most comfortable. This pressure setting was labeled as (G) in Table 3-4.

Table 3-13: Mean force percentage distribution of the user-selected cushion inflation pressure (G), with and without the back support.

Region	Full back support	No back support
	F %	F %
M01	10.1%	6.1%
M02	4.4%	5.1%
M03	11.4%	15.4%
M04	11.6%	16.6%
M05	5.7%	8.6%
M06	4.1%	6.2%
M07	1.1%	2.2%
M08	0.8%	1.6%
M09	6.2%	6.8%

The mean force distribution corresponding to this user-selected inflation pressure combination were subsequently evaluated and summarized in Table 3-13.

3.5 Summary

In this chapter it was attempted to correlate the subjective comfort evaluation to objective measures of a prototype air cushion seat. The overall seat cushion area was divided into 9 regions and the interface force, area and mean pressure were individually measured using a pressure mat technology as described in section 2.4.2. In order to simulate different cushion stiffness in different regions (M01 to M09) the air bladders were inflated according to eight pressure combinations described in Table 3-4. In order to minimize the seating asymmetry influence, the air bladders on the right and left hand sides of the cushion were internally connected. The inflation pressures were selected so that localized pressures were created on different regions to be subjectively evaluated. The measurements were repeated for two sitting postures, fully supported back and unsupported back. By performing intra-subject variability analysis the mean percentage of the seated body weight supported by the seat cushion was determined for both sitting postures, with and without backrest. In addition

to that, the mean overall force, area and the mean pressure distribution on the seat cushion was derived across eight pressure settings, however, due to the large inter-subject variability the overall and the segmental force was normalized to the subject body weight to provide comparison among different cushion inflation pressures. The results of this analysis were further analyzed to correlate the subjective evaluation to that of the measured mean force percentage value.

The results discussed in this chapter are mainly based on static sitting and do not take into account the effect of dynamic excitations through the seat suspension and the effect of the human body in perception of dynamic comfort. Hence, in the following chapter, the dynamic comfort of the seat occupant is studied via vibration attenuation effectiveness of the PUF cushion and the seat suspension.

4. DYNAMIC ANALYSIS OF SUSPENSION SEAT

4.1 Introduction

The comfort analysis of a vehicle seat in a dynamic environment requires evaluation of transmitted vibration to the seated body. The vibration of most road and off-road vehicles occurs in the frequency range of 0.5 to 5 Hz, while the magnitudes of such vibration are invariably large in many road and off-road vehicles [42]. Prolonged exposure to such low frequency and large amplitude vibration has been associated with various health risks among the exposed human drivers. The heavy road and off-road vehicles generally employ suspension seats to limit the exposure to vehicle whole-body vibration, since the magnitudes of vertical vibration are most significant in majority of these vehicles. Considering that the human body is most sensitive to whole body vibration in the low frequency range, the suspension seats are designed with a low natural frequency (1 to 1.5 Hz). Such low frequency suspensions may yield excessive dynamic suspension deflection that could exceed the permissible travel under severe excitations arising from discrete obstacles in the terrain. The resulting dynamic interaction with the travel limiting stops cause high magnitude shock motions of the seated body, which are known to pose greater health risks [42, 51]. A suspension seat should thus be designed to limit both shock and vibration transmission, which pose contradictory design requirements [42].

The prototype suspension seat considered in this study could provide a better design compromise in view of shock and vibration isolation. The suspension could be locked under operations involving very rough terrains or frequent abrupt terrain elevations such as pot holes, to limit excessive suspension travel. The air cushion in these situations would be expected to provide some vibration isolation in addition to adequate body support. Under

operations on terrains leading to continues vibration, both the suspension and the air cushion may be tuned to yield enhanced vibration isolation.

The majority of the seat suspensions of heavy vehicles employ air springs to achieve sitting comfort in a convenient manner. The variations in air spring pressure to achieve desired height directly influence the spring rate, and thus the natural frequency and the vibration attenuation properties of the suspension seat [42]. The prototype suspension seat with independently inflatable air bladders offers potential advantages in realizing desirable body support, although it may directly affect the vibration isolation properties of the suspension.

In this chapter, the vibration isolation effectiveness of the air cushion and the combined air-cushion-suspension seat are experimentally evaluated in the laboratory. The evaluations are performed with adult male subjects and a broad-band random vibration in the 0.5 to 20 Hz frequency range. A series of experiments are also performed to identify resonant frequencies and frequency response characteristics of the air cushion and the suspension, when loaded with a passive load.

4.2 Static and Dynamic Properties of the Seat Suspension System

The prototype seat cushion is applied to a typical air seat suspension, schematically illustrated in Figure 4-1. Apart from the minor differences in design, the seat suspension mechanisms are composed of an elastic and a dissipative component together with the elastic end-stops, and vertical and fore-aft adjustment mechanisms.

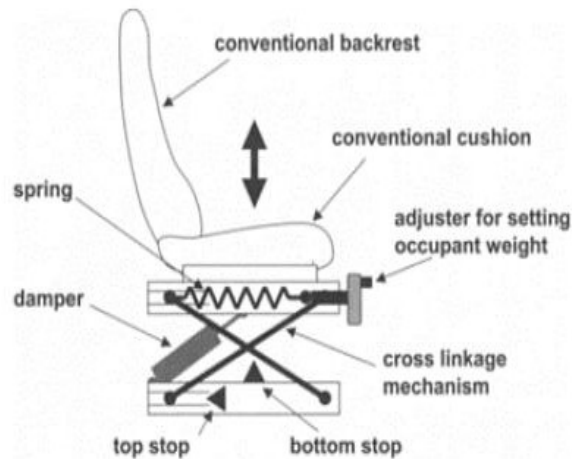


Figure 4-1: Typical suspension seat configuration [42].

The modern seat designs generally employ air bladders, which also provide variable sitting height in a convenient manner. The suspension system also includes a hydraulic damper for dissipation of vibration energy and to control the magnitude of resonant oscillations. Seat pan and cushion is supported on the spring and damper through a linkage mechanism that ensures nearly vertical motion of the seat. The suspension seats are designed to yield limited motion of the seated driver to maintain adequate visibility and access to controls. Owing to low natural frequency design, the control of relative body motion with respect to the cabin is realized by introducing elastic limit stops in the compression and rebound travel directions.

The vibration transmission properties of a suspension seat are directly related to the static and dynamic properties of its components. In particular, the force-displacement and force-velocity properties of the suspension determine the vibration transmission characteristics. The force-deflection properties of the air suspension may also be affected by the seated body weight. Consequently an experiment was designed to measure the static force-deflection properties of the suspension under different loads. For this purpose, both the

cushion and the damper were removed from the suspension and the suspension was installed in the test system described in section 2.3.1. The SAE indenter with the load cell was positioned between the seat pan and the fixed horizontal beam to measure the total force, while the displacement was measured using the LVDT integrated within the hydraulic actuator.

The measurements were performed under three different pre-loads: 46.2, 53.8 and 70.2 kg. These represent the total body weight supported by the seat for standee body weight of 61.6, 71.73 and 93.6 kg, assuming that the 75% of the total body weight is supported by the seat [53]. A harmonic displacement at a very low frequency of 0.088 Hz was subsequently applied with magnitude of 0.025 m. The resulting force was measured and plotted against the displacement to identify the static stiffness of the suspension. The results presented in Figure 4-2 show dependence of stiffness on the pre-load and considerable hysteresis attributed to the friction of mechanism joints. The stiffness constants of the suspension were identified from the mean force-deflection curves corresponding to each pre-load near static equilibrium, which are summarized in Table 4-1. Assuming negligible contribution of the cushion these would yield suspension natural frequency in the range of 1.9 to 2 Hz. This mathematical estimation of the natural frequency is compared to that of the experimental results and detailed discussion is provided in section 4.4.

Table 4-1: Static stiffness of the seat suspension.

Pre-Load (kg)	46.2	53.8	70.2
Equivalent Stiffness (kN/m)	7.2	8.0	10.0

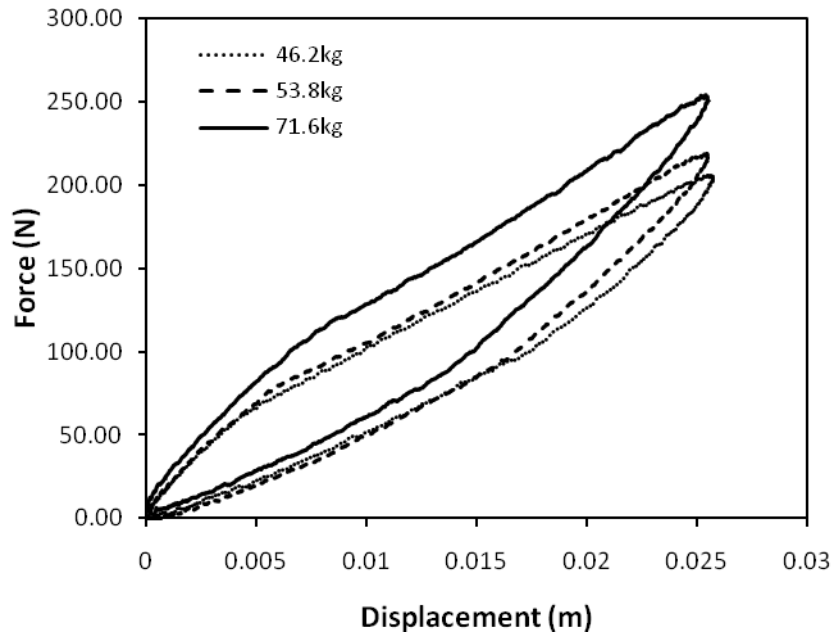


Figure 4-2: Static force-deflection characteristics of the seat suspension.

The damping properties of the suspension were characterized in the laboratory by installing the damper in the same experimental setup between the hydraulic actuator and the fixed inertial beam. A force transducer was installed between the damper and the fixed beam to capture the dynamic force developed by the damper. A linear velocity transducer (LVT) was mounted within the actuator in parallel with the LVDT to measure the damper velocity. The force-velocity properties of the damper were measured under harmonic excitations of different amplitudes in the 0.5 to 8 Hz frequency range. The measured data acquired under different inputs revealed consistent force-velocity characteristics. The results revealed nearly constant but asymmetric damping in compression and rebound. The damping coefficients in compression and rebound were identified from the measured data at each excitation frequency.

Table 4-2 illustrates the force-velocity properties measured under displacements varying in the range of 10 to 25 mm. The table reveals relatively smaller damping constant

in rebound. An increase in the excitation frequency resulted in lower rebound damping constant, most likely due to entrapped air in the hydraulic fluid at higher speeds. The damping coefficients in the 1-5 Hz frequency range, however, exhibit peak variation of approximately 10% about the mean values. The mean values could thus be considered to describe the damping properties reasonably accurately.

It should be noted that the prototype suspension considered in this study employs two dampers in a parallel arrangement. Furthermore, each damper is mounted with inclination within the linkage mechanism, as illustrated in Figure 4-3. The effective vertical damping constant would thus be lower and could be estimated from the geometry. In Figure 4-3, H refers to the damper height in static equilibrium and a is the damper inclination, while Z_s and Z_0 define the vertical motions of the pan and the seat base, respectively.

Table 4-2: Measured damping coefficients in compression (C_c) and rebound (C_r).

Frequency [Hz]	1	2	3	4	5	8	Mean (1-5 Hz)
C_c (N.s/m)	217.30	211.92	200.69	185.64	179.26	152.17	198.96
C_r (N.s/m)	101.59	103.77	105.88	112.03	103.90	104.14	105.43

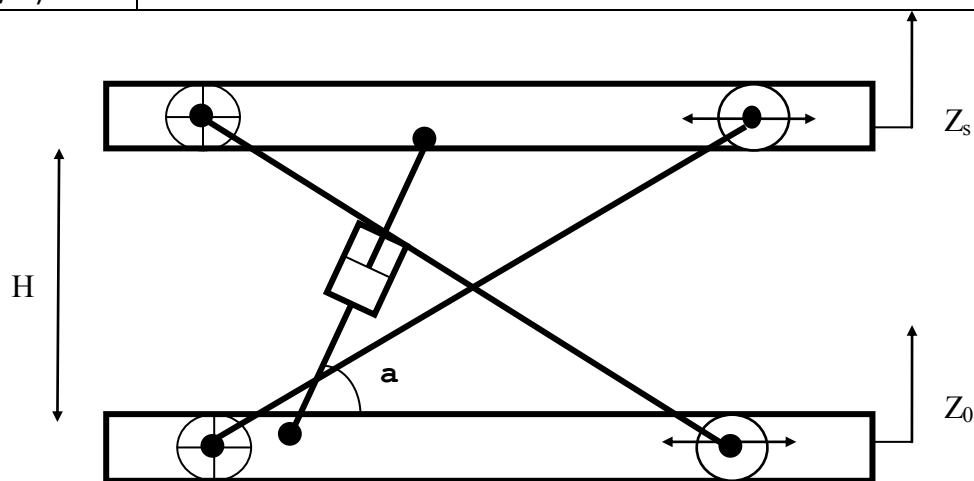


Figure 4-3: Orientation of the dampers within the suspension mechanism.

4.3 Experimental Characterization of Vibration Isolation of the Suspension

Comfort evaluation of a seat is a complex function of both the static and dynamic characteristics of seat, in addition to the vibration environment of the vehicle. The cushion stiffness influences the static comfort the most, while the static and dynamic properties of the suspension and the cushion directly influence the vibration comfort properties of the seat. Furthermore, the human occupant tends to absorb appreciable vibration energy that is attributable to visco-elastic properties of the biological system [27]. Vibration isolation properties of seats are therefore mostly evaluated in conjunction with the seated human body. Owing to the complexities associated with the characterization of the human body dynamics, the dynamic comfort or vibration properties of seats have been mostly evaluated through field or laboratory measurements. An international standard, ISO 7096 [16] defines a standardized laboratory test methodology for assessing vibration performance of suspension seats.

4.3.1 Test Apparatus

The vertical vibration attenuation properties of the suspension seat with the inflatable cushion were measured in the laboratory using the whole-body vehicle vibration simulation (WBVVS). The simulator comprises a vibration platform supported by two servo-hydraulic actuators capable of generating vertical motion up to ± 100 mm in the 0 to 50 Hz frequency range. A closed-loop wave form generator and controller (Vibration Research Corporation) is interfaced with the servo-controller to synthesize a desired vibration spectrum. The suspension seat is installed on the vibration platform, which is also equipped with a steering column, as schematically shown in Figure 4-4.

The following safety features have been implemented in the simulator design in order to ensure the safety of the human subjects and to fulfill the requirements for the human-suspension seat system:

- Emergency safety switches available on the mock steering wheel, servo control panel and on the hydraulic pump controller to interrupt the WBVVS motion by either the subject or the experimenter in an emergency situation. The activation of any of the emergency stop brings the simulator platform to a halt in a ramp-down manner.
- The magnitudes of the compressive and extensive forces are continuously monitored and limited, while the peak acceleration and displacement levels of the excitation signal are limited to 2 m/s^2 and 0.1 m , respectively.
- The simulator is designed to reproduce the vibration environment of various vehicle classes in the frequency range of 0.5 to 35 Hz .
- The simulator is designed to safely support the load due to the platform, subject, seat and the steering wheel.
- Slow ramp-up and ramp-down circuits are incorporated to the controller interface to ensure smooth operation under transient motions, start up, stoppage and in case of power interruption.

The vibration attenuation property of a seat is invariably evaluated from the acceleration measured at the human-seat interface. For this purpose, a standardized seat-pad accelerometer, a 200 mm round elastic disc with an integrated three-axis accelerometer, is widely used [23]. This standardized measurement system, however, could not be adequately installed on the air cushion, particularly where the air bladders in the vicinity of the IT region were inflated to a higher pressure. Consequently, two micro-accelerometers, ADXL 330, were mounted on the cushion over the air bladders within the IT region, which provided adequate contact between the seated body and the cushion.

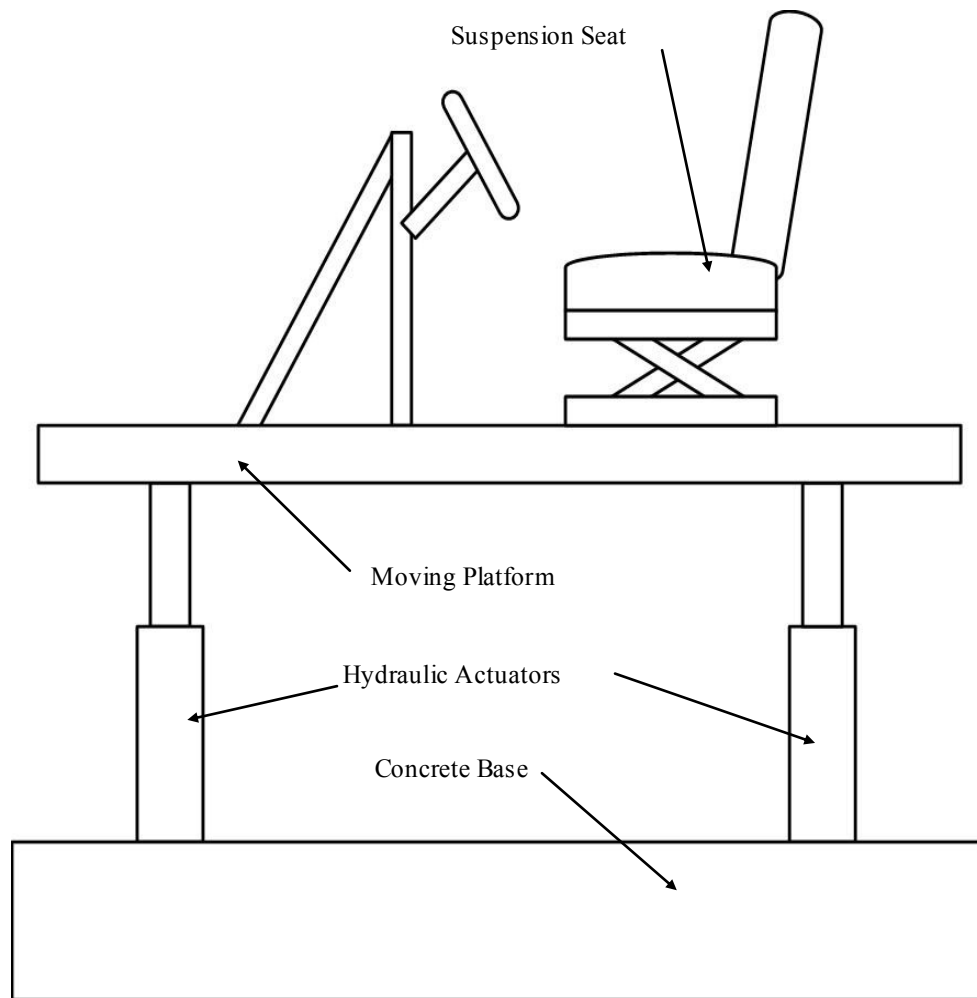


Figure 4-4: Schematic of the whole-body vehicle vibration simulator (WBVVS) and the test suspension seat.

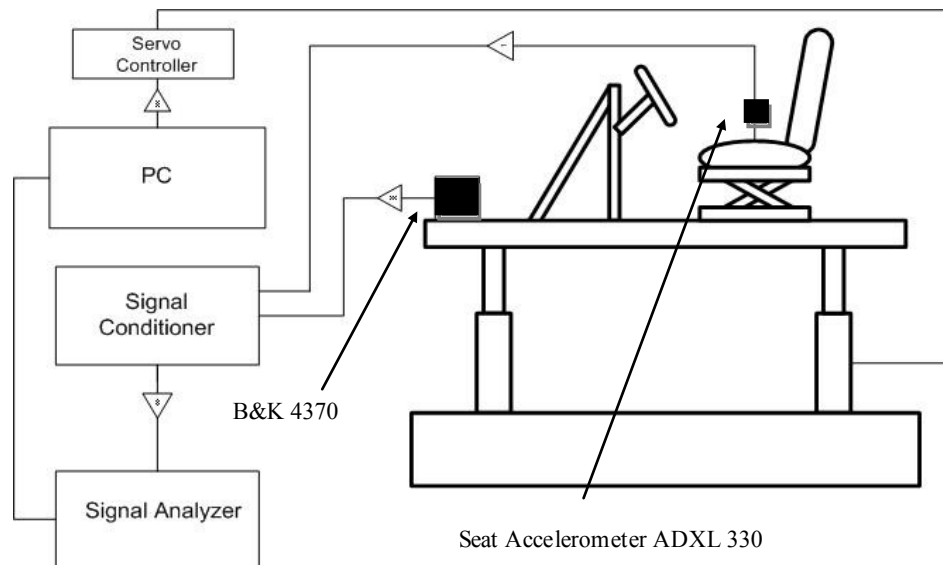


Figure 4-5: Schematic of the measurement and data acquisition system

The validity of this alternate measurement system was also examined by installing the standardized seat pad accelerometer B&K 4322 on the cushion together with the two ADXL accelerometers. The measurement performed with relatively low bladder pressure revealed very similar results with peak deviation below 5%. Furthermore, both the ADXL sensors revealed nearly the same acceleration levels. Consequently, the signal from one of the ADXL sensors was considered for evaluation of vibration transmitted to the seated body.

A single-axis accelerometer, B&K 4370 was also placed on the WBVVS platform for measurement of acceleration due to excitation. This accelerometer signal also served as the feedback to the vibration controller. The signals from the cushion and platform accelerometers were acquired in the multi-channel vibration analyzer (Puls Labshop) for subsequent analysis. Figure 4-5 shows a schematic of the measurement and data acquisition system.

4.3.2 Test Matrix

The experiment was conducted to characterize vibration transmission properties of the prototype cushion, and the combined cushion and suspension seat. The test matrix involved: (i) two levels of sitting posture; (ii) one levels of input vibration; (iii) two levels of suspension configuration; and (iv) three adult male subjects.

The vibration transmission performance of a seat is strongly affected by various posture-related factors. These include the hands support (steering wheel, armrest, or thigh) and the backrest. In this experiment two alternatives were selected for the backrest configuration: (i) full backrest support and (ii) no backrest. In each case the subjects were seated with their hands on the thighs, knee angle 110° , and in case of the full back supported, a backrest inclination angle of 100° was adopted. The seat height was adjusted to normal driving posture as a function of subject height and knee angle of 110° . The vibration controller was programmed to synthesize a white-noise random signal with nearly constant acceleration power spectral density (PSD) in the 0.5 to 20 Hz frequency range. For this purpose, the closed-loop controller was employed to synthesize vibration spectra of overall root mean square (rms) acceleration of 0.5 m/s^2 .

The experiments were performed with two different configurations of the seat. In the first configuration, the suspension was locked so as to access the vibration transmissibility of the air cushion alone. In the second configuration, the suspension was un-locked in order to measure the vibration isolation properties of the suspension with an air cushion. These also include the variations in pressure in the bladders in the vicinity of the buttocks and thighs in the 0 to 6.88 kPa (1.0 psi) range. The selected pressure combinations are summarized in Table 4-3. In the un-locked suspension configuration, the mechanism was adjusted to ensure adequate sitting height.

Table 4-3: Selected combinations of individual bladders pressure coupled with locked and un-locked suspension.

Inflation Pressure kPa (psi)			
Locked Suspension		Un-Locked Suspension	
Buttocks Area	Thighs Area	Buttocks Area	Thighs Area
0.00 (0.0)	0.00 (0.0)	0.00 (0.0)	0.00 (0.0)
3.44 (0.5)	3.44 (0.5)	3.44 (0.5)	3.44 (0.5)
6.88 (1.0)	6.88 (1.0)	6.88 (1.0)	6.88 (1.0)

4.3.3 Test Method

Each subject was advised to sit on the seat with selected configuration. The individual cushion bladders were then inflated to achieve an inflation pressure combination in accordance with those listed in Table 4-3. The seat height was adjusted to achieve desired height and knee angle, while the subject was advised to place his hands on thighs. The WBVVS was subsequently operated to realize the desired platform vibration and acceleration signals were acquired in the Pulse analyzer. The acquired data were analyzed using a bandwidth of 100 Hz with a frequency resolution of 0.125 Hz. Each measurement was repeated three times.

Apart from the above, additional measurements were performed to identify the resonances of the seat and the seat structure. For this purpose, the seat pad accelerometer was mounted directly on the cushion, as shown in Figure 4-6 (a), and the seat was loaded with two different passive loads (53.8 and 70.2 kg). The WBVVS was operated to generate 0.5 m/s^2 white noise excitation. The vibration excitation and response data were acquired for both locked and un-locked suspension, and analyzed in the Pulse analyzer. The measurements revealed significant backrest motion and two distinct peaks in the frequency response, in the vicinity of 7 and 12 Hz. In order to identify the resonance attributed to the

backrest, additional measurements were undertaken with the seat with locked suspension but without the cushion. In this case the seat pad accelerometer was mounted directly on the seat pan as shown in Figure 4-6 (b), while it was ensured that the backrest hinge was sufficiently tight.

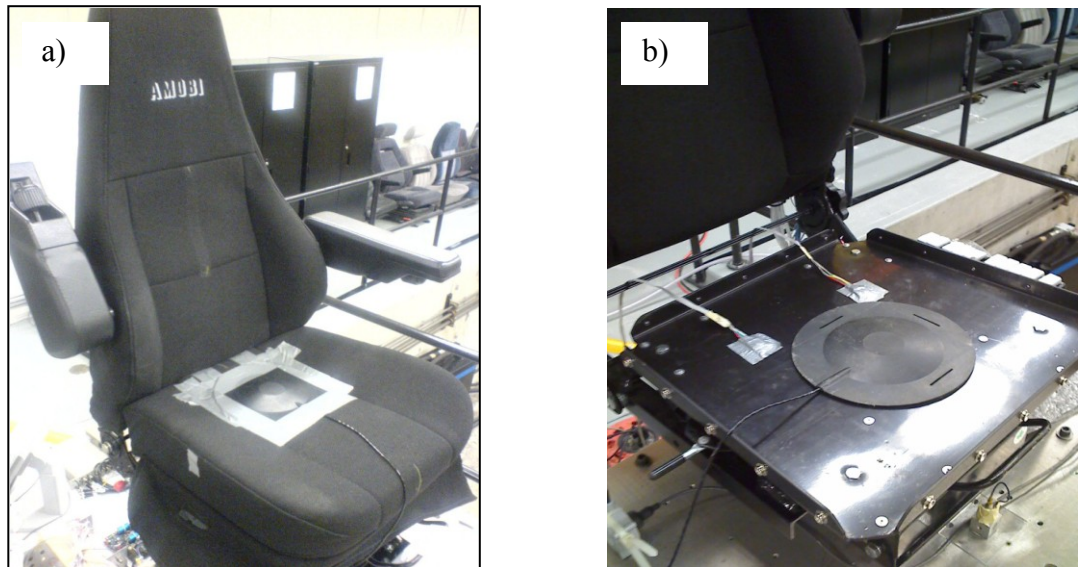


Figure 4-6: Three-axis seat accelerometer pad mounted on (a) seat cushion and (b) seat pan.

The measured acceleration signals were analyzed to derive the vibration transmission properties of different seat configurations with either passive load or the human subjects. The H_1 function available in the analyzer was applied to derive the magnitude of vibration transmissibility such that:

$$T_z = \frac{S_{Z_0 Z_s}}{S_{Z_0}} \quad (4.1)$$

where T_z is the acceleration transmissibility of the seat, $S_{Z_0 Z_s}$ is the cross-spectrum of the base and seat accelerations, and S_{Z_0} is the auto spectrum of the platform acceleration.

4.4 Resonant Frequencies of the Seat and the Structure

The vibration transmissibility analysis of the coupled human-seat system requires identification of those resonance frequencies, which are directly correlated to human health and comfort. These frequencies include cushion and suspension damped natural frequencies, which not only relate to effectiveness of the seat in attenuating vibration, but also reveal important information related to suspension design.

Apart from the primary suspension, the resonances of other components also contributed to the vibration transmitted to the seated body. The data acquired with the locked suspension without the cushion are used to identify the structural resonance. The frequency response characteristics of the structure loaded with two different passive loads and subject to 0.5 m/s^2 broad-band excitation are illustrated in Figure 4-7. The results show three notable peaks in acceleration transmissibility of the seat structure. An increase in the passive load from 55 kg to 70.2 kg resulted in shifts of the two primary peaks to lower frequencies. These two lower frequency peaks in the 7.0 - 8.5 Hz and 11.5 - 13.5 Hz ranges were attributed to be the deflection of the backrest and compression of the seat pan of the locked suspension.

In order to identify the frequencies corresponding to specific modes, the data acquired with backrest stiffened was considered. The acceleration transmissibility of the seat with stiffened backrest is also illustrated in Figure 4-7. This measurement was performed with seat loaded with 70.2 kg passive load. The results show that the peak near 7 Hz shifts towards a higher frequency of 7.6 Hz, when the backrest is stiffened. The second primary peak near 11.45 Hz, however, shifts only slightly. It was thus concluded that the peaks occurring in the 7 - 8.5 Hz, 11.5 - 13 Hz and 20 - 23 Hz correspond to backrest pitch, the plastic pan and steel frame deformation modes, respectively.

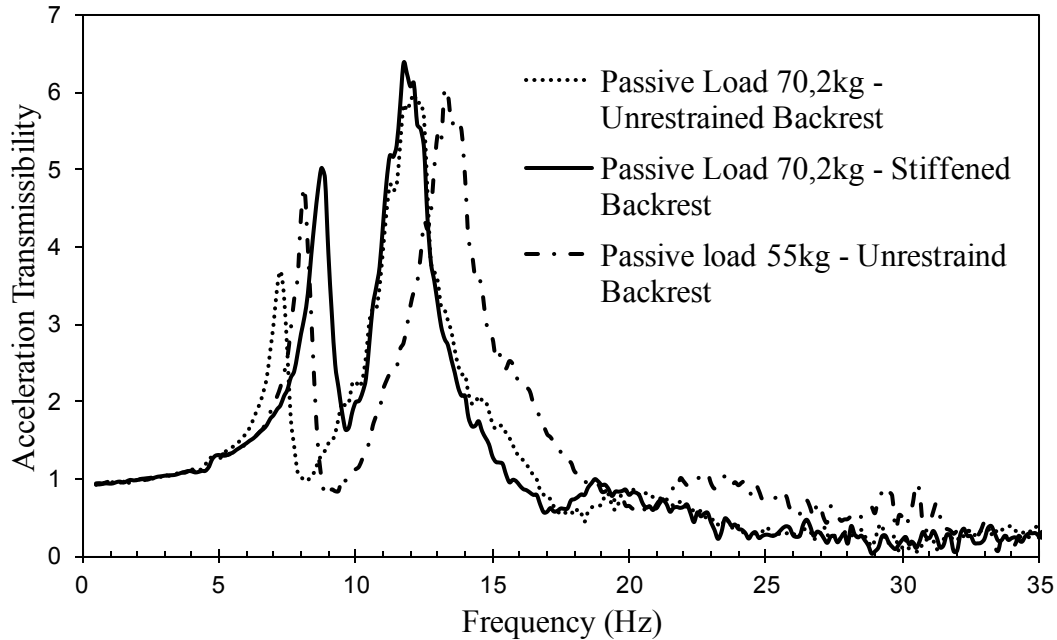


Figure 4-7: Acceleration transmissibility of the seat with locked suspension and no cushion.

The primary resonant frequency of the suspension alone was identified from the acceleration transmissibility response of the seat without the cushion, while loaded with different passive loads (53.8 and 70.2 kg). The results showed primary suspension frequency in the 4-5 Hz range, and an increase in the load resulted in lower damped natural frequency and acceleration transmissibility depending on the load, as it would be expected. The results also revealed that the peak transmissibility ranges from 2.75 to nearly 3.5 as shown in Figure 4-8. Furthermore, the resonant frequency (4-5 Hz) is considered to be high for applications in heavy vehicle and is close to vertical mode resonance of the seated body. The addition of the human body to the seat, however, would alter the resonant frequency and the peak magnitude.

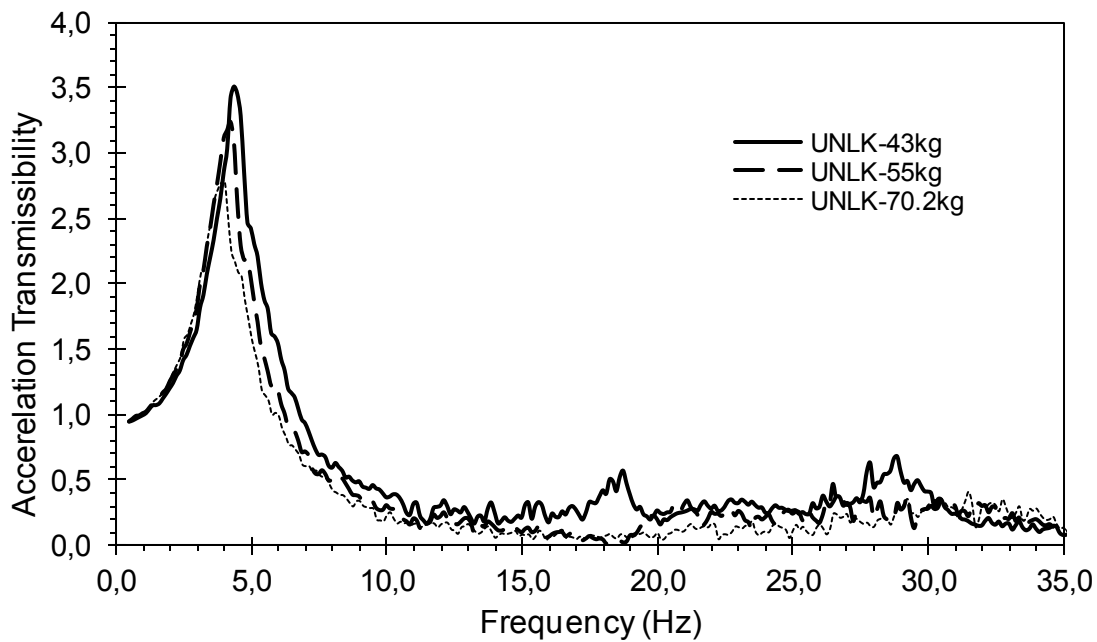


Figure 4-8: Suspension acceleration transmissibility with different passive loads.

The prototype seat employs polyurethane foam (PUF) in the cushion integrating inflatable bladders. The air cushion is composed of 4 air bladders located under the PUF layer and supported by the plastic tray, as shown in Figure 4-9. The resonant frequency and vibration transmission properties of the cushion rely upon the inflation pressure in individual air bladders, which could be conveniently identified from acceleration transmissibility of the seat with locked suspension. Cushion acceleration transmissibility test was thus performed by installing two ADXL 330 accelerometers within the PUF layer. The accelerometers were installed in the region of the cushion where human IT bones are located. This ensured maximum adhesion between the seated body and the cushion. Furthermore, the resonance frequency of the PUF cushion layer alone was measured by completely deflating the air bladders and locking the suspension.



Figure 4-9: Cushion air bags' location on the plastic support.

Figure 4-10 illustrates the measured acceleration transmissibility of the PUF layer loaded with a passive load and subject to 0.5 m/s^2 white-noise excitation. The results suggest a resonant frequency near 5.5 Hz due to the PUF layer alone. The peak transmissibility approaches nearly 6.5, which is attributed to very light damping due to the PUF layer. The results show an additional smaller peak in the 12 - 13 Hz range, which is attributed to deflection of the plastic seat pan.

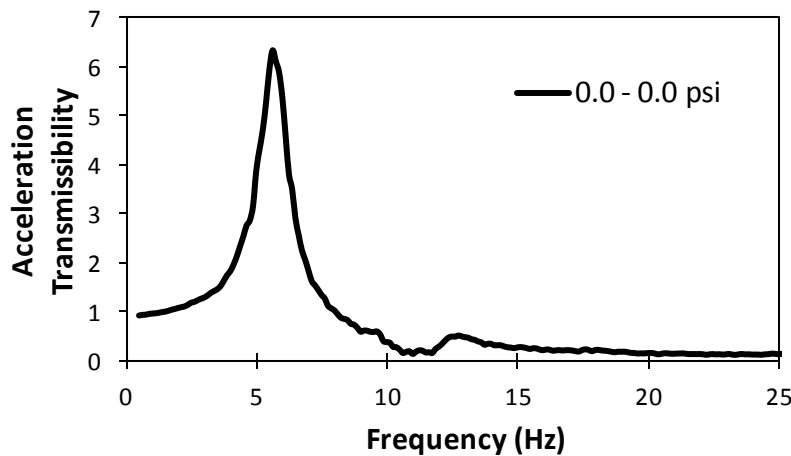


Figure 4-10: PUF cushion acceleration transmissibility with a passive load of 70.2 kg and locked suspension.

Table 4-4: Seat components resonance frequencies - 70.2 kg passive load.

Suspension	Frame	Plastic Tray	Cushion	Backrest
4 Hz	20 Hz	12 Hz	5.5 Hz	7 Hz

Table 4-4 summarizes the identified resonant frequencies corresponding to different components of the seat loaded with 70.2 kg passive load. The above results in view of the suspension resonant frequency contradict the frequencies corresponding to measured suspension stiffness, presented in Table 4-1. The suspension natural frequency was estimated to be in the 1.9-2.0 Hz range on the basis of the measured stiffness, while the above results suggest this frequency in the vicinity of 4 Hz. The resonant frequency of the suspension was also expected to be somewhat lower than 2 Hz considering the additional mass due to pan, the seat structure and the seat rails. This prompted additional investigations and experiments. Upon examination of all the suspension components, it was found that the two dampers used in the suspension were misaligned due to defective bushings. Figure 4-11 illustrates a pictorial view of the defective damper bushing. No further attempts, however, were made to acquire alternate dampers for the subsequent experiments.

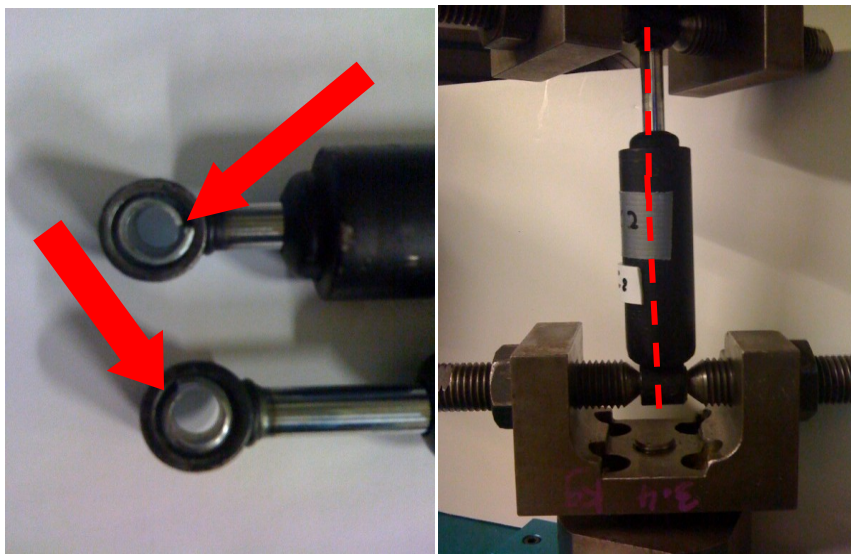


Figure 4-11: Bushing defects (left) and resulting damper eyes misalignment (right).

4.5 Vibration Transmissibility of the Inflatable Cushion

4.5.1 Cushion Vibration Transmissibility Loaded with Passive Loads

Figure 4-12 illustrates the acceleration transmissibility characteristics of the cushion with selected inflation pressure combinations. The notation ‘0-0’, ‘0.5-0.5’ and ‘1-1’ refer to the inflation pressure of the buttocks and the thighs air bladders, as presented in Table 4-3. The results are presented for three different passive loads: 46.2, 53.8 and 70.2 kg. The results show that the peak acceleration transmissibility increases with increase in the cushion air pressure beyond 3.44 kPa (0.5 psi) under the light and medium load, which is mostly attributed to greater deformation of the PUF layer. Increase in the bladder pressure causes greater force at the load-cushion interface leading to higher deformations of the PUF layer. The cells of the PUF layer may collapse under either higher pressure or load leading to reduced damping effect of the PUF layer. Furthermore, the cushion can be considered as a series combination of elasticity of the PUF layer and the bladder. The bladder with lower inflation pressure undergoes larger deformation and thus larger pressure change. The progressively hardening property of the air under compression in this case would yield higher effective stiffness. A lightly inflated bladder may encounter bottoming under a high load leading to higher overall stiffness.

The lower inflation pressure combinations (0 and 3.44 kPa) yield lower peak frequency with increase in the passive load. The results thus show a slight reduction in the resonant frequency with increasing pressure. The frequency, however, increases slightly with increase in the load for the lower inflation pressures of 0 and 3.44 kPa, as shown in Figure 4-13. This is attributed to partial or total bottoming of the lightly inflated air bladders under higher loads.

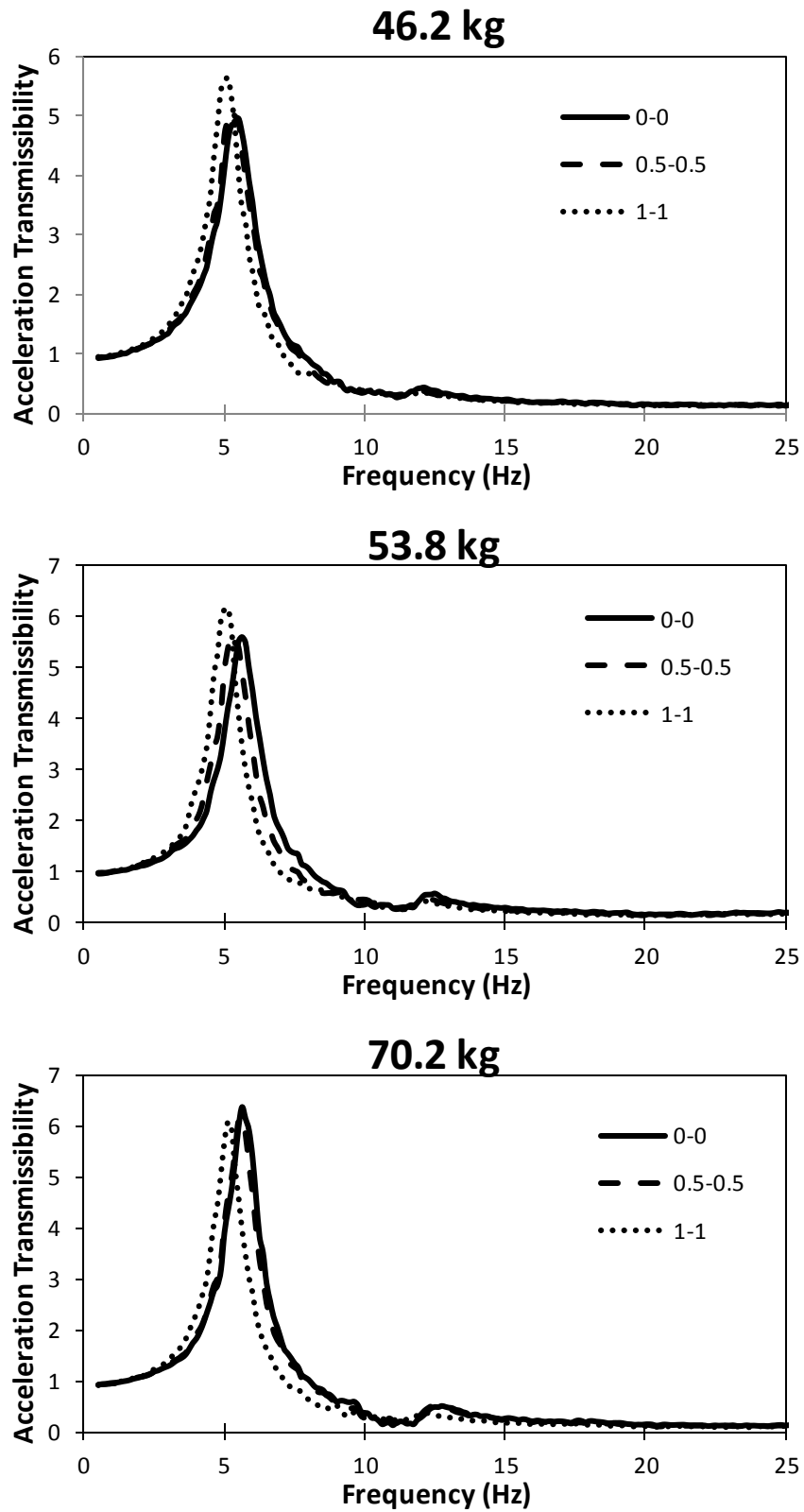


Figure 4-12: Comparison of acceleration transmissibility characteristics of the seat with locked suspension and cushion air bladders inflated at different pressures (passive loads).

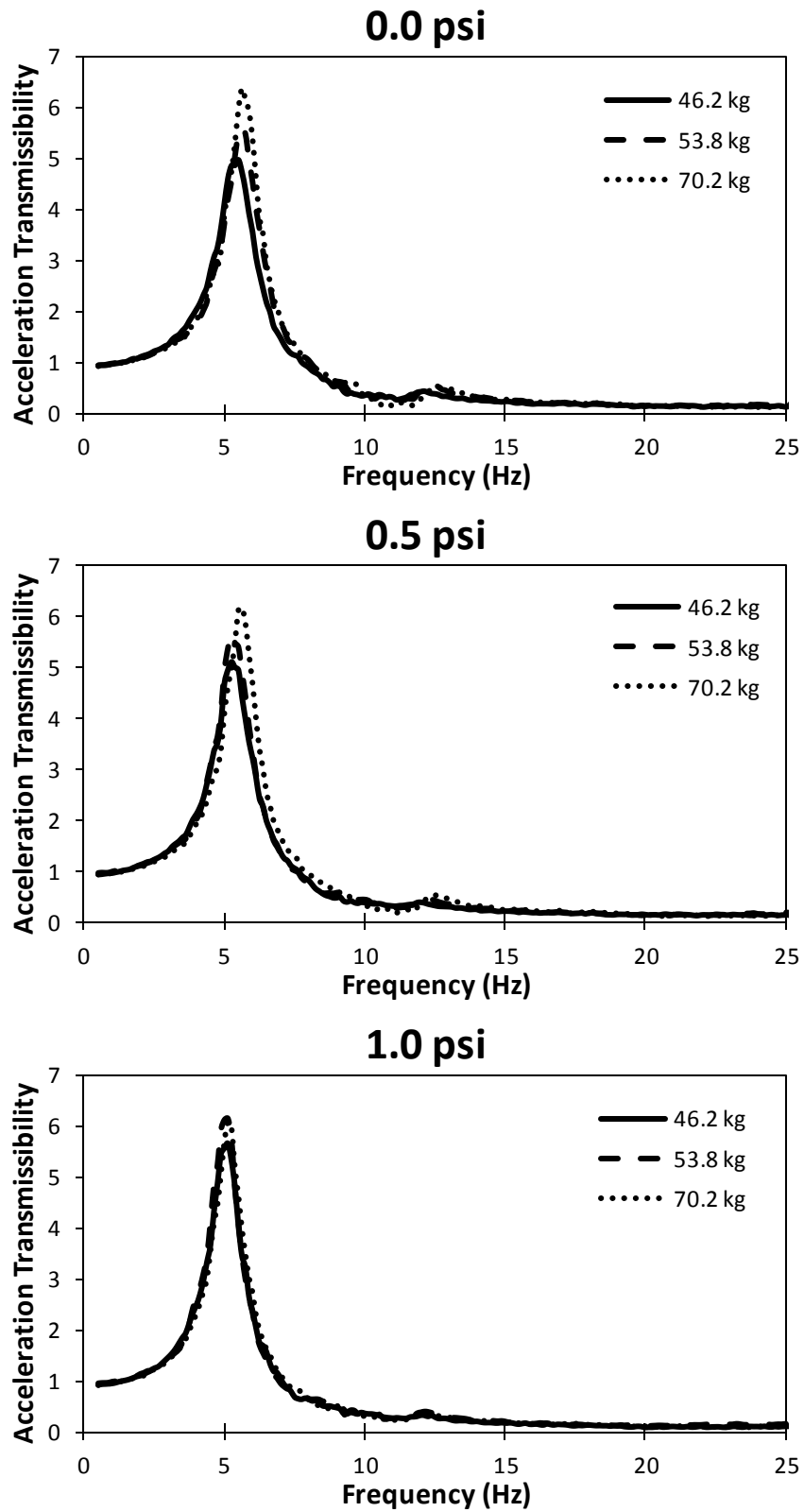


Figure 4-13: Comparison of acceleration transmissibility characteristics of air cushion with different passive loads and inflation pressures (locked suspension).

4.5.2 Cushion Vibration Transmissibility Loaded with Human Subject and Influence of Back Support

Interaction of the human body with the seat can greatly influence the vibration transmissibility response of the seat. In chapter 1, the factors affecting the driver's comfort were studied extensively. One of the factors that considerably contributes to driver's perception of comfort is the backrest. In order to assess the vibration transmissibility of the cushion with human subjects, the experiments were performed with three adult male subjects (total body weight of 61.6, 71.73 and 93.6 kg) and different combinations of inflation pressures. The body mass supported by the seat cushion was measured for each subject with 0 kPa inflation pressure. These were measured as 46.2, 53.8 and 71.2 kg. The human body weight, here after, is denoted by the masses supported by the seat, even though the total body masses are considerably larger. Furthermore, the passive loads used in the prior experiments were configured as per the three subjects used in the study.

Figure 4-14 illustrates the acceleration transmissibility characteristics of the inflated cushion with and without the backrest under 0.5 m/s^2 excitation. The notation 'B' and 'NB' refer to sitting with back fully supported and not supported at all, respectively. The inflation pressure of the buttocks and the thighs air bladders was selected to be 0.0, 0.5 and 1.0 psi for three different subjects with body weights of 43, 55 and 71.2 kg. The results show that the peak acceleration transmissibility decreases with increase in seated cushion load. Comparison between the results of the tests with passive load and those of the tests with human subjects revealed that the acceleration transmissibility is considerably less when using human subjects. This is related to biodynamic contribution of human subjects when it interacts with seat in a vibrating environment.

Figure 4-14 also illustrates the presence of a secondary peak in the acceleration transmissibility when using human subjects. This was attributed to the backrest deflection

mode in the 8-10 Hz frequency range. The magnitude of the secondary peak increased when using a backrest compared to the case with no backrest, which can be related to backrest pitch resonance.

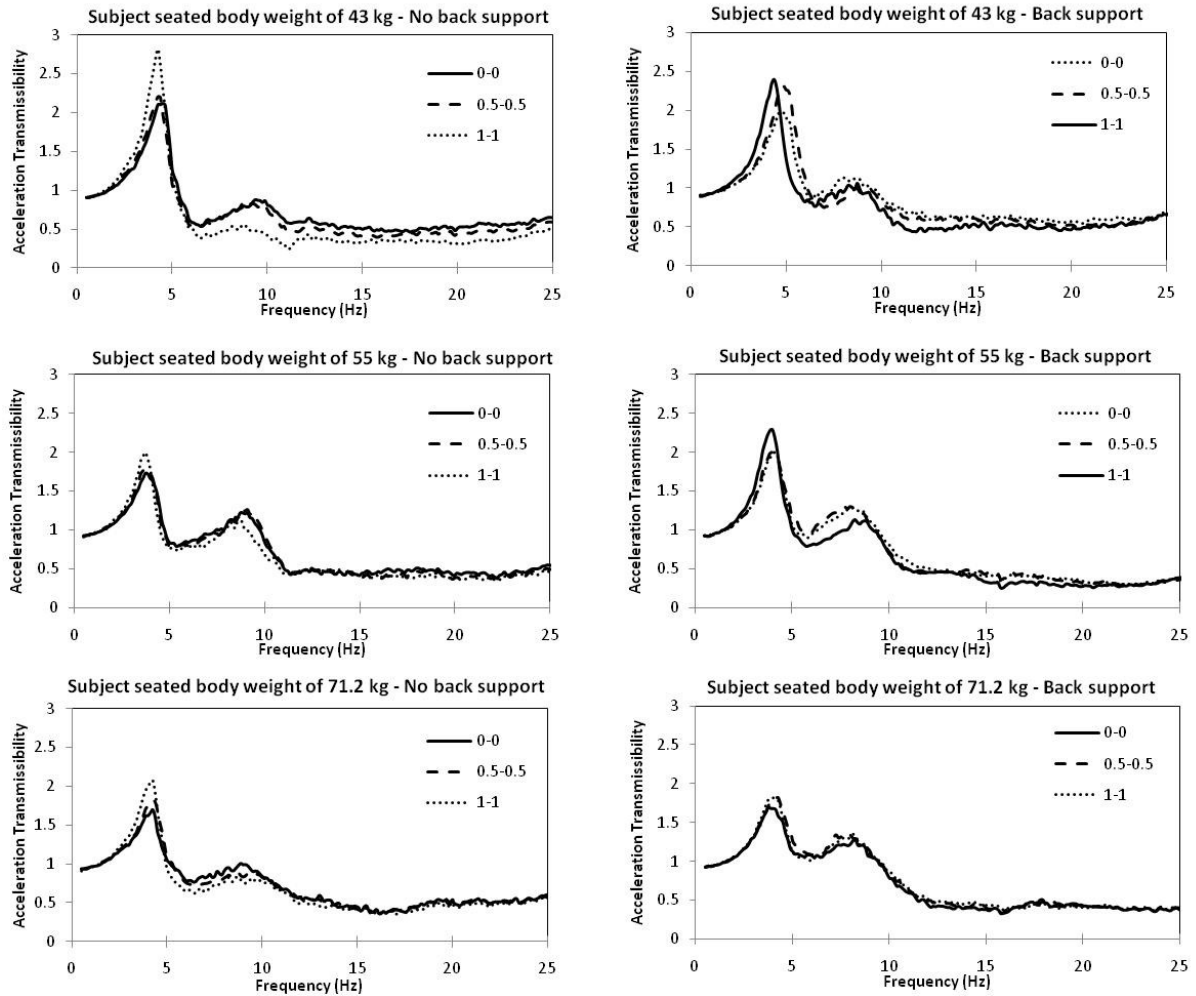


Figure 4-14: Comparisons of acceleration transmissibility characteristics of the cushion with three different subjects and three inflation pressure combinations (locked suspension).

4.6 Vibration Transmissibility of the Suspension Seat

Relative vibration isolation performance of seats can be assessed either through field measurements or in the laboratory using passive loads or anthropodynamic manikins or human subjects. From the results shown in Figure 4-14, it is evident that human body contributes considerably to the overall vibration isolation performance. This has also been reported in [58]. It is thus, essential to account for human body contributions. A few designs of anthropodynamic manikins have evolved in the recent years to eliminate the use of human subjects in the laboratory tests. The manikins are designed on the basis of the biodynamic behavior of the seated body exposed to vertical vibration. A recent study has assessed two different anthropometric manikins for their applications in assessing vibration isolation properties of seats [60]. It was concluded that the vibration response of the seat loaded with manikins differ considerably from those of human-seat system.

Apart from the contribution of the human biodynamics, the interactions of the human body with the environment of the vehicle cabin affect the posture and the contact area at the human-seat interface. Backrest contact, arm rests and the foot supports, can all alter the transmitted vibration to the seat [60], which cannot be characterized by the manikins. Alternatively, the vibration isolation properties of seats may be conveniently evaluated using passive loads, when the suspension natural frequency and excitation frequency are well below the primary resonance of the body. This approach however, yields considerable error in the measurements under excitations close to the body resonance and high magnitude excitations.

In this thesis, the seat suspension responses are investigated in terms of base to cushion vibration transmissibility, for both the locked and un-locked suspension. For the sake of convenience, the measurements of the relative vibration transmissibility responses of the seat

with locked and unlocked suspension are performed only with passive loads. The responses of the locked suspension describe the acceleration transmissibility of the cushion alone, while those of the un-locked suspension yield performance of the combined inflatable cushion and suspension system.

4.6.1 Vibration Transmissibility of Seat Suspension Loaded with a Passive Load

Figure 4-15 illustrates the acceleration transmissibility characteristics of the suspension with selected inflation pressure combinations. The notation ‘0-0’, ‘0.5-0.5’ and ‘1-1’ refer to the inflation pressure of the buttocks and the thighs air bladders, as presented in Table 4-3. The results are presented for three different passive loads: 46.2, 53.8 and 70.2 kg. The results show that the peak acceleration transmissibility decreases with increase in the passive load, however, the cushion inflation pressure has negligible influence on the acceleration transmissibility. Comparisons of responses of the locked and un-locked suspension modes clearly show the vibration attenuation by the suspension, which is attributed to effective suspension damping mechanism. Irrespective of the air cushion pressure, the peak acceleration transmissibility occurs around 3.8 Hz, which is considered as the resonant frequency of the suspension with air cushion. This resonant frequency is considered to be high in relation to the primary ride frequencies of the wheeled off-road vehicles to achieve adequate vibration isolation.

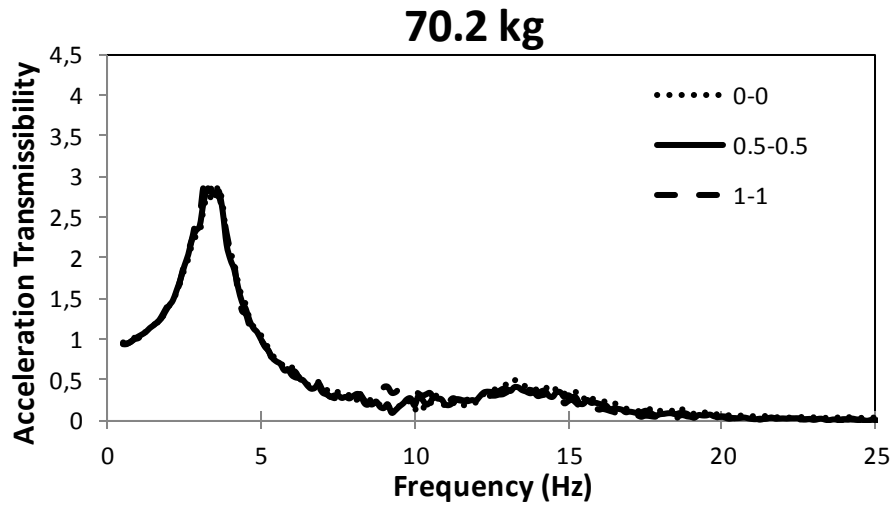
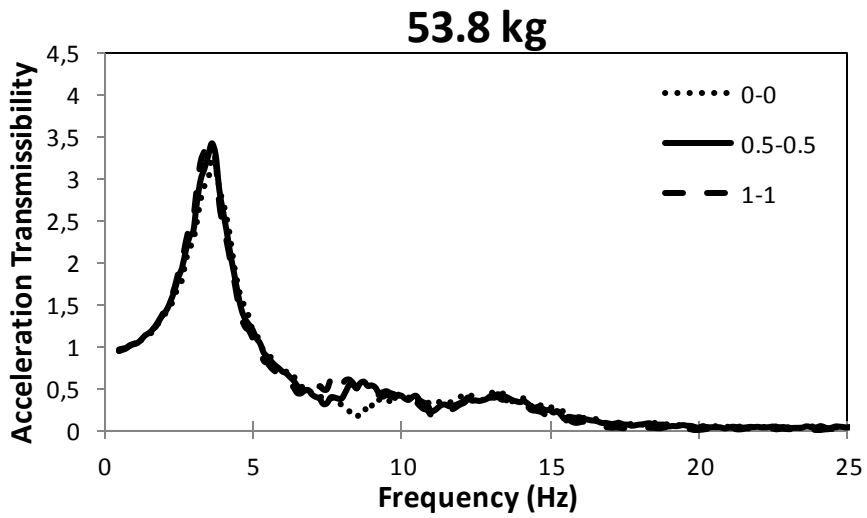
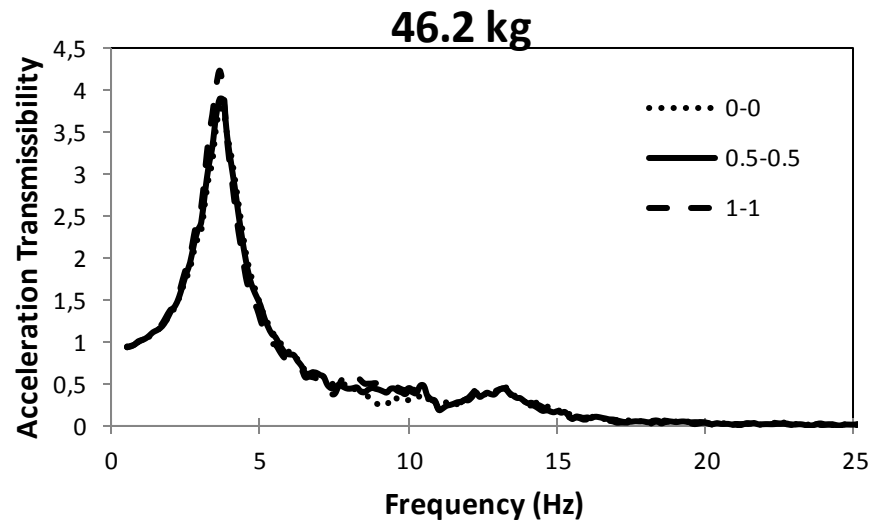


Figure 4-15: Comparisons of acceleration transmissibility characteristics of the suspension with different passive loads and inflation pressures (un-locked suspension).

Figure 4-16 further compares the vibration transmissibility of the seat with locked and unlocked suspension with uninflated cushion. The unlocked suspension exhibits primary peak near 3.8 Hz, denoted as ‘1’. The primary peak due to the locked suspension, labeled as ‘2’, occurs near 5.5 Hz. This is attributed to the resonance of the cushion with the PUF layer alone. The comparisons clearly show the vibration attenuation by the damped suspension. Considering that vast majority of the wheeled off-road vehicles cause substantial vertical ride vibration below 5 Hz, further design efforts are essential to reduce the suspension natural frequency. This may be realized by selecting appropriate damper mountings and suspension air bag with larger volume and lower pressure. The transmissibility responses also show additional minor peaks, labeled as ‘3’ and ‘4’ in the figure, which correspond to backrest pitch and plastic pan deformation, respectively. The results suggest that the suspension can effectively attenuate vibration above 5 Hz.

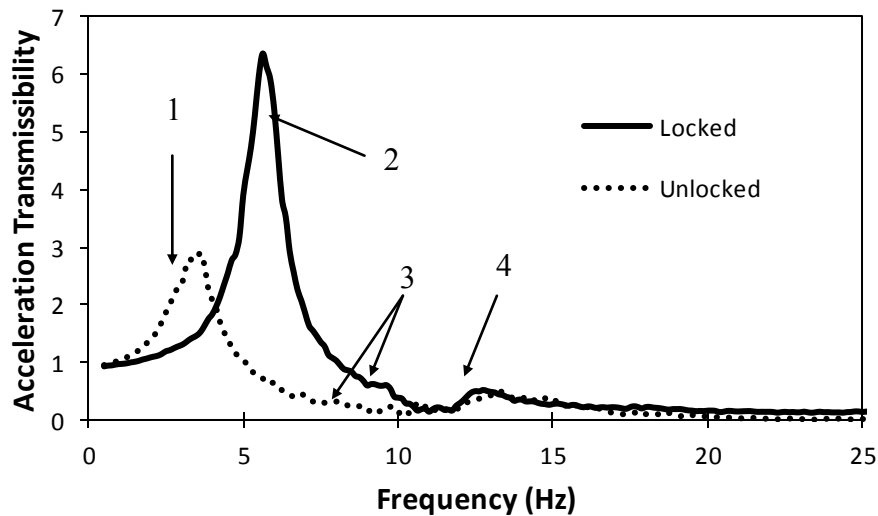


Figure 4-16: Comparisons of acceleration transmissibility of the locked and un-locked suspension (passive load = 70.2 kg; 0 psi air cushion pressure).

4.6.2 Vibration Transmissibility of Seat Suspension Loaded with Human Subjects and Influence of Back Support

The vibration attenuation performance of a suspension seat is strongly influenced by seated human body as it was illustrated in Figure 4-14. The vibration performance of the seat is also affected by many other factors such as body mass, seated body weight distribution on the cushion, interaction with the backrest, armrest and foot support. The international standard ISO-7096 [16], thus requires that the vibration attenuation performance of a suspension seat be investigated with human subjects of three different body masses. The vibration performance of the seat loaded with three different human subjects is thus measured in the laboratory. The measurements were performed using three subjects of total body masses of 61.6, 71.73 and 93.6 kg which yield seated body weight of 43, 55 and 71.2 kg, respectively, and 0.5 m/s^2 white noise random excitation. Each subject was advised to sit on the seat assuming two different postures: Upright with no back support (NB) and relaxed with back support (B). Figure 4-17 illustrates the vibration response characteristics of the seat with locked and unlocked suspension when loaded with passive load and human subject, while the subjects assumed no-back (NB) posture and the cushion inflation pressure of 0 psi. Figure 4-18 compares the acceleration transmissibility responses of the seat with unlocked suspension with subject sitting with two different postures; fully supported back and no supported back. The results show that the use of a back support causes the peak acceleration transmissibility to be slightly higher. This is attributed to the differences in the load supported by the cushion due to posture difference and to the biodynamics of the seated body. The use of back support tends to reduce the body mass proportion supported by the seat cushion and the suspension which transfers greater weight to the buttock region of the cushion. This tends to cause higher resonant peak, particularly for the medium and larger body masses.

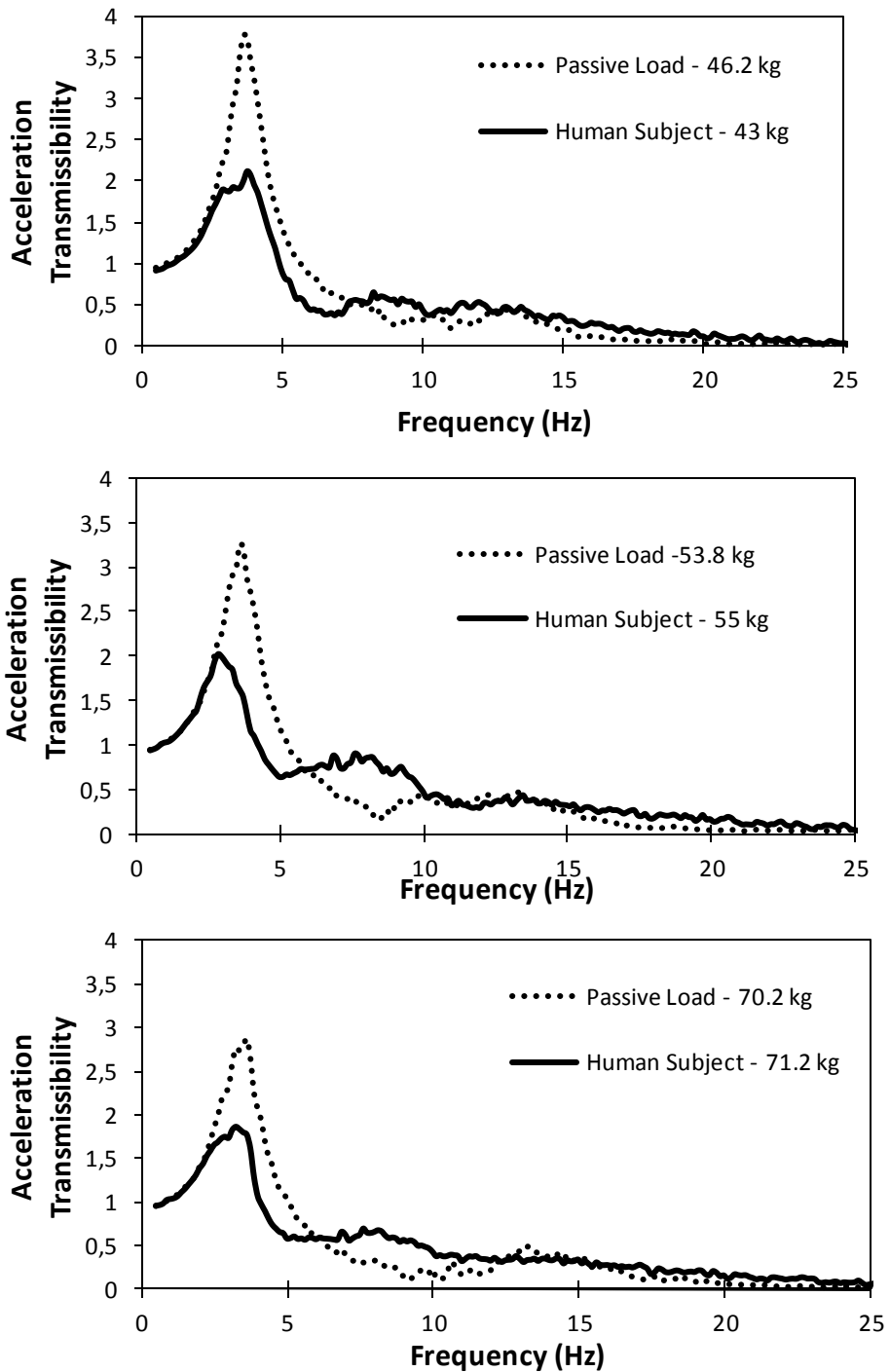


Figure 4-17: Comparisons of acceleration transmissibility of the seat suspension with passive load and human subjects sitting without back support and 0 psi air cushion pressure.

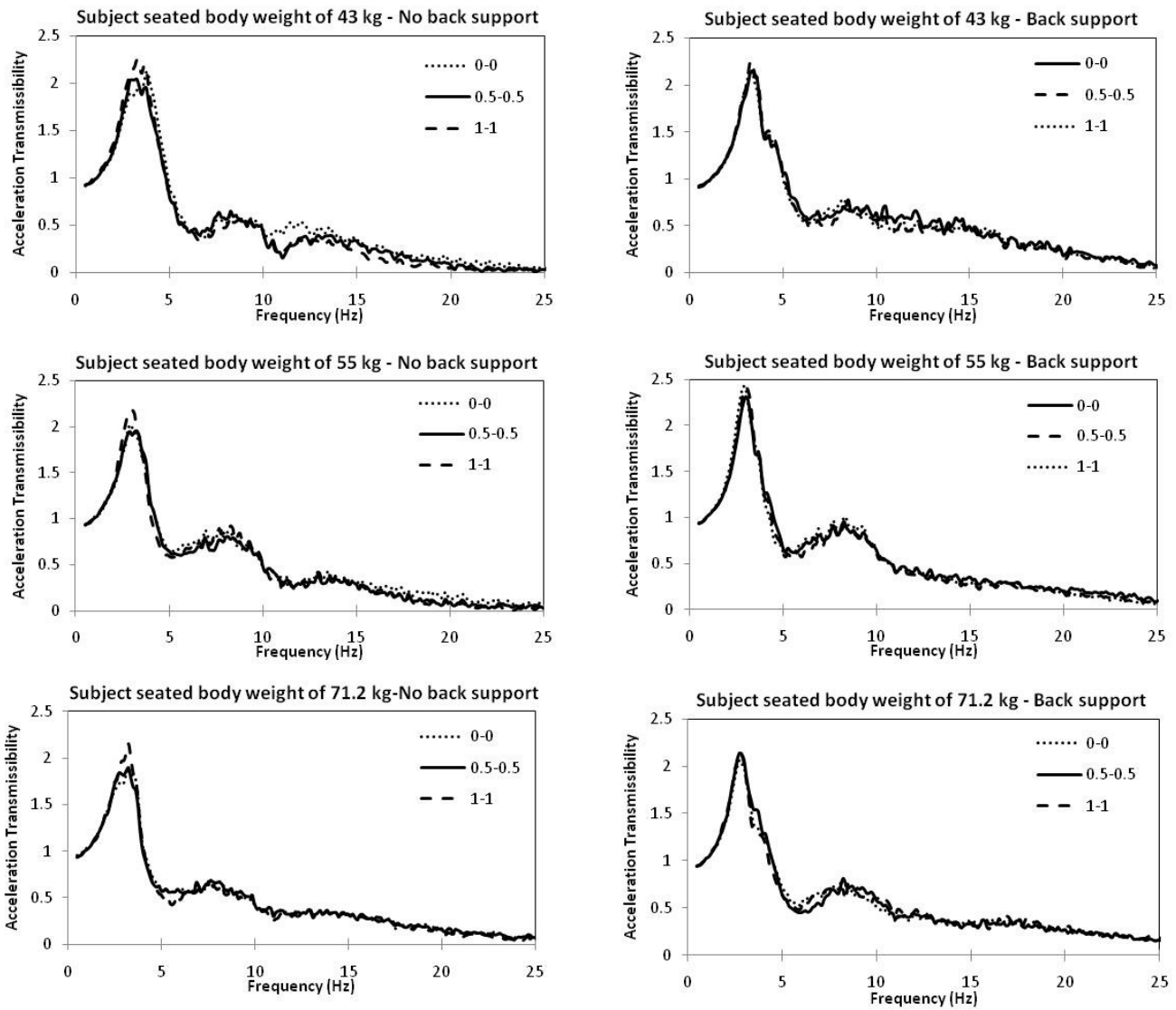


Figure 4-18: Comparison of acceleration transmissibility of the seat suspension with subject sitting with and without the back support (un-locked suspension).

4.7 Summary

In this chapter, the vibration attenuation performance of the prototype suspension seat was measured with passive loads and human subjects. The suspension components characteristics were also measured in the laboratory under different pre-loads and excitation magnitudes. The data could be used to develop component models and a model of the seat suspension system. Since the seat is equipped with built-in air bladders, the effectiveness of air cushion in vibration attenuation was also measured in addition to that of the PUF layer and the suspension mechanism. In order to distinguish the resonant frequency of each component, the vibration responses of the PUF layer, the air bladders and the suspension mechanism have been individually studied under controlled vibration environment. During the preliminary measurements, it was observed that the suspension pan deflection and the backrest pitch also contribute to vertical vibration responses of the seat in the higher frequency range. Vibration responses of the air cushion revealed that increase in inflation pressure yields increase in vibration transmissibility magnitude. An increase in the cushion load also resulted in higher transmitted vibration due to bottoming of the air bladder. The tests with human subject showed the significant human body's contribution in attenuation of vibration. Sitting with fully supported back, however, tends to increase the vibration transmissibility slightly.

5. CONCLUSIONS AND RECOMMENDATIONS FOR FUTURE WORK

5.1 Highlights of This Research Thesis

The comfort performance of automotive seats is a complex function of various seat design parameters such as cushion geometry, contours, stiffness and damping characteristics of the cushioning material. In addition to these, the seat static and/or dynamic characteristics contribute to the overall seat comfort to a great extent. The comfort performance of a seat, however, is related to subjective sensations in a highly complex manner, apart from its vibration attenuation performance.

This thesis research concerns the comfort performance analysis of a prototype seat with a vertical suspension and a cushion with a number of independently inflatable air bladders to provide controlled support for the body. The evaluations were performed using objective approaches through measurements at the human-seat interface pressure and vibration attenuation together with subjective evaluations of the support properties. The subjective evaluations were performed using a questionnaire for the subjects to rate the level of comfort/discomfort as a function of the inflation pressure.

A total of ten male subjects participated in the subjective and objective study of pressure distribution. The interface pressure was measured over nine segments at the human-seat interface and eight pressure combinations were created to simulate different cushion stiffness and contouring. The effect of backrest support was also investigated. The total contact area was divided into nine anatomical segments in order to study the pressure distribution and corresponding contact force over the individual segments. To eliminate the inter subjects variations due to variations in total body weight and buttocks contact area, the

segmental forces within each region were normalized to the total body weight. The proposed methodology permitted the identification of contact pressure, area and force in various segments that are considered comfortable by the subjects. The results, however, were found inconclusive for some of the anatomical regions. These were mostly caused by variations in subject's anthropometry such as height, buttocks and leg size.

The static and dynamic properties of the seat cushion were investigated using three different combinations of inflation pressures and two different indenters. The indenters included the 20 cm diameter disk recommended in SAE J1051 and a buttock-shaped indenter developed following the recommendations in ISO/DIS 16840-2.

The dynamic performance of the suspension seat was evaluated in the laboratory using human subjects as well as passive loads. In order to investigate the effect of air cushion on vibration transmissibility of the seat, three different experiments were designed. In the first series, the bladders were deflated completely and the suspension was locked to record the acceleration transmissibility characteristics of the PUF layer alone. In the second design, the vibration performance of the cushion and the PUF layer were measured using inflation pressures of 0.5 and 1.0 psi, while the suspension was kept locked. In the final series, the vibration performance of the seat with inflated and deflated cushions were measured under white noise random excitations. These experiments involved three different passive loads and human subjects.

5.2 Conclusions

The present study is a preliminary fundamental effort on building methodologies for assessing subjective and objective comfort performance of a suspension seat with individual inflatable air bladders. The experimental study provided considerable knowledge that would

be applicable in deriving models of the prototype seat and in identify important design guidance. The major findings of the study are summarized below:

- The SAE indenter tends to underestimate the cushion stiffness when compared to that derived from buttock-shaped indenter. The buttock-shaped indenter yields greater contact area, which is more representative of a seated human.
- The most significant anatomical region for assessing the objective comfort via the interface pressure is the ischium region, which showed good correlation with the subjective sensation. It was concluded that excess pressure in the ischium region would cause greater discomfort.
- The contact force in the tail bone zone becomes more significant when using a backrest due to greater load shifting towards the backrest and rotated pelvic.
- The buttock-shaped indenter simulates the interface pressure distribution that is more representation of that observed with human subjects. The results indicated similar trend in pressure concentration under ischial regions of the indenter when compared to the human buttocks.
- Dynamic stiffness of the cushion is a more realistic measure of total cushion stiffness in a dynamic environment. The incremental quasi-static measure always tends to underestimate the stiffness due to lack of cushion relaxation under static loads.
- Although the air cushions are generally more effective in distributing the interface pressure, an overinflated cushion tends to generate higher pressure concentration under the thighs and under ischial bones. On the other hand inadequate inflation pressure leads

to bottoming effect and body contact with the seat frame resulting in higher contact pressure.

- Among different components of the prototype seat, the PUF cushion and suspension showed damped natural frequencies near 5.5 and 3.8 Hz. These frequencies are close to the seated body vertical mode fundamental frequency (near 5 Hz). The current prototype seat design is thus considered inadequate for effective vibration isolation.
- The vast majority of the wheeled off-road and heavy road vehicles exhibit dominant vertical vibration at frequencies well below 5Hz. The prototype suspension would thus be expected to amplify the vehicle vibration.

The above conclusions with respect to analysis of body pressure distribution and vibration transmissibility of the dynamic seat in combination with cushion characteristics can provide important guidelines for design of automotive seats with enhanced comfort performance. These are summarized below:

- Force-deflection characteristics of the PUF material reveal nonlinear stiffness. A very soft cushion tends to distribute contact force over a larger area and thus reduces the localized pressure concentration at the seat-human interface but can cause bottoming with heavier subject. A soft cushion would also impose greater loads on the side wings and the femur bone. A seat cushion or the air bladders therefore must be selected to accommodate wide range of subjects' weight and yet prohibits hard interface contact. Jelly foams are highly recommended for this purpose however further investigation in the static and dynamic characteristics would be highly desirable.

- The cushion characteristics evaluated using the commonly used SAE indenter cannot be considered representative of the load distribution by the seated human. The buttock-shaped indenter can serve as an effective tool to estimate realistic load distribution.
- Air cushions are capable of distributing the interface force more evenly, when inflation pressure is regulated. Cushions made of a number of independent or coupled air bladders would be desirable. The aircushions, however, offer negligible damping to limit the vibration transmission. Hence application of air filled cushions in automotive seat is highly recommended when combined with PUF materials with adequate damping.
- Higher number of cushion bladders used in the seat cushion can provide greater flexibility to select the most comfortable force distribution and thus the support by the user. Such a design would also permit variations in contact pressure, which is desirable under prolonged sitting.
- The lateral support region of the cushion should be designed with lower stiffness in order to accommodate subjects with wide anthropometric variations. This would also reduce the localized pressure concentration in the side wings.
- Use of a back support helps to transfer some portion of the upper body weight to the back rest. Furthermore, this constitutes a preferred posture by many subjects. The back support, however, causes pelvic rotation and generates high contact pressure near the tail bone area, which may lead to fatigue and sensation of discomfort. Implementation of an adjustable lumbar support both in the fore-aft and vertical directions is highly recommended.

- Suspension mechanism in dynamic seat must be able to reduce vibration transmissibility close to natural frequencies of the human body. Therefore tuning the damper and spring characteristics for the range of 5th to 95th percentile subjects is essential. The suspension natural frequency should be in the 1-1.5 Hz range to effectively attenuate vertical vibration of the vehicles.
- A typical industry solution to provide adjustable height in heavy vehicles is to utilize the air spring as a mean to elevate or to descend the seat. This leads to change in the spring stiffness and hence the fundamental frequency of the suspension seat. It is recommended to decouple the lifting mechanism from the suspension mechanism.

5.3 Recommendations for Future Work

In this thesis the performance of a prototype heavy vehicle seat has been measured through objective evaluations in terms of comfort perception and vibration isolation. Although a suspension coupled with an air cushion with a number of inflatable air bladders offers considerable potential to provide improved body support and vibration isolation, the present study can be considered only as a preliminary laboratory-based effort. Far more additional efforts would be desirable to deduce more reliable assessments and design guidelines. Some of the possible further works are summarized below:

- The current cushion stiffness measurement method employs a circular disc to draw force-deflection characteristics of the seat cushions. However this indenter poorly represents a typical human buttocks contact with the seat. In this thesis, a buttock-shaped indenter was designed and fabricated, which showed more representative human-seat load distribution. It is highly recommended to add soft material all

around the exterior surface of the indenter to simulate human body soft tissue. This could permit simulation of the human-seat contact more accurately and thus the stiffness and damping characterization of the cushion.

- While the analysis of pressure measurement at the human-seat interface has provided valuable information regarding segmental cushion loading and pressure distribution, higher numbers of subjects and air bladders are recommended.
- Application of visco-elastic material within the seat cushion would be desirable so as to achieve improved vibration isolation by the cushion.

Appendix A

Sample Questionnaire

Name:						
Significant (?)	Region	Very Un-comfortable	Un-comfortable	Satisfactory	Comfortable	Very comfortable
	1					
	2					
	3					
	4					
	5					
	6					
	7					
	8					
	9					
Significant (?)	Region	Very Un-comfortable	Un-comfortable	Satisfactory	Comfortable	Very comfortable
	1					
	2					
	3					
	4					
	5					
	6					
	7					
	8					
	9					
Significant (?)	Region	Very Un-comfortable	Un-comfortable	Satisfactory	Comfortable	Very comfortable
	1					
	2					
	3					
	4					
	5					
	6					
	7					
	8					
	9					
Significant (?)	Region	Very Un-comfortable	Un-comfortable	Satisfactory	Comfortable	Very comfortable
	1					
	2					
	3					
	4					
	5					
	6					
	7					
	8					
	9					
Significant (?)	Region	Very Un-comfortable	Un-comfortable	Satisfactory	Comfortable	Very comfortable
	1					
	2					
	3					
	4					
	5					
	6					
	7					
	8					
	9					

References

- [1] Donald, D., Harrison, Sanghak, O., Harrison, Arthur, C., Crot, Deed, E., Harrison, Stephan, J., Troyanovich, 2000/01 "Sitting Biomechanics, Part II: Optimal Car Driver's Seat and Optimal Driver's Spinal Model," *Journal of Manipulative and Physiological Therapeutics*, vol. 23
- [2] International Standardization Organization 2631, 1985, "Mechanical Vibrations and Shock Evaluation of Human Exposure to Whole-Body Vibration" Part 1: General Requirements, First Edition, p. 17.
- [3] Eklund, J., Liew, M., 1991/8, "Evaluation of seating: The influence of hip and knee angles on spinal posture," *International Journal of Industrial Ergonomics*, vol. 8, pp. 67-73.
- [4] Rosegger, R., Rosegger, S., 1960, "Health effects of tractor driving," *Journal of Agricultural Engineering Research*, vol.5 pp. 241-275.
- [5] Donald, D., Harrison, Sanghak, O., Harrison, Arthur, C., Crot, Deed, E., Harrison, Stephan, J., Troyanovich, 1999/12 "Sitting Biomechanics, Part I: Review of the literature" *Journal of Manipulative and Physiological Therapeutics*," *Journal of Manipulative and Physiological Therapeutics*, vol. 22. pp. 594-609.
- [6] Harrison, DD., Janik, TJ., Troyanovich, SJ., Harrsion, DE, Colloca, CJ., 1997/5, "Evaluation of the assumptions used to derive an ideal normal cervical spine model," *Journal of Manipulative and Physiological Therapeutics*, vol. 20, issue 4, pp. 246-56.
- [7] Rakheja, S., Ahmed, A.K.W., Sankar, S., and Afework, Y., 1991/112, "Ride Performance Characteristics of Seat-Suspension Systems and Influence of the Seated Driver", ASAE Paper No. 917569, ASAE International Winter Meeting, Chicago, Illinois, Dec. 17-20 1991, p. 26.
- [8] Wu, X., Rakheja, S., Boileau, P.-ED., 1999, "Distribution of human-seat interface pressure on a soft automotive seat under vertical vibration," *International Journal of Industrial Ergonomics*, vol. 24, pp. 545-557.
- [9] Andersson, BJG., Ortengren, R., Nachemson, A., Elfstrom, G., 1974, "Lumbar disc pressure and myoelectric back muscle activity during sitting. I. Studies on an experimental chair," *Scandinavian Journal of Rehabilitation Medicine*, vol. 6, pp.104-114.
- [10] Damkot, DK., Pope, MH., Lord, J., Frymoyer, JW., 1984/5, " The relationship between work history, work environment and low-back pain in men," *Spine*, vol. 9 issue 4, pp. 395-399.
- [11] Andersson, BJG., Ortengren, R., Nachemson, A., Elfstrom, G., 1974, "Lumbar disc pressure and myoelectric back muscle activity during sitting. IV studies on a car driver's seat," *Scand J Rehab Med* vol. 6, pp. 128-133.
- [12] Schoberth, H: *Sitzhaltung, Sitzschaden, Sitzmobel*. Berlin, Springer-Verlag, 1962.

- [13] Williams, M., Lissner, HR., 1977 "Biomechanics of human motion," Philadelphia: Saunders, pp. 90-92.
- [14] Thomas M. Frusti, David J. Hoffman, 1994, "Quantifying the comfortable seat developing measurable parameters relating to subjective comfort," Automotive Body Interior & Safety Systems, IBEC 94.
- [15] Levart, E., Voisin, A., Bombardier, S., and Bremont, J., 1997, "Subjective Evaluation of Car Seat Comfort with Fuzzy Set Techniques," International Journal of Intelligent Systems, vol. 12, pp. 891-913.
- [16] International Standardization Organization 7096, "Earth-Moving Machinery-Operator Seat-Transmitted Vibration", ISO/TR 5007-1980, p. 29.
- [17] Wenqi, S., Parsons, K.C., 1997, "Validity and reliability of rating scales for seated pressure discomfort," International Journal of Industrial Ergonomics, Vol. 20, pp. 441-461.
- [18] Ebe, K., and Griffin, M. J., 2000, "Qualitative Models of Seat Discomfort Including Static and Dynamic Factors," Ergonomics, vol. 43 issue 6, pp. 771-790.
- [19] Andreoni, G., Santambrogio, G. C., Rabuffetti, M., 2002/11, "Method for the Analysis of Posture and Interface Pressure of Car Drivers," Applied Ergonomics, vol. 33, issue 6, pp. 511-522.
- [20] Wolfe, HW., 1982, "Cushioning and fatigue," Mechanics of Cellular Plastics, (London: Applied Science), pp. 99- 142.
- [21] Ebe, K., Griffin, M. J. 1994, "Effect of polyurethane foam on dynamic sitting comfort," in Proceedings of Inter-Noise 94, vol. 2 (Yokohama: Institute of Noise Control Engineering and Acoustical Society of Japan).
- [22] Ebe, K., and Griffin, M. J., 2001, "Factors Affecting Static Seat Cushion Comfort," Ergonomics, vol. 44 issue 10, pp. 901-921.
- [23] Griffin, M.J., 1990, "Handbook of Human Vibration", Academic Press, London.
- [24] Christ, W., Dupuis, H. Uber die beanspruchung der wirbelsaule unter dem einfluss sinusformiger und stochastischer schwin gungen Internationales Zeitschrift fur Angewandte Physiologie 1966; 22:258-78.
- [25] Ahmadian, M., Seigler, M., 2002, "A comparative Analysis of Air-Inflated and Foam Seat Cushions for Truck Seats" SAE Technical papers, Detroit, Michigan November 18-20.
- [26] Boggs, C., Ahmadian, M., 2005/4, "Field Study to Evaluate Driver Fatigue Performance in Air-Inflated Truck Seat Cushions-Objective Results," SAE Technical papers, Detroit, Michigan, 2005-01-1008.
- [27] Griffin, M.J. 1998, "Fundamentals of human responses to vibration," In "Fundamentals of Noise and Vibration," Fahy, F.J., Walker, J.G., Eds. London: E&FN Spon, pp. 179-223.

- [28] Raphael Zenk, Christian Mergl, Jurgen Hartung, Olaf Sabbah, Heiner Bubb, 2006/4, "Objectifying the Comfort of Car Seats", SAE Journal of Ergonomics, 2006-01-1299.
- [29] Lee, J., Grohs, T., Milosic, M., 1995, „Evaluation of Objective Measurement Techniques for Automotive Seat Comfort,” SAE Technical Paper no. 950142.
- [30] Park, S.J., Min, B.C., Lee, J.K., Kang, E.S., 2001, ”Development of the Evaluating System for Ride Comfort and Fatigue in Vehicle,” SAE. Technical Paper no. 2001-01-0388.
- [31] S. Na, S. Lim, H. Choi and M. K. Chung, 2005/12 "Evaluation of driver's discomfort and postural change using dynamic body pressure distribution," International Journal of Industrial Ergonomics, vol. 35, pp. 1085-1096.
- [32] Staarink, H.A.M., 1995 “Sitting posture, comfort and pressure,” Delft University Press 1995.
- [33] Ebe, K., M. J., Griffin, 2000/12, "Qualitative models of seat discomfort including static and dynamic factors," International Journal of Industrial Ergonomics, vol. 43, pp. 771-790.
- [34] Gibson, L.J., Ashby, M.F. Cellular Solid Structure and Properties, Pergamon Press, New York, 1988.
- [35] Wu, X., Griffin, M.J., 1998, “The influence of end-stop buffer characteristics on the severity of suspension seat end-stop impacts,” Journal of Sound and Vibration, vol. 215 issue 4, pp. 989–996.
- [36] Vever, M.M., Lange, R., Hoof, J., Wismans, J.S.H.M., “Aspects of seat modeling for seating comfort analysis”, Journal of Applied Ergonomics 36 (2005) 33-42.
- [37] Ebe, K., 1994, " Effect of Thickness on Static and Dynamic Characteristics of Polyurethane Foam", International Congress of Noise Control Engineering.
- [38] Hostens, I., Papaioannou, G., Spaepen, A., Ramon, H., 2001, "Buttock and back pressure distribution tests on seats of mobile agricultural machinery," Applied Ergonomics, vol. 32, pp. 347-355.
- [39] Society of Automotive Engineers, 1988/12. “Force-Deflection Measurements of cushioned components of Seats for Off-Road Work Machines,” SAE J1051. Society of Automotive Engineers.
- [40] Thomson, W. T., Dahleh, M. D., 1998, “Theory of Vibration with Applications”, Prentice Hall.
- [41] Blair, G.R., Milivojevich, A., Van Heumen, J.D., 1997, "Automotive Seating Comfort: Investigating the Polyurethane Foam Contribution - Phase I" SAE Paper No. 980656, Detroit, Michigan, 1997.
- [42] Mansfield, N. J., 2004, “Human Response To Vibration”. CRC Press; 1 edition (Oct 28, 2004).

- [43] Pheasant, S., 1988, "Body Space", anthropometry, ergonomics and design, Taylor & Francis.
- [44] Wu, X., Rakheja, S., Boileau, P.-ED., 2006. "The role of seat geometry and posture on the mechanical energy absorption characteristics of seated occupants under vertical vibration," *International Journal of Industrial Ergonomics*, vol. 36, pp. 171-184.
- [45] Wilder, DG., Woodworth, BB., Frymoyer, JW., Pope, MH., 1982, "Vibration and the human spine," *Spine* vol. 7, pp. 243-54.
- [46] Pope, MH., Wilder, DG., Frymoyer, JW., 1980/5, "Vibration as an aetiologic factor in low back pain," In: *Proceedings of Institution of Mechanical Engineers, Conference on Engineering Aspects of the Spine*, Westminster, London.
- [47] Panjabi, MM., Andersson, GBJ., Jorneus, L., Hult, E., Mattsson, L., 1986, "In vivo measurements of spinal column vibrations:." *Journal of Bone and Joint Surgery*, 68A, pp. 695-702.
- [48] Levert, E., Voisin, A., Bombardier, S., Bremont, J., 1997, "Subjective Evaluation of Car Seat Comfort with Fuzzy Set Techniques," *International Journal of Intelligent Systems*, vol. 12, pp. 891-913.
- [49] Kolich M., Seal N., Taboun, S., 2004/5, "Automobile seat comfort prediction: statistical model vs. artificial neural network," *Applied Ergonomics*, vol. 35, pp. 275-284.
- [50] Lee, J., Ferraiulo, P., 1993, "Seat comfort," SAE Paper, 930105 (Warrendale, PA: Society of Automotive Engineers).
- [51] Wu, X., Griffin, M.J., 1996, "Towards the standardization of a testing method for the end stop impacts of suspension seats," *Journal of Sound and Vibration*, vol. 192 issue 1, pp. 307-319.
- [52] Japanese Automobile Standards Organization, 1982, "Test Code of Seating Comfort for Automobile Seats," JASO B407-82. The Society of Automotive Engineers of Japan, Inc.
- [53] Rakheja, S., Stiharu, I., Boileau, P.-E., 2002, "Seated Occupant Apparent Mass Characteristics under Automotive Postures and Vertical Vibration", *Journal of Sound and Vibration*, vol. 253, issue 1, pp. 57 – 75.
- [54] Kolich, M., 1999, "Reliability and validity of an automobile seat comfort survey", SAE paper 1999-01-3232.
- [55] Milivojevich, A., Stancie, R., Russ, A., Blair, G. R. and van Heumen, J. D. 2000, "Investigating psychometric and body pressure distribution responses to automotive seating comfort", SAE technical paper 2000-01-0626.
- [56] Krouskop, T. A., Graber, S. L., 1989, "Interface pressure confusion", *Decubitus*, vol. 2, issue 3, p. 8.
- [57] International Organization for Standardization ISO/DIS 16840-2, 2003, *Wheelchair Seating – Part 2: Test methods for determining the physical and mechanical characteristics of devices intended to manage tissues integrity – Seat Cushions*.

- [58] Boileau, P.E. 1995/3, "A Study of Secondary Suspension and Human Driver Response to Whole-Body Vehicular Vibration and Shock" PhD Thesis, Concordia University, pp. 310-314.
- [59] Magnusson, ML., Pope, MH., Wilder, DG., Areskoug B., 1996, "Are occupational drivers at an increased risk for developing musculoskeletal disorders?", Spine vol. 21 pp.710-717.
- [60] Nélisse, H., Patra, S., Rakheja, S., Boutin J., Boileau, P.-É., "Assessments of two dynamic manikins for laboratory testing of seats under whole-body vibration," 2008/5, International Journal of Industrial Ergonomics, vol. 38, issue 5-6, pp. 457-470.
- [61] Seigler, M., Ahmadian, M., 2003, "Evaluation of an alternative seating technology for truck seats," Heavy Vehicle Systems, vol. 10, issue 3, pp. 188-208.
- [62] Hilyard, N. C., and Collier, P., 1984/12, "Effect of vehicle seat cushion material on ride comfort," Paper presented at Plastic on the Road, The Plastic and Rubber Institute International Conference, London.